Electrical energy conversion with distributed parameter modelling: A study of a step-down converter

Nicholas Reuss

Faculty of Engineering and the Built Environment
University of the Witwatersrand
February 2025

Declaration

I declare that this dissertation is my own, unaided work. It is being submitted for the degree of Master of Science in Engineering to the University of the Witwatersrand, Johannesburg. It has not been submitted before for any degree or examination to any other university.

Signed on 2025-09-14

Nicholas Reuss

Abstract

Energy is converted in an electric circuit. For example, when a DC-DC power converter uses the current in an inductor to decrease the input voltage. However, the underlying physical mechanism by which energy is converted is not visible on a circuit diagram that uses lumped parameter models. The spatial information is missing but can be included via distributed parameter modelling with transmission lines. The mechanism of energy conversion using transmission line modelling is yet to be reported in literature.

A theoretical step-down converter topology is studied with the inductor substituted for a high impedance, one-dimensional, lossless transmission line model. Simulated outputs show that the converter functions comparably with the lumped and distributed inductor models for a 10 V input and 50 % duty cycle at 25 kHz. The converter switch initiates step waves that propagate in the transmission line and produce a characteristic stepped output waveform.

A reflection diagram for the transmission line inductor yields spatial distributions of voltage, current and instantaneous power. These distributions show the energy conversion process produces voltage and current from energy at rest purely in the magnetic field. The wavefront is the site of energy conversion where energy at rest is converted and brought into motion. The wavefront power is decomposed into components for the electric field and magnetic field on the basis of changes in energy density. These components provide a means to describe the energy conversion process with respect to the action of the wavefront on the underlying electromagnetic fields.

Reflections of the wavefront show the energy conversion process within the inductor is biased towards the storage of energy purely in the magnetic field. Wavefronts diminish in magnitude over time, so the repeated switching of a converter creates new wavefronts that sustain the energy conversion process. Examining the effects of impedance mismatch reveals a trade-off between converting energy in-place and transporting energy to the load.

This work supplies greater insights into the fundamental mechanisms of energy conversion in inductors, which may be a prerequisite step for further significant innovation in power converters.

Contents

List of Figures

List of Tables

Acronyms

DC Direct Current

FEM Finite Element Method

KCL Kirchhoff's Current Law

KVL Kirchhoff's Voltage Law

RF Radio Frequency

Chapter 1

Introduction

Inductors, capacitors and semiconductors are the fundamental building blocks in many DC-DC power converters. In recent years, much attention has been directed towards the improvement and optimization of semiconductor switches with impressive results. However, little has been done to understand the fundamental operating mechanisms of the inductors and capacitors in the context of power converters. Petroianu [1], [2] concedes that the power electronics industry has thrived despite an incomplete understanding of foundational concepts, and this success has further emphasised procedural research efforts over conceptual knowledge.

Power electronics research is generally driven by technology rather than theoretical breakthroughs. A new technology must first become available before it is integrated into a power converter; the power converter is not a precursor to the technologies used in its construction. For other fields this is not always the case where theoretical developments predict what will come in the future. Consider the work done in material science which led to the creation of wide bandgap semiconductors like gallium nitride (GaN). The foundational theory from that field predicted that GaN would be a promising material for semiconductor switches before the technology existed to manufacture them [3]. Perhaps a deeper understanding of inductors and capacitors is a prerequisite for further significant innovation in power converters.

The electric circuit is the foundation of every power electronics textbook and is the essential tool for analysis and design [4]. For power converters, circuit elements are arranged in a topology to process electrical energy from the input to the output, as measured by voltages and currents. Changes in voltage and current of energy storage elements point to the conversion of electrical energy. The typical DC-DC power converter processes energy from a source with inductors and capacitors which undergo a cycle of energy accumulation and discharge modulated by the switching action of the converter [5]. Work by Ferreira [6] using the Poynting vector suggests that the processes governing the conversion of energy are rooted within capacitors and inductors.

Lumped capacitor and inductor models remain the ubiquitous modelling technique for energy storage elements in power converters. These models describe the physical components in terms of differential equations for the voltage and current at the terminals. By definition a lumped component model considers a physical quality, like inductance, to be concentrated at a point, so physical dimensions are abstracted away leaving only the fundamental electrical properties. This abstraction allows the engineer to focus on circuit analysis and design aspects of converters while disregarding unnecessary details.

Lumped component models have given good results in the past. However, with the advent of wide bandgap semiconductors, the advances in switching performance have made new effects visible which these lumped models did not originally predict [7]. When these effects are not modelled, they cannot be designed for. In literature this has led to renewed interest in the modelling of power converter circuits using techniques from electromagnetics [5], [8].

The functioning of lumped capacitor and inductor models used in electric circuits cannot be directly explained from an electromagnetic field perspective [9]. The use of lumped parameter models results in a shortfall of spatial information since there is no volume described by the model in which fields may be observed. A physical inductor or capacitor must occupy a volume. Therefore, an alternative modelling approach is necessary to describe the functioning of inductors and capacitors.

For example, consider the process of charging a physical inductor. The outcome of energy flowing into the terminals is the accumulation of energy in the magnetic field. Importantly, a voltage and associated electric field must also be present within the inductor for it to charge. Part of the charging process includes the conversion of electric field energy to magnetic field energy. Similarly, for a discharging inductor, energy at rest purely in the magnetic field must be converted into a voltage and current before leaving at the terminals. This internal conversion of energy is not visible using lumped models as it requires consideration of volume and electromagnetic fields.

One approach for analysing the conversion of energy in capacitors and inductors would be to conduct a 3D FEM analysis of the fields. However, this is complex and intensive for circuit applications, particularly if the conversion process arises in the context of a larger circuit like a power converter. In this work we propose to use transmission line models as an intermediary between lumped component models and 3D FEM analysis for identifying and describing the mechanism of energy conversion in inductors and capacitors.

As a form of distributed modelling, the transmission line considers parameters like inductance and capacitance to be spread out in space rather than concentrated at a point. Transmission lines have been used before as alternatives to lumped parameter models of inductors and capacitors [7], [9], [10]. Inductors are modelled as high-impedance transmission lines terminated in a short circuit. Capacitors are modelled as low-impedance transmission lines terminated in an open circuit. A detailed description of the mechanism of energy conversion in inductors or capacitors using transmission line models is yet to be reported in literature.

The innate presence of wave effects in transmission lines leads to the hypothesis that energy conversion can be explained by the propagation and reflection of wavefronts.

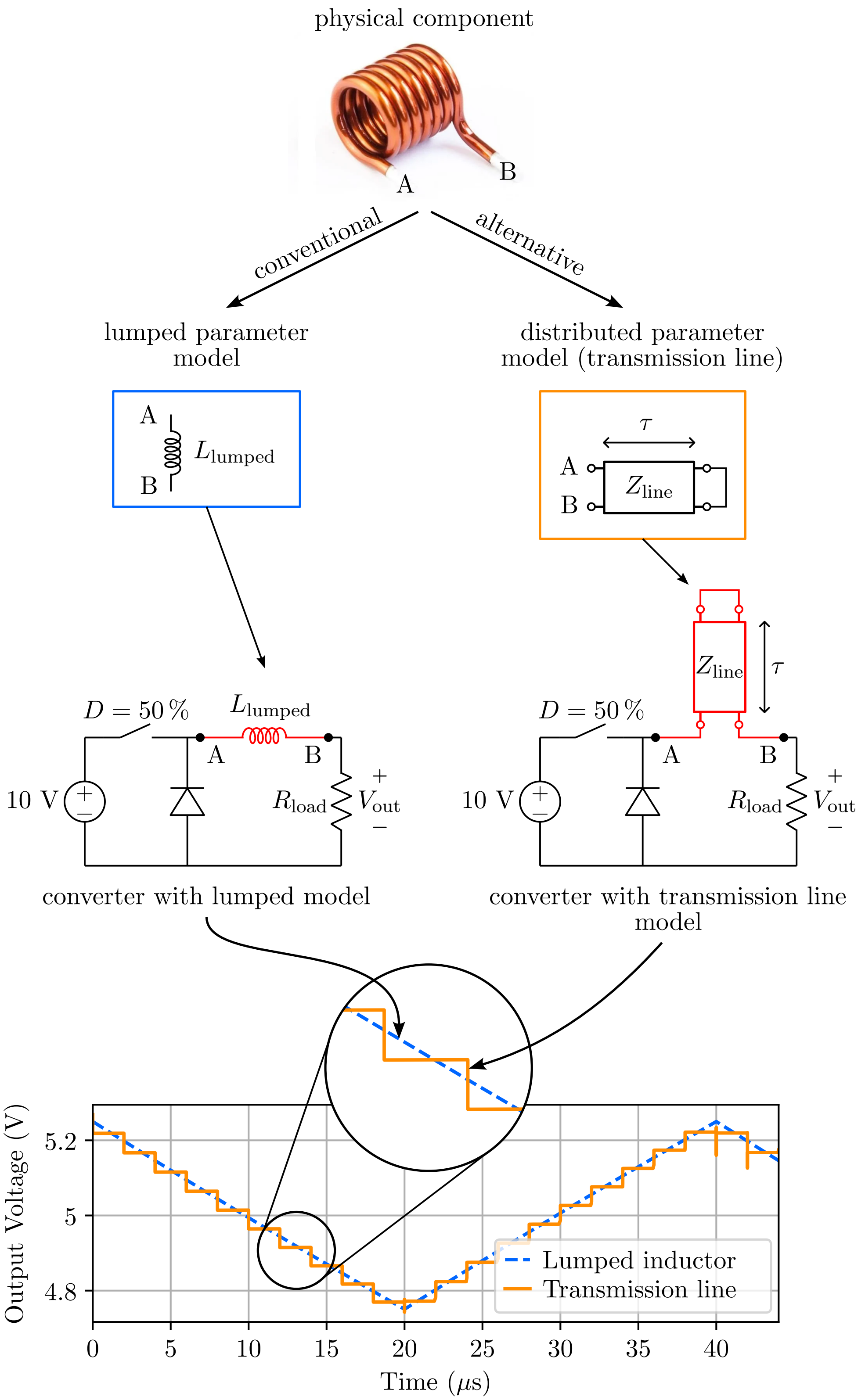

Figure 1.1: Power converter output with a transmission line inductor as an alternative to the conventional lumped parameter inductor model

1.1 Terminology

The primary function of a DC-DC power converter is to process electrical energy by supplying voltages and currents optimally suited to load requirements [3]. The term power converter is ubiquitous in power electronics but is perhaps a little misleading when interpreted literally. A perfectly efficient power converter has an output power equal to its input power and therefore conserves power. As we do not desire to use new terminology for well established engineering concepts, we will continue to use the term power converter in this text but will refer to the process of changing the properties of electrical energy, namely the voltage and current, as *electrical energy conversion*. As this work deals exclusively with electrical energy, the term energy conversion is used interchangeably with electrical energy conversion.

1.2 Objective

The objective of this research is to identify and describe a mechanism that shows the energy conversion process in an inductor when the inductor is viewed as a lossless, high impedance transmission line. This description should be rich in detail on the mechanisms of energy conversion: where it takes place, how it changes over time, and its sensitivity to parameter variations like a mismatch in impedance between the transmission line and broader circuit.

1.3 Method

Figure 1.1 provides a high-level outline of the approach taken in this work. A physical inductor is represented with a conventional lumped inductor model and an alternative transmission line model. These models are then used in a simplified theoretical power converter circuit to produce comparable outputs via simulation. The added spatial dimension that accompanies the transmission line provides extra information on the underlying physical component which is not visible in lumped models. Using insights from the spatial dimension of the transmission line we identify a mechanism that shows the energy conversion process.

Chapter 2 provides an overview of literature to contextualize this work. Distributed techniques for modelling inductors and capacitors are discussed along with existing applications of transmission lines in power converters. A direct energy perspective is noted to benefit descriptions of energy conversion and informs the approach taken in subsequent chapters.

Chapter 3 introduces transmission line models of inductors and capacitors. The 3D structures of physical capacitors and inductors are briefly presented to contextualize the abstractions applied for transmission line models. The modelling assumptions applied to transmission lines and switches are stated upfront for clarity and apply to all work that follows. In subsequent chapters, the inductor is studied in detail while the capacitor is left for future work which could take advantage of the duality that exists between transmission line models of inductors and capacitors to draw equivalent conclusions.

In chapter 4, standard converter design principles are applied to create a theoretical step-down converter with a lumped inductor model. The lumped model is substituted for an equivalent transmission line inductor model to produce another converter circuit as outlined in figure 1.1. Timing constraints are established for the transmission line to eliminate some of the complex wave effects described in literature. The two converters are simulated, and output waveforms compared serving to validate the substitution. The time domain inductor waveform informs the choice of new transmission line parameters to magnify the transmission line effects to a scale where they are easily perceptible. The theoretical converter circuit is divided into two equivalent circuits based on the switch position. Analysis of the equivalent circuits follows in chapters 5 and 6.

Chapter 5 presents the scenario where the transmission line inductor discharges into the load resistor. A reflection diagram is used to create spatial distributions which show the action of the wavefront. The wavefront appears to be the centre of activity for energy conversion, so the approach of wavefront power components is formulated to aid the description. The energy conversion process is described over time as the wavefront undergoes several reflections in the inductor.

In chapter 6, the discussion is extended to the other equivalent circuit of the step-down converter where the transmission line inductor is charged up by the voltage source. The results from each equivalent circuit are combined for a full switching period. A discussion of results considers the relationship between lumped and distributed model and the role of converter switching in the energy conversion process of the inductor.

Chapter 7 assesses the impact of impedance mismatch on the energy conversion process in a transmission line inductor using a Thévenin equivalent circuit with simple values. The Thévenin resistance is varied while keeping the transmission line impedance fixed so that the stored energy remains constant. The effect on the wavefront power and its components is described with emphasis on load resistances which show salient features. A discussion addresses the trade-off between the degree of energy conversion and the ability of the inductor to absorb or supply energy.

Lastly, chapter 8 concludes with a summary of key findings and provides recommendations for future work.

Chapter 2

Background

The pursuit of compact, high efficiency power converters combined with advances in switching technology have led to a long-standing trend of increasing switching frequency [6]. The challenges posed by increased operational frequencies have been known for several decades [8], [11]. These challenges are trying the limits of conventional circuit theory modelling for power electronics [11], [12]. Ferreira and Van Wyk [13] argue that the electromagnetic operation of switched power converters needs further treatment to enable meaningful innovation. In this chapter we consider which techniques and approaches used by other work in the field show promise for identifying and describing the mechanism of energy conversion in inductors and capacitors.

2.1 Distributed capacitors and inductors

The idea of modelling inductors and capacitors as transmission lines has existed for many years [7]. However, distributed modelling of reactive components did not initially begin with transmission line models for inductors and capacitors. Rather, efforts were directed into merging inductors and capacitors for modelling and realization of resonant mode converters [14]. This led to the field of integrated passives where inductors and capacitors were electromagnetically integrated into a single distributed structure with the objective of reducing component footprints and improving ease of manufacture [14]. It was speculated that total integration of discrete components was the future direction for power electronics [13], but this has yet to materialize. In hindsight, it more likely represented a shift in thinking for power-electronics where an electromagnetic power-conditioning perspective emerged [12].

Sullivan and Kern [7] pursue the idea that the transmission line can be directly applied to model a physical capacitor. They note that discrepancies between simulations of RLC lumped models and measurements of physical components are reconciled using distributed models, particularly at high frequencies. Their work was focused on modelling accuracy at the terminals of the capacitor in the time domain. They suggest that transmission lines are more suitable than lumped models in instances where switching transitions are faster than the period of the capacitor's self-resonant frequency. A benefit of the approach of Sullivan and Kern is that it facilitates terminal-for-terminal substitution and does not merge the behaviour of the capacitors and inductors. The lumped parameter model in a circuit can be replaced by a transmission line model which shares the same terminal connections. This minimises the number of changes made to the circuit diagram and permits direct comparisons between lumped parameter models and transmission line models.

2.2 Power converters with distributed models

The idea of distributed modelling was not restricted to components alone. Shmilovitz and Singer [8] recognise that lossless transmission lines can be used as the primary energy storage component for the realization of power converters and proceed to build a working prototype. In a later paper [10], they identify the benefits of the transmission line model for the construction of power converters. Namely, inductance and capacitance are spread out along its length rather than concentrated at a point. This gives rise to a resistor-like surge impedance but without the loss of a resistor, thereby permitting high frequency converter operation with rapid rise and fall times. However, their approach is strictly limited to the time-domain terminal behaviour and therefore does not provide insight into the internal processes taking place within the transmission line.

Sander [5] is also concerned with the development of power converters using transmission lines but appears to be unaware of the earlier work of Shmilovitz and Singer [8]. Both papers describe and model the primary converter element using a transmission line but realise this model differently in their prototypes: Shmilovitz and Singer use a length of $50\,\Omega$ coaxial cable [8] while Sander uses a cascaded network of discrete inductors and capacitors [5].

Sander [5] differs from earlier work by considering the spatial dimension of the transmission line using plots of voltage and current plots versus position. The use of the spatial dimension is significant because new underlying behaviours begin to surface. One of these behaviours is the accumulation of energy in a transmission line shorted at one end. However, these insights remain untreated with focus diverted to experimental success of developing an operational converter prototype with a new topology. We note the value of the spatial dimension and specifically incorporate into our discussions.

Sander and Karvonen [15] revisit the initial work by Sander [5] to position the new topology as a solution for cost reduction in the manufacture of power converters due to a decreased semiconductor count. Here they explain the high-level operating principle of the converter in terms of voltages and currents but neglect to mention any underlying means of energy storage which leaves the mechanism of energy conversion within the transmission line unclear.

Huang, Woittennek and Röbenack [16] present a distributed power converter using an integrated passive which combines the inductor and capacitor of a regular buck converter into a single transmission line. Their work is preoccupied with rigorous mathematical treatment of the converter under the assumption of ideal switching. They conclude that the introduction of transmission line models may yield comparable results to lumped models but introduces effects that are not visible with the classical buck converter. Specifically, they identify switching edges in the converter output which they attribute to the wave nature of the solution. This is a poignant result which we consider in more detail in chapter 5 through the discussion of wavefronts. They further note that it is desirable to have a transmission line with a high characteristic impedance relative to the load resistance to reduce output ripple. Thus, we explore the potential implications of impedance mismatch for energy conversion in chapter 7.

2.3 Power converters from an energy perspective

Li et al. [17] propose an energy-centric representation of an electric circuit called an energy topology. In an energy topology the circuit elements like inductors and capacitors are given equivalent energy models obtained using Poynting vector. The components are considered to be separated in space at different coordinates on a 2D plane. The components are joined by interconnects which are modelled as lossless transmission lines. The energy topology makes it obvious that energy in a power converter moves in an open loop, from source to sink unlike the closed loop of current flow in a circuit.

An energy topology is visualised for a buck converter and other topologies. Bar charts at different coordinates represent the energy stored or dissipated in each component. This highlights the movement and distribution of energy over time. Despite the consideration of spatial layout, they fail to mention a significant limitation of their approach: it does not account for the distributed nature of physical components, which themselves have an internal construction which the energy must permeate. We overcome this limitation by using transmission lines directly for the components rather than as interconnects. They conclude that viewing converters directly from an energy perspective benefits converter design and control because it is more intuitive than the simultaneous consideration of voltage and current. We build on this observation and focus on the manipulation of the energy in the fields of the transmission line.

Ferreira [6], [11] is an early pioneer of electromagnetics applied to the study of power converters. He proposes that energy flow modelling using electromagnetics is an essential counterpart to circuit theory for the design and optimization of high frequency power electronic converters. Ferreira performs Poynting vector analysis on transmission lines terminated in different circuit elements. Notably, he does not consider the inductors or capacitors themselves to be modelled as transmission lines preferring to draw them as structures in 3D space. His work is restricted to qualitative descriptions of the energy flow in transmission lines and the fields of inductors and capacitors. While Ferreira's approach is promising, it ultimately needs further development.

Ferreira arrives at a similar conclusion to Li et al. [17]. The primary objective of power converters is the conditioning and conversion of electrical energy, therefore, modelling energy flow via voltage and current is an indirect approach when compared to Poynting vector analysis. Ferreira alludes to energy being transformed by the propagation of waves in the transmission line. A large number of these waves arise from reflections due to a mismatch in impedance between interconnects and the source or load. The reflection of energy flux causes additional energy to build up in the field of the transmission line beyond the transfer requirements set out by the Poynting vector. This raises questions about the role of wavefronts in the manipulation of energy. However, his approach is constrained to a quasi-steady state analysis which is an aggregated view of all wave activity. In our work we consider individual wavefronts on a reflection diagram so that function of the wavefront within the transmission line is visible. Ferreira explicitly chooses a simple circuit because complex modes of operation may obscure the effects of interest, an approach which we replicate in this work.

Work by Mofu [18] marks a departure in approach from other literature by considering individual wavefronts within distributed models in an attempt to describe energy manipulation processes within reactive components. The idea of describing individual wavefronts is shown to have merit. Mofu identifies a complex effect which arises due to the interaction of two transmission lines and proposes a hierarchical classification for its description. In a process called wave fragmentation, a single switching event results in a vast number of wavefronts propagating in the transmission lines. However, complexity from many wavefronts appears to overwhelm the attempt to describe the energy conversion process within the transmission line. In this work we use these learnings to intentionally limit additional sources of complexity, like wave fragmentation, so that the action of individual wavefronts remains the core focus.

In much of the literature surveyed, it appears to be common practice to disregard the spatial information provided by the transmission line model and focus only on the time-domain characteristics at the terminals [6], [8], [14], [16]. There is additional insight in work which considers the spatial dimension. Therefore, in this work we place continued emphasis on the spatial dimension, particularly through the use of reflection diagrams as our foundational theory for studying transmission line models of inductors and capacitors.

Chapter 3

Transmission line modelling for energy storage elements

The circuit diagram is the primary tool used by engineers for the design and modelling of power converters. Lumped component models used in circuit diagrams have abstractions which reduce the visibility of activity inside components, particularly with regard to the functioning of energy storage elements like inductors and capacitors. Generally these abstractions are desirable since they eliminate irrelevant information. However, the literature surveyed in chapter 2 suggests that a spatial dimension is valuable for describing the electromagnetic operation of these components.

The discipline of power electronics is not typically concerned with wave effects that are present in the RF domain. In the past, the wavelengths of the signals in power converters were much larger than the physical dimensions of the components so the lumped parameter models were sufficient. However, as the switching frequencies of power converters increase, signal wavelengths are beginning to approach the physical dimensions of the components [7]. This increases the relevance of spatial dimensions described by distributed models.

Distributed models are based on fewer abstractions of the underlying physical structures compared to lumped models. A distributed parameter model considers parameters to be spread out in space rather than being concentrated at a single point, as in a lumped model. The transmission line is a popular form of distributed modelling.

This chapter summarises an approach for obtaining transmission line models of a physical capacitor and inductor. The assumptions and constraints governing all transmission lines in this work are presented and justified, forming the foundation for the analysis conducted in subsequent chapters.

3.1 Capacitor modelling

Physical capacitors are 3D devices which occupy a volume. Figure 3.1a shows a parallel plate capacitor with terminals labelled a and b. The parallel plates have a length l, width w and separation d. The plates are perfect conductors, and are

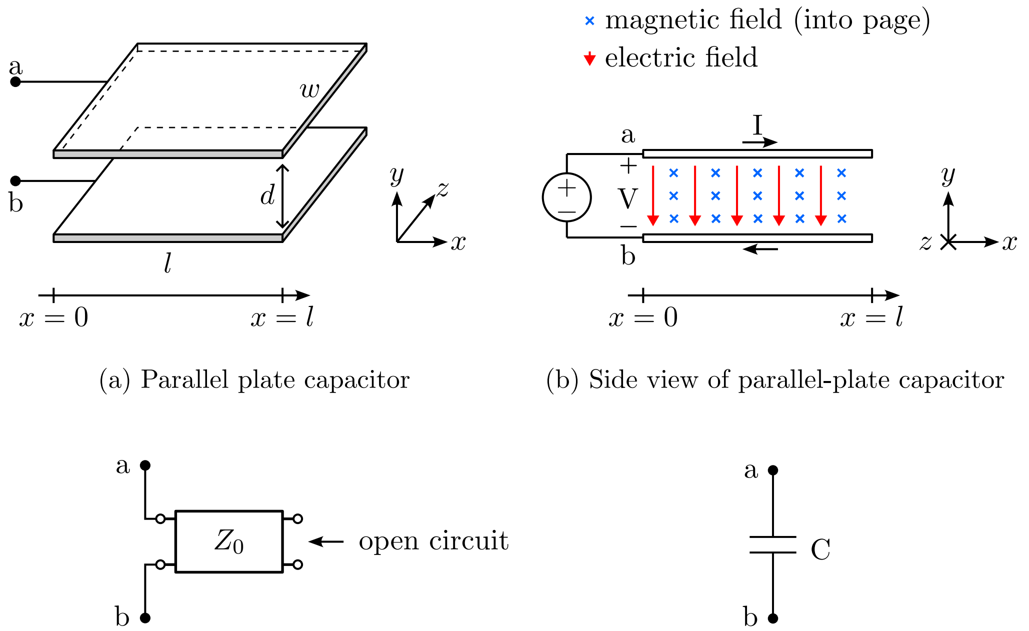

(a) Parallel plate capacitor

(b) Side view of parallel-plate capacitor

(c) Transmission line capacitor

(d) Lumped model capacitor

Figure 3.1: Capacitor models

separated by free space. When the width and length are much greater than the plate separation, the electromagnetic fields are confined to the volume sandwiched between the plates and fringing can be neglected [19].

When figure 3.1a is modelled as a lumped capacitor in figure 3.1d, the assumption applied is that the fields are uniform and application of a voltage at the terminals instantaneously permeates the structure. The lumped capacitor therefore considers energy to be stored exclusively in the electric field between the plates. The lumped capacitance (3.1) is determined by the plate separation, surface area and permittivity of free space ε_0 [19]. A small separation and large surface area lead to a large lumped capacitance.

$$C = \frac{\varepsilon_0 w l}{d} \tag{3.1}$$

To arrive at the transmission line model of the capacitor in figure 3.1c, a different set of assumptions are used. The transmission line model assumes the length l is the dominant dimension and therefore changes in the fields are instantaneous and uniform in the yz plane, but not along the x-axis. Thus, the analysis becomes quasi-one-dimensional. The 3D capacitor in figure 3.1a is reduced to a distributed capacitance C' and inductance L' in (3.2) where ε_0 and μ_0 are the permittivity and permeability of free space [20].

$$
\begin{aligned}
C' &= \frac{\varepsilon_0 w}{d} \\
L' &= \frac{\mu_0 d}{w}
\end{aligned}
\tag{3.2}
$$

Equation (3.2) shows that if the plates are brought closer together, the distributed capacitance increases and the distributed inductance decreases. Thus, a capacitor modelled in this fashion will have a large distributed capacitance and small distributed inductance.

The length of the plates, together with the distributed capacitance and inductance determine the transmission line properties. Namely, the characteristic impedance Z_0, propagation delay τ and propagation velocity v_p as shown in (3.3). A transmission line with a large distributed capacitance, and small distributed inductance will have a low characteristic impedance.

$$
\begin{aligned}
Z_0 &= \sqrt{L'/C'} \\
\tau &= l\sqrt{L'C'} \\
v_p &= \frac{1}{\sqrt{L'C'}}
\end{aligned}
\tag{3.3}
$$

The transmission line capacitor can store energy in both the electric and magnetic field. A transmission line capacitor is an intuitive extension of figure 3.1b which shows a side view of the parallel plate capacitor in figure 3.1a. A voltage difference between the plates will give rise to an electric field. Similarly, a current flowing along the plates will give rise to a magnetic field. The fields are orthogonal with the electric field directed from the positive to the negative plate and the magnetic field directed into the page.

In a transmission line there exists a duality between voltage and current and the electric and magnetic fields, respectively [20]. This is expressed in (3.4) which linearly relates the electric field E to the voltage V and the magnetic field H to the current I. Thus, the voltage and current on the transmission line can be used as a proxy for the strength and polarization of the underlying electric and magnetic fields. This has the benefit that a full 3D field analysis is not required to understand the electromagnetic operation of the capacitor.

$$
\begin{aligned}
E &= V/d \\
H &= I/w
\end{aligned}
\tag{3.4}
$$

3.2 Inductor modelling

An inductor can be modelled in a similar fashion to a capacitor. Figure 3.2a shows a single-turn foil inductor with an air core. This inductor is derived by modifying the parallel plate capacitor with a perfect short circuit the ends of the plates opposite to the inductor terminals. This is one realization of an inductor and there are many others. However, the similarity to the capacitor model means it is equally described by (3.2) to (3.4).

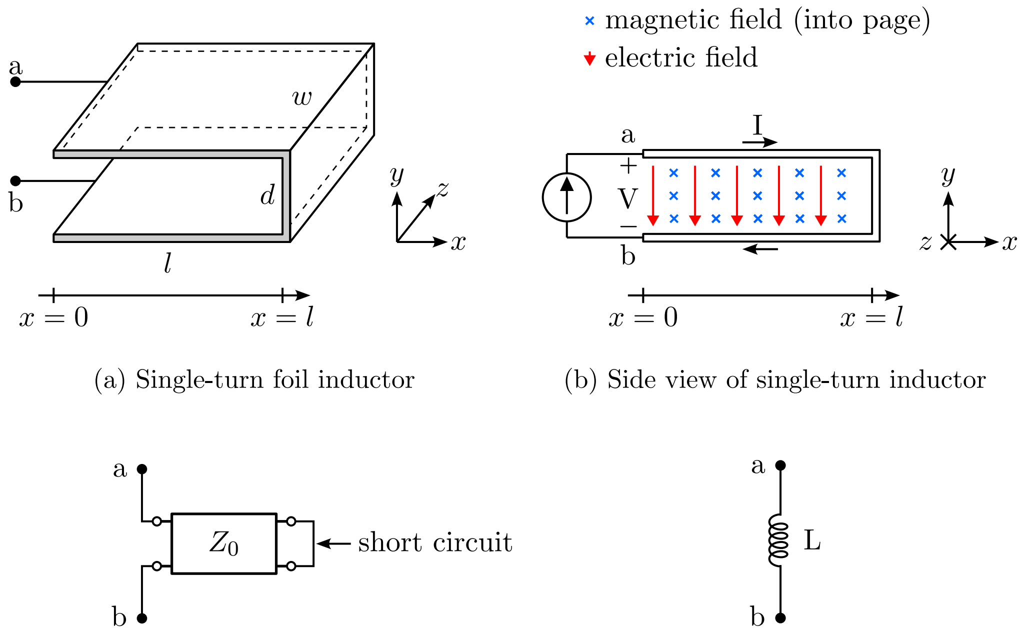

(a) Single-turn foil inductor

(b) Side view of single-turn inductor

(c) Transmission line inductor

(d) Lumped model inductor

Figure 3.2: Inductor models

For an inductor, the separation of the conductive plates is typically larger than that for the capacitor. This drives up the distributed inductance and reduces the distributed capacitance leading to a high characteristic impedance for the transmission line in figure 3.2c.

Figure 3.2b shows the electric and magnetic fields are again orthogonal and confined within the volume between the plates when a current is applied to the terminals. Thus, the voltage and current along the length of the inductor are again linearly related to the electric and magnetic fields.

The 3D inductor in figure 3.2a is reduced to a lumped inductor in figure 3.2d under the assumption that an applied current instantaneously permeates the structure. The lumped inductor therefore considers the energy to be stored exclusively in the magnetic field between the plates. The lumped inductance (3.5) is determined by the plate separation, surface area and permeability of free space μ_0 [19]. A large separation and narrow conductor strips create a large lumped inductance.

$$L = \frac{\mu_0 d l}{w} \tag{3.5}$$

3.3 Abstraction of geometry

There are various physical realizations of transmission lines with different cross-sections. Popular options include parallel plates, coaxial conductors and two-wire structures [19]. The derivation of transmission line parameters for different physical structures is the subject of many electromagnetics textbooks [19], [20]. A transmission line model is an abstraction over the underlying geometry. It emphasises the length of the component so the voltage and current vary with respect to position along a single dimension of the transmission line and not with respect to a general position in space.

The variation seen in the circuit symbols used to represent the transmission lines is often rooted in the underlying geometry. For example, a symbol with coaxial cylinders suggests the underlying physical structure is a coaxial cable with central conductor surrounded by a conductive cylinder. This work is not concerned with any one particular physical realization of a transmission line. The parallel plate models shown earlier are purely for illustrative purposes. The transmission line symbols used in this work are not intended to represent any specific underlying physical structure. Instead, we leverage the abstraction afforded by the transmission line model to ensure our observations are generally applicable to all geometries of inductors and capacitors which may be modelled as transmission lines. Table 3.1 records the parameters and their respective units used to quantify transmission lines in this work.

In this work, capacitors and inductors are modelled as separate transmission line structures. Capacitors are represented with low impedance transmission lines terminated in an open circuit. Equally, inductors are represented with high impedance transmission line terminated in a short circuit [7], [9]. We take the view that there is no salient characteristic impedance at which a transmission line becomes an inductor or capacitor. Rather, it is the termination in an open or short circuit which ultimately determines the operating behaviour of the transmission line. High impedance transmission lines work better as inductors and low impedance transmission lines work better as capacitors. An impedance is defined as high or low relative to the impedance of other components in the circuit.

Table 3.1: Common transmission line parameters describe electrical properties without reference to underlying geometry

Parameter	Description	Unit
L'	Distributed line inductance	H/m
C'	Distributed line capacitance	F/m
L_{line}	Total line inductance	H
C_{line}	Total line capacitance	F
Z_0	Characteristic impedance	Ω
v_p	Propagation velocity	m/s
l	Length	m
τ	Propagation delay	s

Table 3.2: Summary of lumped and distributed models for inductors and capacitors

		Capacitor	Inductor
Lumped model	Circuit symbol	C 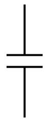	L 
	Means of energy storage	electric field	magnetic field
Distributed model	Circuit symbol	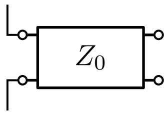	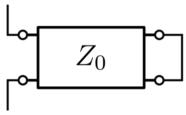
	Characteristic impedance	low	high
	Terminated by	open circuit	short circuit
	Means of energy storage	electric & magnetic field	electric & magnetic field

3.4 Duality of inductors and capacitors

Table 3.2 compares key characteristics across inductors and capacitors for lumped and distributed models. The lumped model is a simple abstraction that is easy to work with and is commonly used in power electronics. The distributed model is more complex but provides an additional spatial dimension which will be utilized in this work to identify and describe a mechanism of energy conversion in capacitors and inductors. The modelling approaches are different but complementary, although it should be noted that there is no universal procedure for converting between lumped and distributed capacitor models.

In the remainder of this work we focus primarily on the inductor. This is not because capacitors are less important, rather, transmission lines applied to capacitors and inductors exhibit a duality of behaviour as seen in table 3.2. This means that conclusions for transmission line inductors will have equivalent outcomes for transmission line capacitors. The detailed treatment of capacitors is left to future work. The use of inductors in this work does not limit the generality of the transmission line approach.

3.5 General modelling assumptions and constraints

In practice, power converters are not perfectly efficient. Semiconductor switches have switching and conduction losses while capacitors and inductors are constructed from lossy materials and cannot support an electromagnetic field indefinitely [3]. However, these practical considerations only serve to add complexity without significantly altering fundamental behaviour. Therefore, we intentionally apply assumptions and constraints which maintain the core behaviours of transmission lines while eliminating additional sources of complexity. These assumptions are commonplace in literature on transmission line modelling [19], [20]. The assumptions lead to a model that is impossible to build physically and does not match the complex construction of a real capacitor or inductor but ultimately creates a setup in which fundamental processes of energy conversion can be studied. We adopt the view that energy is stored in the electromagnetic field [20].

3.5.1 Transmission lines

In this work we exclusively use a one dimensional, lossless transmission line model with a uniform material and cross-section. Waves propagate strictly in the transverse-electromagnetic mode in the absence of fringing. This means that the electric and magnetic fields are orthogonal to the direction of propagation and the fields are completely confined within the transmission line. We neglect all the loss mechanisms present in physical materials. The conductors are perfect conductors with infinite conductivity. The dielectric medium is free space, which is a linear material and has a propagation velocity equal to the speed of light (3×10^8 m/s).

As a result of these constraints, variables in the transmission line model vary only in one dimension, along the axis of propagation. When the voltage or current is described at a position in the transmission line, this position refers to the distance in meters along the axis of propagation which is denoted with the variable x.

3.5.2 Switches and diodes

The shape of voltage and current waveforms in transmission lines is primarily determined by the switching action of the semiconductor devices. Advances in semiconductor technology have lead to increasingly faster switches. In light of this trend and for the purposes of simplification, in this work we assume switches and diodes to be ideal with no internal resistance and an infinitesimal rise and fall time. Using an ideal switch produces step changes in voltage and current which are easily identifiable and simplify the mathematics of their analysis. These step waveforms work well with reflection diagram analysis of transmission lines [21] and have been applied in other works [6], [15], [18].

Chapter 4

Step-down converter with distributed inductor model

This chapter introduces a transmission line in the context of a theoretical DC-DC power converter circuit. A simple converter design is presented using lumped parameter techniques before the lumped inductor model is substituted for a transmission line inductor model. The converter establishes the necessary context for chapters 5 and 6 which identify and discuss the process of energy conversion in the inductor of the converter. While many converter topologies are suitable candidates, the overarching approach is to favour simplicity so that the energy conversion aspect of the transmission line inductor model remains priority, rather than the converter topology itself. This applies also to the use of concrete component values, which are chosen to be conceptually representative rather than realistic values for realization of a physical device.

The converter is simulated to demonstrate agreement between the lumped and distributed modelling approaches from the view of the converter output. A discussion explores the significance of the transmission line delay as a design parameter for the experiment. A timing constraint is imposed for the transmission line to limit additional sources of complexity which could confound the description of energy conversion. A reflection diagram is drawn for the transmission line inductor to visualise the wavefronts which result from the switching action of the converter. The reflection diagram is used to construct exact voltage and current waveforms for the inductor at its terminals and serves as the essential modelling tool in the chapters that follow.

4.1 Step-down converter topology

The complexity of a DC-DC power converter increases with larger numbers of semiconductors and energy storage elements [15]. Energy storage elements interact with the source, load, and each other during normal converter operation. These interactions when considered through distributed models are a significant source of complexity. This is the topic of the work by Mofu [18] and is out of the scope of this work.

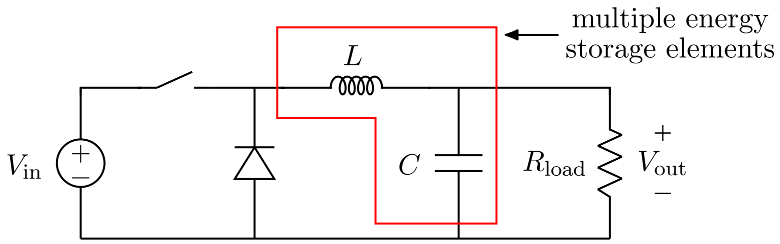

(a) Buck converter circuit

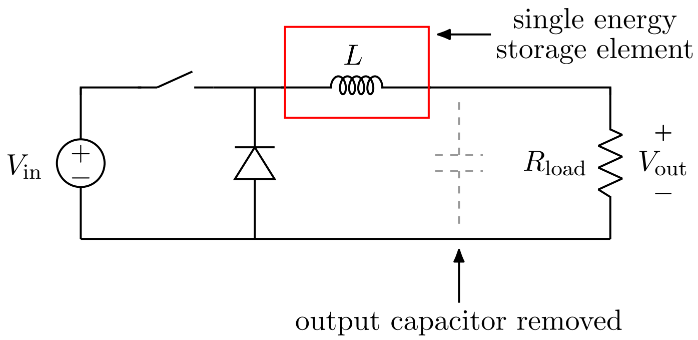

(b) Step-down converter circuit

Figure 4.1: The output capacitor of the buck converter is removed to create the step-down converter

Table 4.1: Step-down converter parameters

Parameter	Symbol	Value
Input voltage	V_{in}	10 V
Output voltage	V_{out}	5 V
Output voltage ripple	ΔV_{out}	0.5 V
Switching frequency	f_{S}	25 kHz
Switching period	T_{S}	40 µs
Duty cycle	D	50 %
Load resistance	R_{load}	50 Ω
Inductance	L_{lumped}	10 mH

Figure 4.1a depicts a classic buck converter circuit with two energy storage elements: an inductor and capacitor. The inductor and load resistor in the buck converter form a first order LR filter for the output of the switching stage. If the time constant of the filter is much smaller than the switching period, the output voltage ripple is small and the output capacitor of the buck converter can be eliminated without significantly compromising the converter operation.

Removing the capacitor results in a circuit with a single energy storage element as shown in figure 4.1b. This new circuit is referred to as a *step-down* converter in this work because it is distinct from the well-known buck converter topology, and it reduces the voltage from input to output. With a single reactive component, only one transmission line substitution is required and the complexities of interacting transmission lines are avoided.

Parameters for the step-down converter are chosen under the assumption that the converter operates in continuous conduction mode with a fixed 50 % duty cycle at 25 kHz. The converter is supplied with 10 V and the current is left as a degree of freedom which varies according to the requirements of the load. The voltage source, switch and diode are modelled as ideal, lossless components as per the assumptions set out in chapter 3. Employing the small ripple approximation technique [4], the appropriate inductor value is determined using (4.1) from the parameters in table 4.1. The theoretical nature of the converter allows for the selection of simple values which are not necessarily realistic choices for a physical circuit.

$$L_{\text{lumped}} = \frac{R_{\text{load}}(1 - D)}{(\Delta V_{\text{out}}/V_{\text{out}})f_S} \tag{4.1}$$

4.2 Distributed inductor model

We proceed to define a transmission line model which can be substituted for the 10 mH lumped inductor and maintain similar converter performance but provide better insight into the internal activity of the inductor. The lumped inductor model in figure 4.2a is substituted for a lossless transmission line terminated in a perfect short circuit to produce figure 4.2b. Suitable transmission line parameters must be calculated, namely the propagation delay τ and the characteristic impedance Z_{line}. The propagation velocity v_p is set to the speed of light as outlined in chapter 3

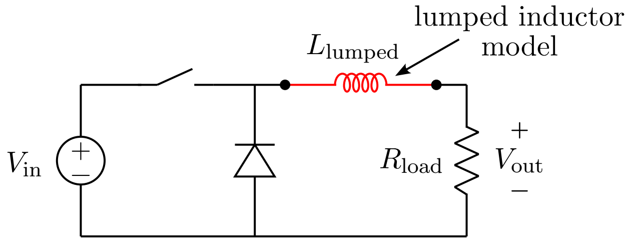

(a) Lumped inductor model

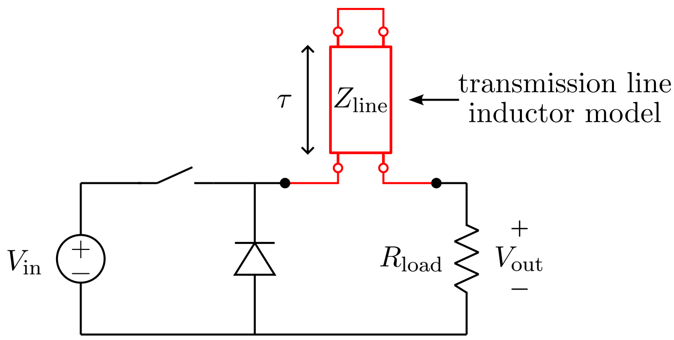

(b) Transmission line inductor model

Figure 4.2: The lumped parameter inductor model is substituted for a transmission line inductor model in the step-down converter

Table 4.2: Transmission line inductor parameters

Parameter	Symbol	Value
Characteristic impedance	Z_{line}	$10\,\text{k}\Omega$
Total inductance	L_{line}	$10\,\text{mH}$
Total capacitance	C_{line}	$100\,\text{pF}$
Propagation delay	τ	$1\,\mu\text{s}$
Propagation velocity	v_p	$3 \times 10^8\,\text{m/s}$

and relates the length of the transmission line to its propagation delay. Due to the extensive use of time domain analysis in this chapter, the propagation delay is used more frequently than the line length unless referring to specific positions in space.

The choice of propagation delay has significant implications for overall converter output. These complexities are covered in further detail in section 4.5. As an initial approach τ is set to $1\,\mu\text{s}$ which is much less than the converter switching period and also cleanly divides into the switching period of $40\,\mu\text{s}$.

To calculate the characteristic impedance of the transmission line, a constraint is imposed that the amount of energy stored in the transmission line U_{line} must equal the energy stored in the lumped inductor model U_{lumped} for a DC current I_{dc}. Equation (4.2) shows that this constraint implies the total inductance of the transmission line L_{line} must be equal to the inductance of the lumped inductor L_{lumped}.

$$\begin{aligned} U_{\text{line}} &= U_{\text{lumped}} \\ \frac{1}{2}L_{\text{line}}(I_{\text{dc}})^2 &= \frac{1}{2}L_{\text{lumped}}(I_{\text{dc}})^2 \end{aligned} \tag{4.2}$$

Applying the constraints produces (4.3) which relates the total transmission line impedance to the lumped inductor and choice of propagation delay. These equations are used to calculate the transmission line inductor parameters in table 4.2.

$$\begin{aligned} L_{\text{line}} &= L_{\text{lumped}} \\ C_{\text{line}} &= \tau^2/L_{\text{lumped}} \\ Z_{\text{line}} &= \sqrt{L_{\text{line}}/C_{\text{line}}} \end{aligned} \tag{4.3}$$

4.3 Converter simulation

The two converter circuits shown in figure 4.2 are simulated in LTspice and compared with respect to output voltages at steady state. The simulation netlist is available in appendix A. The simulation serves to validate the use of the transmission line inductor for the step-down converter with the chosen parameters. The voltage source, diode and switch comprise the supply and switching stages of the converter. For the simulated circuit, these stages are combined and modelled as a single pulsed voltage source so the diode and switch models can be omitted.

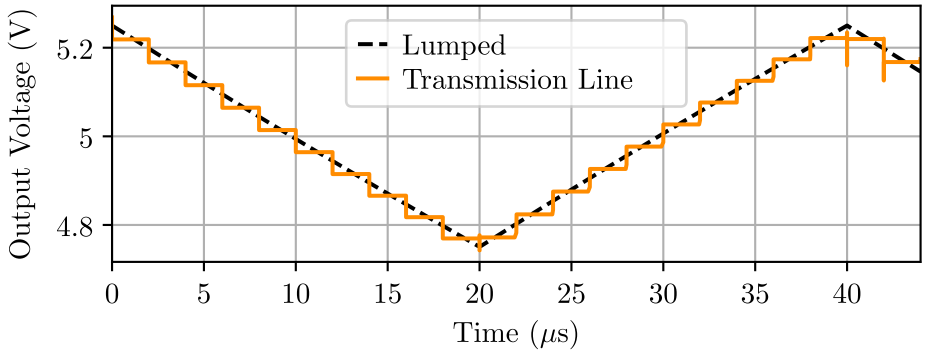

Figure 4.3: Simulated converter output voltage for lumped and transmission line inductor models

4.3.1 Output waveforms

For the converter at steady state, every switching period is identical to the next. The output voltage for the step-down converter with each inductor model is shown in figure 4.3 and conforms to the design specification. The step-down converter with a transmission line inductor shows an output waveform with a staircase pattern which follows the lumped model output. The steps in the converter output waveform are directly attributed to the transmission line inductor model and are a recognisable phenomenon in literature [5], [20].

The overall agreement between output waveforms, despite the differences in modelling approach, is due to the similarity between the terminal behaviour of the inductor models. The use of a transmission line in place of a lumped inductor increases the richness of the inductor model at the cost of increased complexity, which is desirable for this work but perhaps is inappropriate for other applications.

4.3.2 Increased propagation delay

In figure 4.3 the duration of each step in the output voltage waveform is 2 µs, or double the propagation delay τ. However, in figure 4.3 there are many steps which pose a challenge to analyse and present in detail. Thus, a new propagation delay for the transmission line inductor is chosen so that 2 steps occur during charging and discharging, totalling 4 steps in a switching period. Incorporating more steps is an option, but it increases manual analysis effort without providing new insights.

Table 4.3 shows that a change in transmission line delay gives new values for the impedance and total capacitance. All other parameters remain unchanged, including the total inductance due to the constraint imposed on energy storage.

Figure 4.4 shows the output waveform for the step-down converter with the new transmission line delay of 5 µs. While the models are still in agreement, a larger delay results in longer steps with larger changes in voltage for each step. Therefore, the output waveform does not follow to the lumped parameter model as closely as before, although the models are still in agreement overall.

Simulation artefacts described in [9], [18] are visible in figure 4.4 and result from

Table 4.3: Parameters changed for new transmission line delay

Changed parameter	Symbol	Old value	New value
Propagation delay	τ	1 µs	5 µs
Impedance	Z_{line}	10 kΩ	2 kΩ
Total capacitance	C_{line}	100 pF	2.5 nF

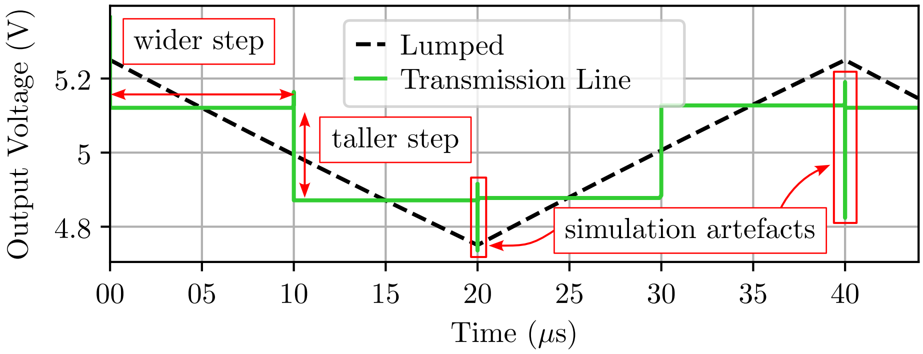

Figure 4.4: Simulated converter output voltage for a propagation delay increased to 5 µs

time-step solver used in the simulation. These artefacts are also present in figure 4.3 but are less discernible due to the shorter step duration. These simulation-specific challenges are not the focus of this work and do not pose a continued problem in subsequent analysis where reflection diagrams are used.

4.3.3 Simulator limitations

The SPICE based simulations typical of the power electronics are not used extensively in this work, primarily because they provide the time-domain terminal behaviour at the ends of the transmission line while the activity within the transmission line remains inaccessible. This is a limitation which stems from the time-based solvers used by circuit simulators.

One workaround would be to divide up the transmission line into many discrete segments by joining shorter transmission lines end-to-end or using a discretised LC network. However, this approach has the risk of amplifying numerical simulation artefacts and introducing a time-step discretization which is a potential source of error [9]. Additionally, we pursue a description of the fundamental mechanism of energy conversion, so reliance on a simulator introduces an undesirable dependency.

4.4 Inductor reflection diagram

The reflection diagram is a well-established tool for analysing transmission lines that has stood the test of time, having been proposed by Bewley in 1931 [21]. The reflection diagram provides an effective solution for extracting the spatial information of the transmission line model. This work makes extensive use of

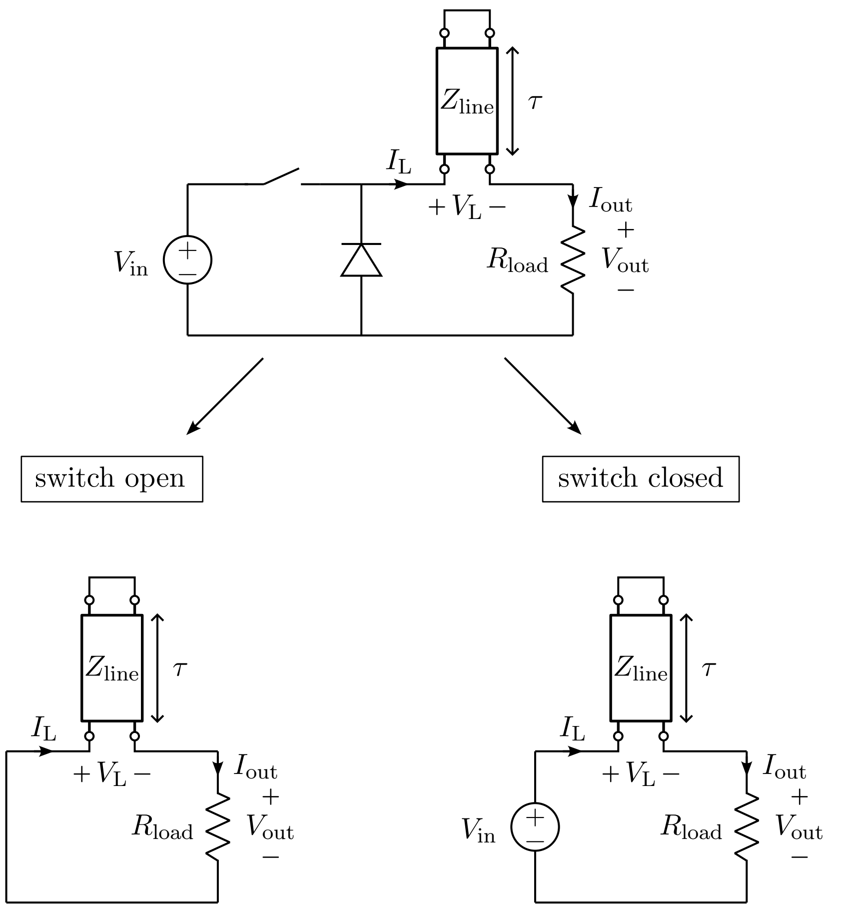

Figure 4.5: Equivalent circuits for the step-down converter based on switch position

reflection diagrams to calculate and visualise variations in voltage and current along the spatial dimension of a transmission line at any point in time.

The step-down converter is simplified to two equivalent circuits based on the switch position as shown in figure 4.5. With the switch open the diode is forward biased, and the transmission line inductor discharges into a load resistor. When the switch is closed, the diode is reverse biased and the transmission line inductor charges from the voltage source via the load resistor. The switching action of the step-down converter continually alternates between these two circuits creating step changes in the boundary conditions at the terminals of the transmission line inductor.

Reflection diagrams generally show the progress of the wavefront assuming that the transmission line has zero initial conditions. However, this is not feasible for the inductor of a converter which may require many switching periods to reach steady state. Instead, a DC offset is specified for the current in the transmission line. Equation (4.4) gives the initial current for the transmission line inductor model based on the small ripple approximation for the start of a discharge cycle and charge cycle. This results in an initial current of 105 mA and 95 mA for the discharge and charge portions respectively.

$$
\begin{aligned}
I_{\text{initial discharge}} &= \frac{V_{\text{out}} + \Delta V_{\text{out}}/2}{R_{\text{load}}} \\
I_{\text{initial charge}} &= \frac{V_{\text{out}} - \Delta V_{\text{out}}/2}{R_{\text{load}}}
\end{aligned}
\tag{4.4}
$$

The equivalent circuits for the converter vary based on switch position, but the impedance seen by a wavefront at the ends of the transmission line is unchanged for the step-down converter circuit. The voltage reflection coefficients are given by (4.5) and apply equally to when the switch is opened or closed. At the transmission line inductor terminals the wavefront is partially reflected and partially absorbed by the load resistor. For the short circuit, the wavefront is totally reflected but with an inverted voltage.

$$
\begin{aligned}
\Gamma_{\text{terminal}} &= \frac{R_{\text{load}} - Z_{\text{line}}}{R_{\text{load}} + Z_{\text{line}}} = -0.95 \\
\Gamma_{\text{short}} &= \frac{0 - Z_{\text{line}}}{0 + Z_{\text{line}}} = -1
\end{aligned}
\tag{4.5}
$$

Figure 4.6 shows the reflection diagram for the transmission line inductor where the time axis grows downward, and the position axis grows to the right. The time axis is marked in multiples of the propagation delay τ. In steady state, the process of charging and discharging the inductor happens in a periodic fashion according to the chosen switching frequency. The wavefront travels back and forth along the length of the transmission line undergoing several reflections. Due to the prior choice of propagation delay, the switching events coincide with the reflection of the wavefront at the terminals of the transmission line. The switching action creates a new wavefront in the transmission line at the same instant the returning wavefront reaches the terminals, causing the arrows of each wavefront in the reflection diagram to be overlaid.

The reflection diagram yields exact waveforms which are not subject to simulation artefacts. Figure 4.7 shows a rotated reflection diagram so that its time axis aligns with the time axis of the current, voltage and power at the terminals of the inductor obtained from the reflection diagram. Step changes in voltage and current waveforms are seen where the wavefront completes a round trip in the transmission line and returns to the terminals at $x = 0$. A round trip is twice as long as the propagation delay so changes in the voltage and current at the terminals occur for even multiples of the propagation delay. When the inductor discharges into the load resistor, the power at the terminals is negative. Similarly, when the inductor charges from the voltage source, the power at the terminals is positive. In all cases the lumped and distributed models show agreement.

The plots of voltage, current and power displayed in figure 4.7 represent the time-domain behaviour of the inductor. However, the transmission line diagram also incorporates a spatial dimension which warrants further in-depth discussion. This is the topic of Chapter 5.

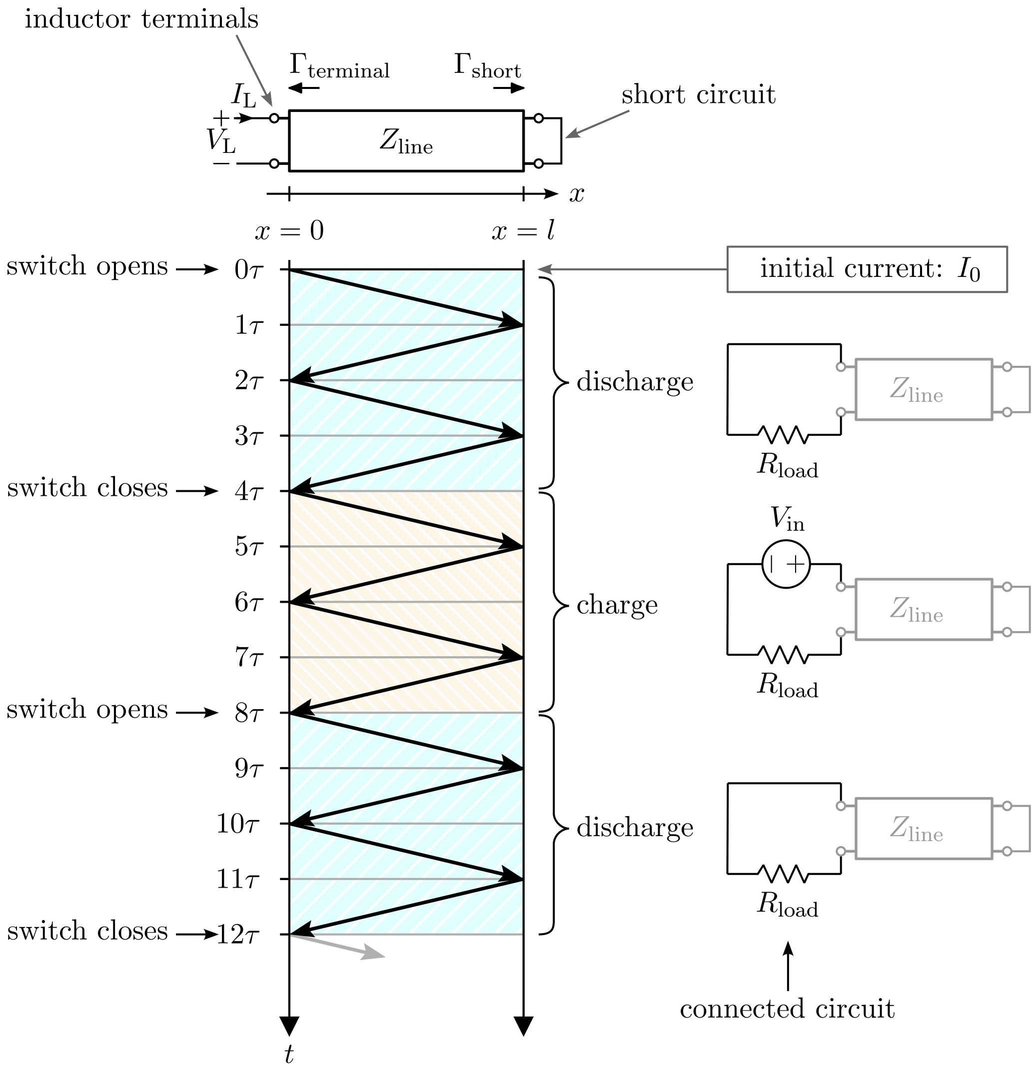

Figure 4.6: Reflection diagram for the transmission line inductor model of the step-down converter at steady state

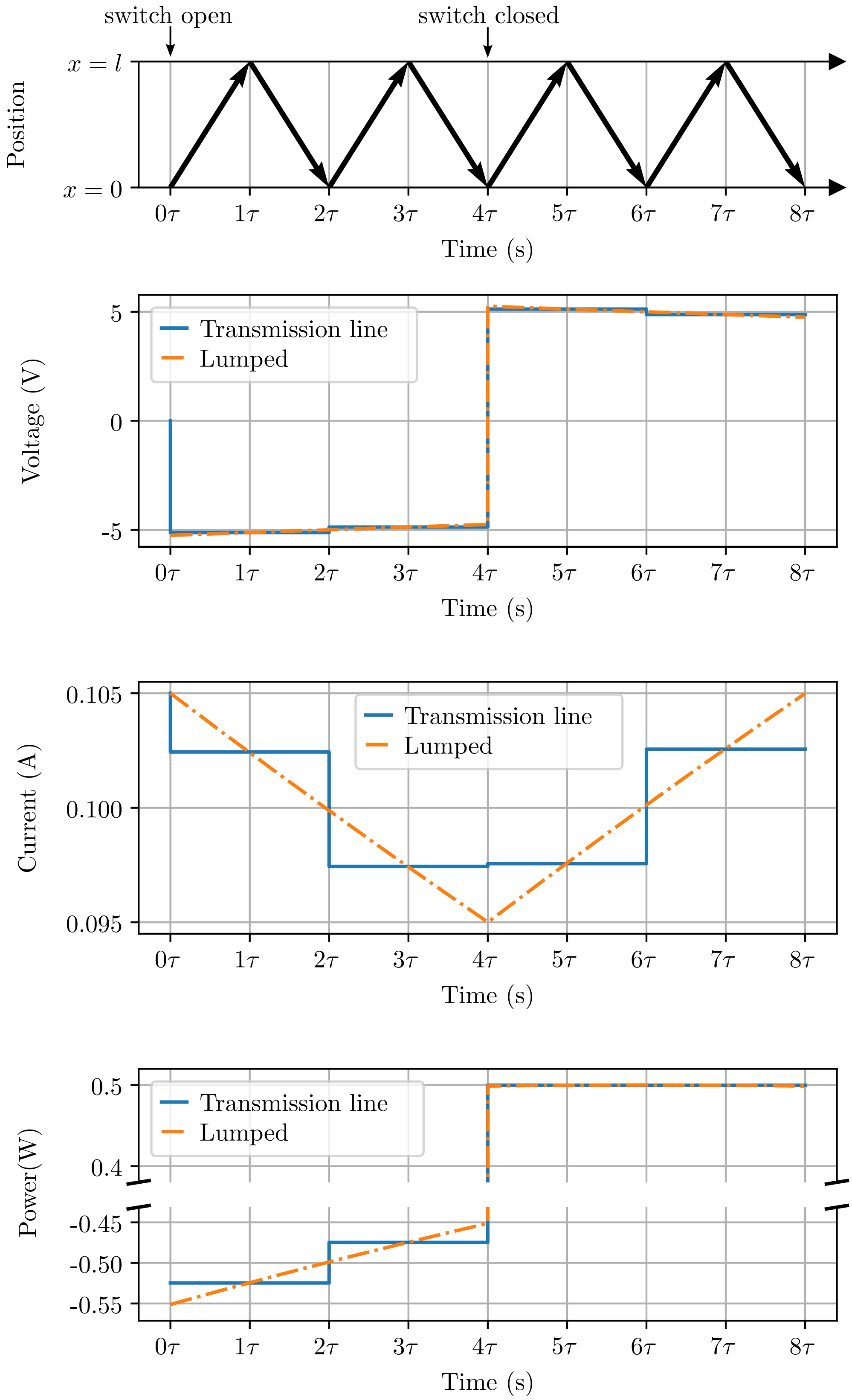

Figure 4.7: Reflection diagram yields waveforms for the terminals of the transmission line inductor over a converter switching period in steady state

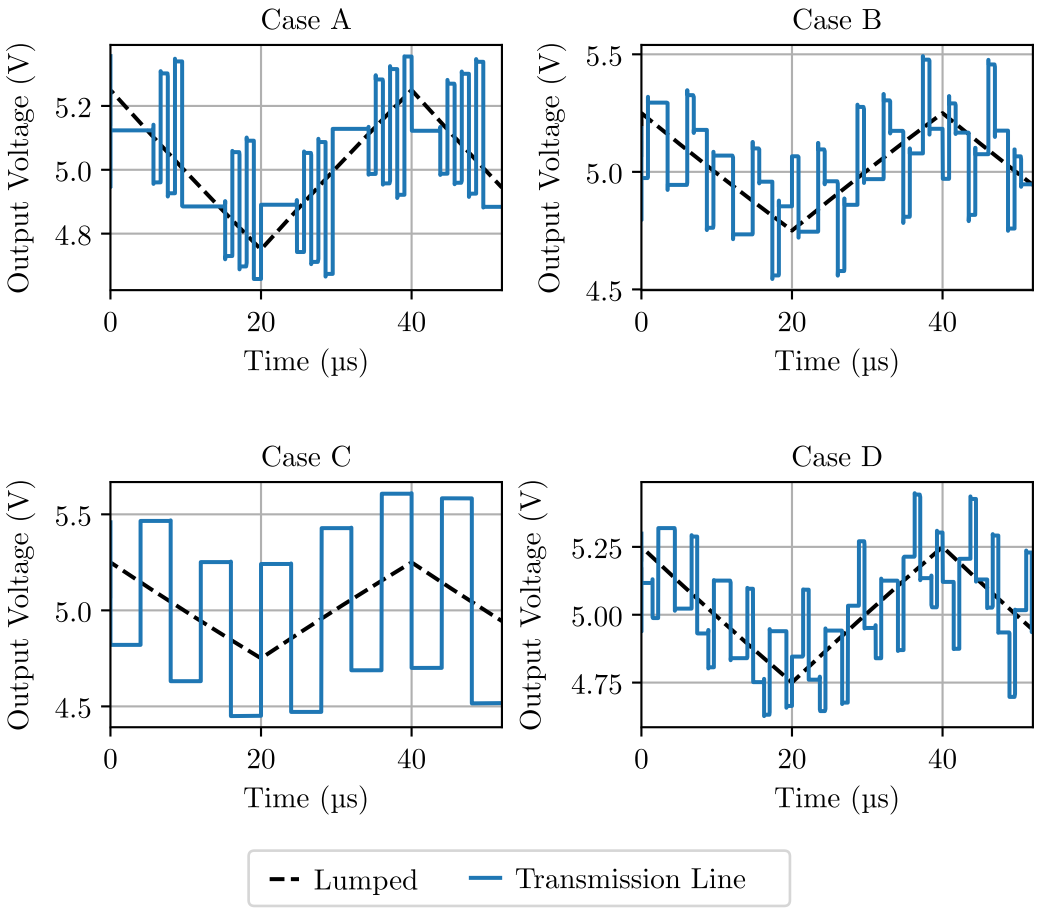

Figure 4.8: Misalignment between switching events and the transmission line propagation delay gives rise to complex output waveforms

4.5 Effect of the propagation delay

Figure 4.8 shows some of the complex patterns that arise in the output voltage waveform of the step-down converter with various values of propagation delay for transmission line inductor model. Similar behaviour is seen in work by Röbenack and Bärnklau [22] where the propagation delay is held fixed but the converter duty cycle is varied. Mofu [18] also identifies this behaviour where two transmission lines interact with different ratios between propagation delays. These complex waveforms arise from a misalignment between an existing wavefront in the transmission line and events which create of new wavefronts. This problem is not normally encountered when using lumped parameter models since they operate in a quasi-static state [20].

In the case of the step-down converter with a single inductor, a new wavefront is introduced into the transmission line for each instance where a switching event occurs out of sync with a returning wavefront as shown in figure 4.9. If the converter's switching period were 3.8τ, a new wavefront would be initiated before the returning wavefront reached the terminals. Figure 4.9 shows the potential for a multiplicity of wavefronts to form in the transmission line. Ultimately these complexities, while valid, obscure the fundamental mechanisms of energy conversion, making it difficult to analyse and interpret. This is a significant source of complexity

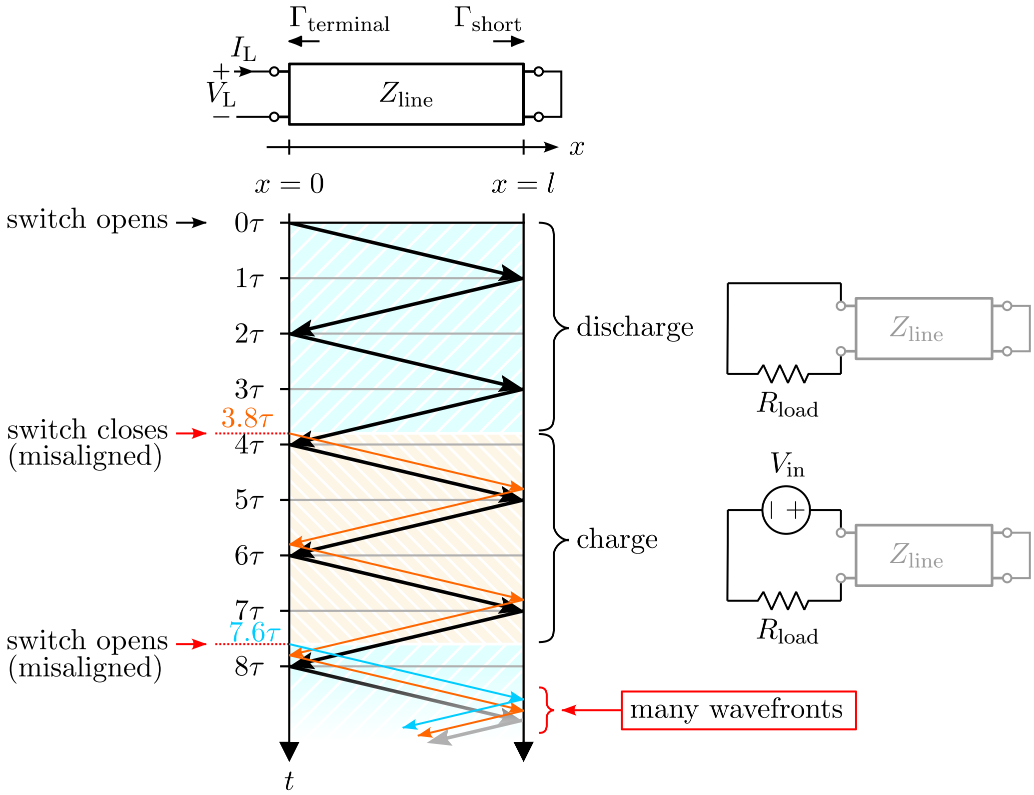

Figure 4.9: Misaligned timing gives rise to new wavefronts inside the transmission line with each switching event

which can be avoided by imposing a timing constraint for the propagation delay of the transmission line inductor.

The converter duty cycle and switching period determine the spacing of switching events. For regularly spaced events, the switching period is set upfront and the duty cycle is held fixed. The values of propagation delay which align with the switching events are expressed by (4.6) where GCF refers to the Greatest Common Factor for real numbers. The natural number k represents the number of round trips which occur. A round trip is twice the delay of the transmission line and is the time needed for a wavefront to leave the terminals, travel down the line, reflect and arrive back at its starting point.

$$\tau = \frac{1}{2k}\mathrm{GCF}\left(DT_{\mathrm{S}}, (1-D)T_{\mathrm{S}}\right) \quad \text{where} \quad k \in \mathbb{N} \tag{4.6}$$

When (4.6) is used, the switching events of the step-down converter coincide with the wavefronts travelling in the transmission line, ensuring that at most one wavefront is present in the transmission line at any time. The value for k is therefore part of the experimental design. Earlier in this chapter, the propagation delay was set to 5 µs and then 1 µs which correspond to $k = 2$ and $k = 10$, respectively.

While the complex behaviour seen in figure 4.8 could occur in physical systems, the constraint applied to the propagation delay is a necessary simplification that allows the mechanism of energy conversion in the transmission line inductor to be identified in chapter 5. The description of the energy conversion mechanism with large numbers of wavefronts is left to future work.

Chapter 5

The wavefront and energy conversion

This chapter considers one of the two equivalent circuits for the step-down converter designed in chapter 4. In the case where the transmission line inductor of the step-down converter discharges into a load resistor, energy at rest purely in the magnetic field of the inductor is made available to the load resistor as a voltage and current because of the energy conversion process within the inductor. This energy conversion process is analysed and described for the transmission line inductor.

Circuit analysis is performed, and a reflection diagram constructed for the transmission line. This reflection diagram describes how the wavefront propagates along the transmission line and its effect on the voltage and current. From the reflection diagram, spatial distributions are developed to show the voltage, current, and instantaneous power along the length of the transmission line. These spatial distributions visually demonstrate the step change associated with the wavefront, including the change in instantaneous power which we call the wavefront power.

These spatial distributions are the basis for further discussion on the location and characteristics of energy conversion within the transmission line. The changes in energy density on either side of the wavefront are used as a means of decomposing the wavefront power into two components: one component for the magnetic field and one for the electric field. The wavefront power components describe the energy conversion process that occurs at the wavefront in relation to the underlying fields, providing insight into the mechanism of the conversion process.

Reflections of the wavefront occur in large numbers under normal operating conditions. The wavefront undergoes reflections at both the ends of the transmission line inductor. The effect of reflections on the energy conversion are discussed by tracking the wavefront power components over several reflections.

5.1 Circuit

The equivalent circuit of the step-down converter as the inductor discharges consists of a transmission line inductor with an initial current and a single load resistor. These conditions are shown in figure 5.1a for a lossless transmission line with

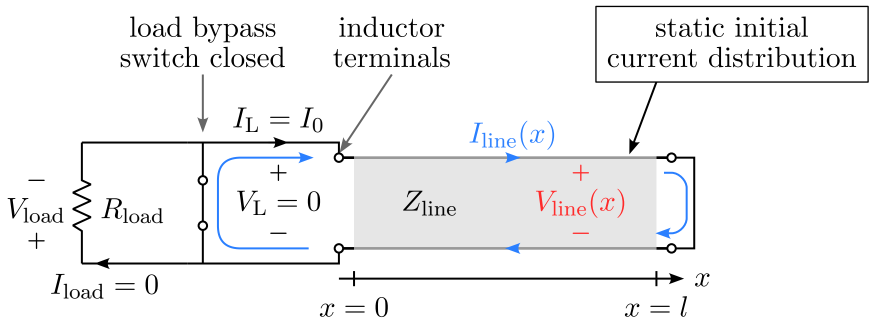

(a) Circuit for initial conditions (bypass switch closed)

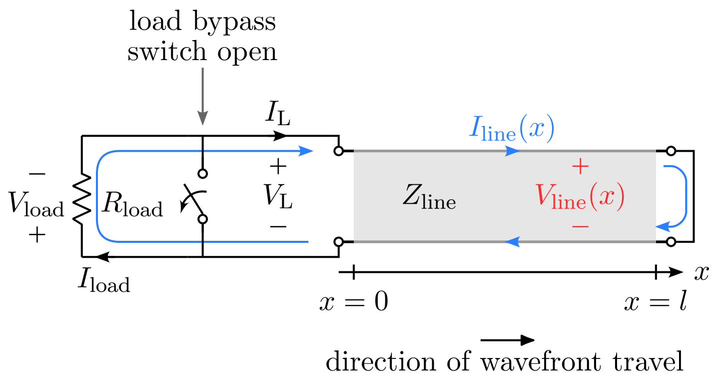

(b) Circuit for analysis (bypass switch open)

Figure 5.1: Transmission line inductor with an initially static current distribution discharges into a load resistor when the load bypass switch opens

Table 5.1: Summary of parameters for the transmission line inductor discharged into a load resistor

Parameter	Symbol	Value
Characteristic impedance	Z_{line}	$2\,\text{k}\Omega$
Propagation delay	τ	$5\,\mu\text{s}$
Propagation velocity	v_p	$3 \times 10^8\,\text{m/s}$
Initial current	I_0	$105\,\text{mA}$
Load resistance	R_{load}	$50\,\Omega$
Voltage reflection coefficient (terminal)	Γ_{terminal}	-0.95
Voltage reflection coefficient (short)	Γ_{short}	-1

characteristic impedance Z_{line} connected to a resistor R_{load} and shorted at the other end. The propagation velocity of the line v_p is fixed at the speed of light as per the assumption set out in chapter 3. The transmission line has a length l, propagation delay τ and initial current I_0. The initial current is statically distributed along the length of the transmission line and there is zero initial voltage. The values for these parameters are obtained for the step-down converter in chapter 4 and reproduced in table 5.1 for ease of reference.

The port of the transmission line connected to the rest of the circuit is described as the *terminals* of the transmission line inductor because it corresponds to the terminals of the lumped parameter inductor which was substituted. The other port of the transmission line is shorted to complete the model of the transmission line inductor. Position $x = 0$ is assigned to the terminals and $x = l$ to the short circuit.

Initially, the load resistor is bypassed by an ideal switch to facilitate the analysis of initial conditions in the circuit diagram. The voltage and current of the terminals are denoted V_{L} and I_{L}. The voltage and current of the resistor are denoted by V_{load} and I_{load}. The bypass switch is opened instantaneously at time $t = 0\,\text{s}$, leaving a single path for the current to flow through the resistor.

Figure 5.1b shows the circuit for $t > 0\,\text{s}$ where a new current and voltage are established at the terminals of the transmission line as a result of opening the bypass switch. The voltage and current in the transmission line vary according to position. Opening the switch causes an instantaneous change in the voltage and current at the terminals. For the instant immediately after the switch opens, the current at the terminal I_{L} is different from that in the remainder of the line, which remains at the initial current I_0. Similarly, the voltage at the terminals V_{L} instantaneously changes while the rest of the line remains at the initial voltage of $0\,\text{V}$.

We use the term *spatial distribution* to describe any quantity in the transmission line that varies as a function of position x. Therefore, the transmission line voltage V_{line} and current I_{line} are spatial distributions with polarities defined in figure 5.1. The terminal voltage and current are therefore the voltage and current at position $x = 0$ as expressed in (5.1).

$$
\begin{aligned}
V_{\mathrm{L}} &= V_{\mathrm{line}}(x)\Big|_{x=0} \\
I_{\mathrm{L}} &= I_{\mathrm{line}}(x)\Big|_{x=0}
\end{aligned}
\tag{5.1}
$$

5.2 Reflection diagram

Figure 5.2 shows the reflection diagram and spatial distributions for the transmission line inductor. The horizontal axis represents the length of the transmission line in meters and is aligned across the charts. The vertical axis represents the amplitude of the voltage, current and instantaneous power at each position.

Under the assumption of ideal diode and switch models, when the switch is opened, the voltage and current at the terminals change instantaneously producing a wavefront in the transmission line. The reflection diagram shows that the wavefront propagates along the transmission line, starting at the terminals and directed towards the short circuit. While a typical reflection diagram may show many reflections, figure 5.2 focuses solely on the initial wavefront generated by the switching event. For clarity, in this work the term reflection is used to describe the process that a wavefront undergoes upon reaching the ends of a transmission line which causes, among other things, a reversal in direction of travel.

The wavefront in the transmission line reaches the short-circuited terminals in τ seconds. The analysis that follows from this reflection diagram is concentrated on the time period of interest $0 < t < \tau$. The wavefront voltage $V_{\mathrm{wavefront}}$ and current $I_{\mathrm{wavefront}}$ are related by the characteristic impedance of the transmission line in (5.2) and share the same polarity as $V_{\mathrm{line}}(x)$ and $I_{\mathrm{line}}(x)$.

$$
\boxed{I_{\mathrm{wavefront}} = \frac{V_{\mathrm{wavefront}}}{Z_{\mathrm{line}}}}
\tag{5.2}
$$

The wavefront voltage and current are also equal to the initial value in the transmission line less the value at the terminals.

$$
\begin{aligned}
V_{\mathrm{wavefront}} &= V_{\mathrm{L}} \\
I_{\mathrm{wavefront}} &= I_{\mathrm{L}} - I_0
\end{aligned}
$$

Performing regular circuit analysis with KVL, KCL and Ohm's law produces the relations:

$$
\begin{aligned}
V_{\mathrm{L}} &= -V_{\mathrm{load}} \\
I_{\mathrm{L}} &= I_{\mathrm{load}} \\
R_{\mathrm{load}} &= V_{\mathrm{load}}/I_{\mathrm{load}}
\end{aligned}
$$

The system of equations is solved simultaneously to produce (5.3) and (5.4) which give the voltage and current for the wavefront and terminals in terms of the initial conditions and circuit parameters. Equations (5.3) and (5.4) show the response

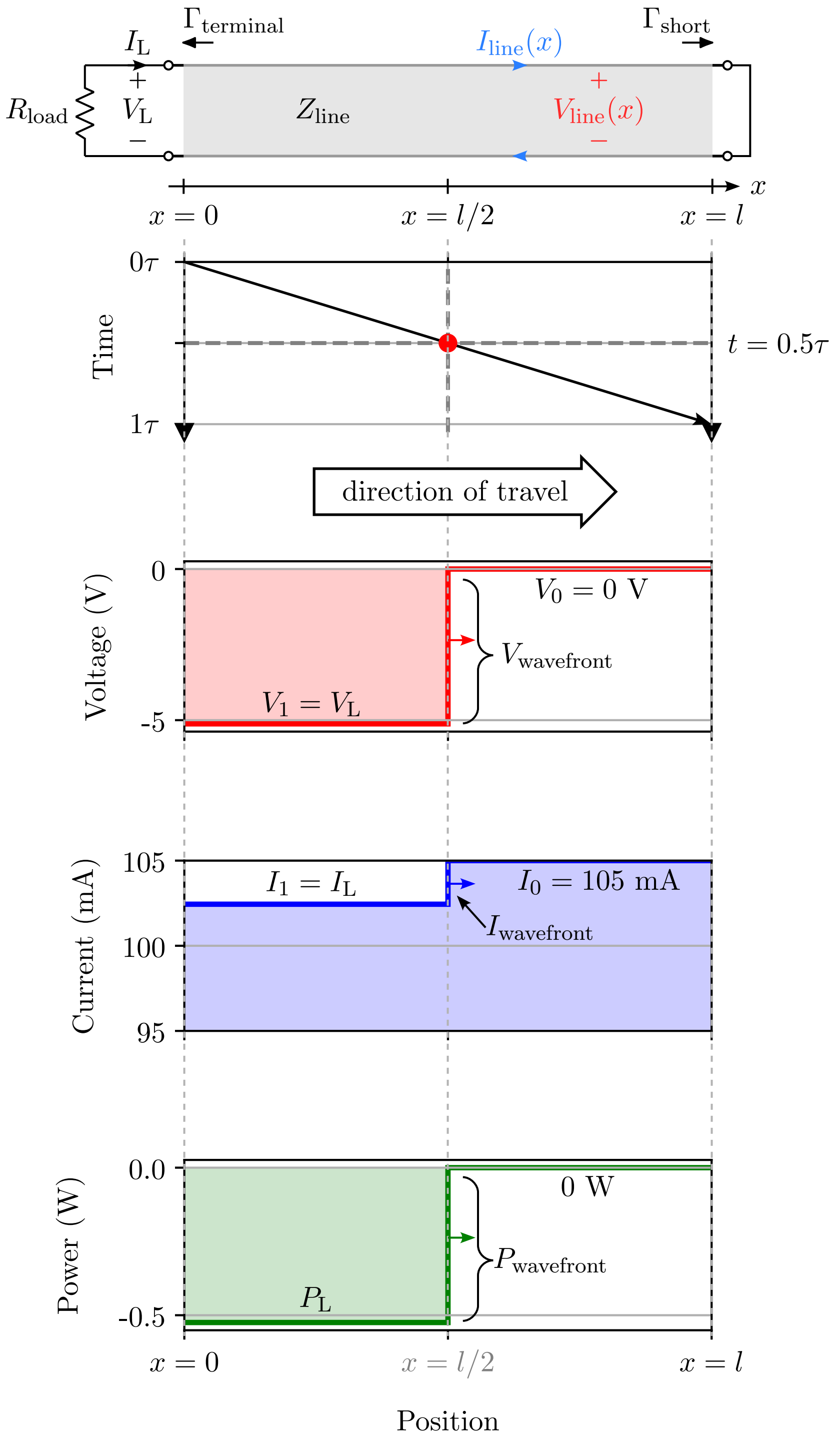

Figure 5.2: Reflection diagram and spatial distribution of voltage, current and instantaneous power for the initial passage of the wavefront at $t = 0.5\tau$

to the instantaneous switching event depends solely on the impedances Z_{line} and R_{load}, as well as on the initial current I_0.

$$\begin{aligned} I_{\text{wavefront}} &= -\frac{R_{\text{load}} I_0}{R_{\text{load}} + Z_{\text{line}}} \\ V_{\text{wavefront}} &= -\frac{R_{\text{load}} Z_{\text{line}} I_0}{R_{\text{load}} + Z_{\text{line}}} \end{aligned} \tag{5.3}$$

$$\begin{aligned} I_{\text{L}} &= \frac{Z_{\text{line}} I_0}{R_{\text{load}} + Z_{\text{line}}} \\ V_{\text{L}} &= -\frac{R_{\text{load}} Z_{\text{line}} I_0}{R_{\text{load}} + Z_{\text{line}}} \end{aligned} \tag{5.4}$$

In figure 5.2 there is a visible step in the amplitude of voltage and current distributions which corresponds to the wavefront. The total current behind the wavefront will drop from its initial value of 105 mA to 102.5 mA. There is a voltage of −5.12 V inside the inductor following the wavefront which was not present before. Thus, it is clear from the spatial distribution that the energy conversion process in a transmission line inductor produces a voltage from energy at rest in the magnetic field.

The instantaneous power in the transmission line is the product of the current and voltage distributions. The instantaneous power distribution describes the flow of energy at each position. The instantaneous power increases in magnitude behind the wavefront. And is the subject of further discussion in the next section.

5.3 Spatial distribution of power

Conventional circuit analysis of a lumped parameter inductor will yield the power at the inductor terminals. The spatial distribution of power in the transmission line inductor provides key insight into the action of the wavefront on the stored energy within inductor. The instantaneous power distribution from figure 5.2 is reproduced

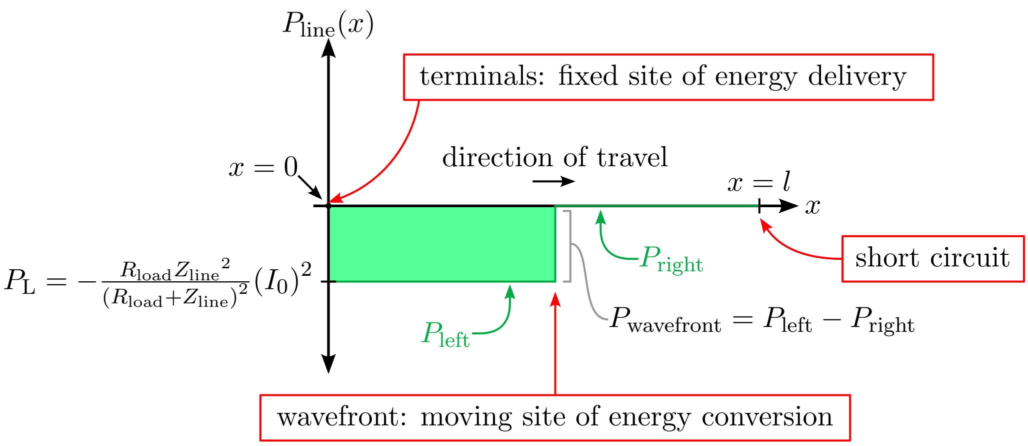

Figure 5.3: Instantaneous power distribution for the initial passage of the wavefront in the transmission line inductor

in figure 5.3 and annotated. The terminals of the transmission line are at position $x = 0$ and the short circuit is at position $x = l$. The wavefront propagates towards the right but has not yet reached the short circuit at the end of the transmission line.

The region behind the wavefront, to the left of figure 5.3, has a constant power distribution equal to the power at the terminals P_L. The region ahead of the wavefront, to the right of figure 5.3, has zero power distribution because energy is initially at rest within the inductor.

5.3.1 Wavefront power

The wavefront is an effect that moves in time and space. The position of the wavefront coincides with a step change in the instantaneous power distribution along the length of the transmission line which we call the *wavefront power*. The wavefront power in the transmission line is defined in (5.5) as the power immediately to the left of the wavefront P_{left} less the power immediately to the right of the wavefront P_{right}. It is important to note that the wavefront power is not the product of the wavefront voltage $V_{\text{wavefront}}$ and current $I_{\text{wavefront}}$.

$$P_{\text{wavefront}} = P_{\text{left}} - P_{\text{right}} \tag{5.5}$$

For the power distribution in figure 5.3, the wavefront power is equal to the power at the terminals of the transmission line P_L. The wavefront power can be expressed in terms of the line impedance, load resistance and initial current in (5.6).

$$P_{\text{wavefront}} = -\frac{R_{\text{load}} {Z_{\text{line}}}^2}{(R_{\text{load}} + Z_{\text{line}})^2} (I_0)^2 \tag{5.6}$$

The wavefront power describes the flow of energy directed along the length of the transmission line due to the presence of the wavefront. Since only the change in instantaneous power is considered, pre-existing flows of energy due to initial conditions or other wavefront are excluded from the wavefront power.

The wavefront power follows a passive sign convention due to the polarities defined in figure 5.1 for $V_{\text{line}}(x)$ and $I_{\text{line}}(x)$. The wavefront power is positive when energy flows left to right in figure 5.3 and negative when the flow is directed right to left. When the transmission line inductor discharges into the load resistor, the flow of energy is directed to the terminals at the left of the transmission line, so the wavefront power is negative. For the case of a transmission line inductor with a single wavefront and zero initial power distribution, the wavefront power for that single wavefront will equal the power at the terminals of the transmission line. This is a result which is frequently referenced in discussions hereafter.

5.3.2 Energy conversion at the wavefront

The source of stored energy in the transmission line inductor is purely the magnetic field described by the initial current. The instantaneous power distribution ahead of the wavefront is zero so the stored energy is initially at rest. Behind the wavefront, the instantaneous power is non-zero, so energy is in motion. This suggests that the wavefront is the mechanism responsible for energy conversion. The energy put into motion at the wavefront is conveyed to the terminals where it is delivered to the load resistor. A continuous supply of energy at the terminals made available as the wavefront travels through the transmission line encountering more stored energy. If energy conversion occurs at the wavefront, after some time it must occur at every position within the transmission line because the wavefront is constantly moving.

5.4 Energy density

The wavefront also accompanies a change in the energy density along the transmission line. We discuss the energy density around the wavefront because it provides insight into the action of the wavefront which we later use to derive wavefront power components. A transmission line model will store energy in a magnetic field and electric field according to it's distributed inductance L' and capacitance C', respectively [20]. Distributed inductance and capacitance in a one-dimensional transmission line are measured per-unit length, so the energy density can be obtained at any position in the transmission line in units of Joules per meter. The magnetic field energy density d_H and electric field energy density d_E are calculated from the current I and voltage V at position x using (5.7).

$$\begin{aligned} d_H(x) &= \frac{1}{2}L'(I(x))^2 \\ d_E(x) &= \frac{1}{2}C'(V(x))^2 \end{aligned} \tag{5.7}$$

Using the fundamental transmission line relations from chapter 3 the energy density can also be expressed in terms of the characteristic impedance Z_{line} and propagation velocity v_p as shown in (5.8a) and (5.8b), respectively. The formulation of density in terms of impedance is favoured in subsequent discussions in this work. A high impedance transmission line like an inductor will have a large magnetic field energy density and a small electric field energy density.

$$\boxed{d_H = \frac{Z_{\text{line}}}{2v_p}I^2} \tag{5.8a}$$

$$\boxed{d_E = \frac{1}{2v_p Z_{\text{line}}}V^2} \tag{5.8b}$$

5.4.1 Initial energy density

The energy densities in the transmission line prior to opening the switch are calculated according to (5.9) using the initial conditions for current and voltage from figure 5.1a. The absence of an initial voltage results in an electric field energy density of 0 J/m. The initial energy of the system is uniformly distributed in the magnetic field of the transmission line.

$$\begin{aligned} d_{H0} &= \frac{Z_{\text{line}}}{2v_p}(I_0)^2 \\ d_{E0} &= 0 \end{aligned} \tag{5.9}$$

The transmission line inductor with a characteristic impedance of $2\,\text{k}\Omega$ and a propagation velocity of 3×10^8 m/s has an initial magnetic field energy density of 36.75 nJ/m when the current is 105 mA.

$$d_{H0} = \frac{(2\,\text{k}\Omega) \cdot (105\,\text{mA})^2}{2 \cdot (3 \times 10^8\,\text{m/s})} = 36.75\,\text{nJ/m}$$

5.4.2 Energy density behind the wavefront

As the wavefront propagates through the transmission line, it modifies the current and voltage in the region swept by the wavefront. If the current and voltage change then the energy densities will also change according to (5.8). Figure 5.4 shows how the density behind the wavefront decreases for the magnetic field but increases for the electric field. The new energy densities for the region behind the line are shown (5.10).

$$\begin{aligned} d_{H1} &= \frac{Z_{\text{line}}}{2v_p}\left(\frac{Z_{\text{line}}}{R_{\text{load}} + Z_{\text{line}}}\right)^2 (I_0)^2 \\ d_{E1} &= \frac{1}{2v_p Z_{\text{line}}}\left(\frac{R_{\text{load}} Z_{\text{line}}}{R_{\text{load}} + Z_{\text{line}}}\right)^2 (I_0)^2 \end{aligned} \tag{5.10}$$

Note that the electric field energy density d_{E1} is now non-zero where previously it was zero. This means that energy which was previously stored in the magnetic field has now been transferred into the electric field thereby increasing the energy density in the portion of the transmission line that was swept by the wavefront. This behaviour is evidence of energy conversion and links the wavefront to the change in energy distribution of the transmission line.

The change in energy density that accompanies the wavefront is the initial energy density (5.9) less the energy density behind the wavefront (5.10).

$$\begin{aligned} \Delta d_H = d_{H1} - d_{H0} &= \frac{Z_{\text{line}}}{2v_p}({I_1}^2 - {I_0}^2) \\ \Delta d_E = d_{E1} - d_{E0} &= \frac{1}{2v_p Z_{\text{line}}}({V_1}^2 - {V_0}^2) \end{aligned} \tag{5.11}$$

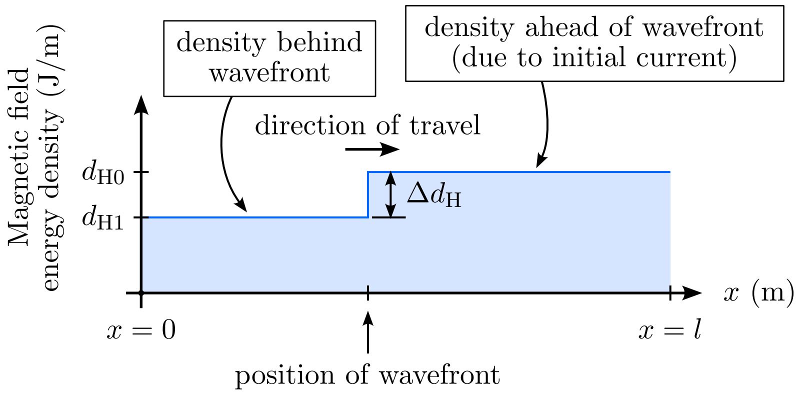

(a) Magnetic field energy density distribution

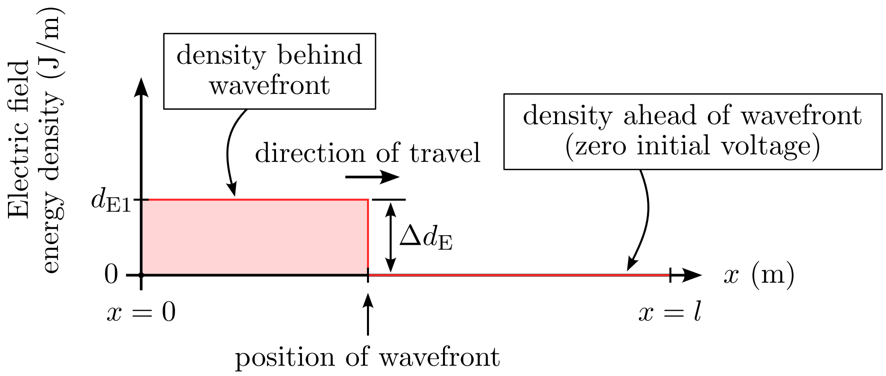

(b) Electric field energy density distribution

Figure 5.4: Energy density distributions in the transmission line for the wavefront travelling from the terminals towards the short circuit

The changes in energy density are labelled in figure 5.4. The reduction in current and gain in voltage at the wavefront corresponds to a negative change in energy density for the magnetic field and a positive change in energy density for the electric field.

5.5 Wavefront power components

The wavefront power defined earlier describes the rate at which energy flows along the length of the transmission line at the position of the wavefront. But this energy is apportioned differently between the magnetic and electric fields. The wavefront power components are proposed as a means to describe the energy conversion process in terms of the action of the wavefront on the underlying fields of the transmission line. The objective is to express the wavefront power as the sum of a magnetic field component p_H and electric field component p_E as shown in (5.12).

$$P_{\text{wavefront}} = \overbrace{p_H}^{\text{magnetic field component}} + \underbrace{p_E}_{\text{electric field component}} \tag{5.12}$$

The electric and magnetic field each have an associated energy density, which is a natural fit for decomposing a single the wavefront power into components. Figure 5.5 shows a generic energy density distribution at time t_0 and later at time t_1. A region of length Δx is defined to the right of the wavefront at t_0. The wavefront travels the distance Δx at a constant propagation velocity v_p, reaching the end of the region at time t_1. A duration of Δt has elapsed between the distributions. The amount of energy stored in the region has changed by $\Delta d \Delta x$.

The wavefront in the transmission line simultaneously changes the energy density distribution of both the magnetic and electric fields as per figure 5.4. The total change in energy for the transmission line in the region is the combined effect of the changes in the electric and magnetic field.

The amount of energy stored in the region can also be expressed in terms of the wavefront power acting for duration Δt. Thus, (5.13) is obtained by conservation of energy.

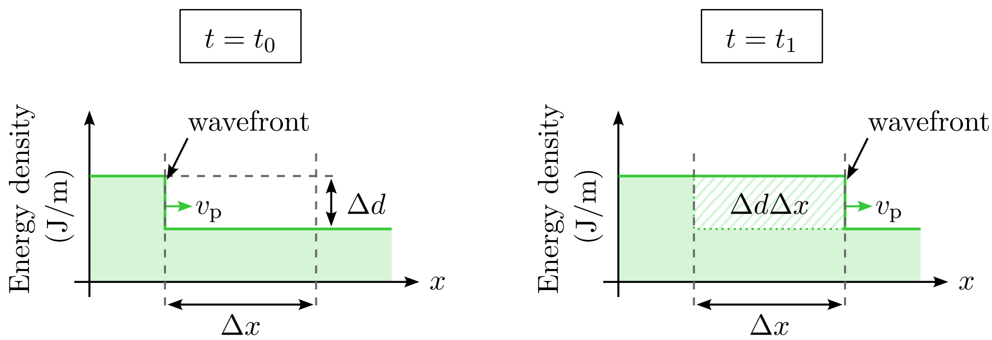

Figure 5.5: A wavefront travelling at a constant propagation velocity changes the energy density distribution in the transmission line

$$\underbrace{P_{\text{wavefront}}\Delta t}_{\text{total energy}} = \overbrace{\Delta d_H \Delta x}^{\text{magnetic field energy}} + \underbrace{\Delta d_E \Delta x}_{\text{electric field energy}} \tag{5.13}$$

The distance travelled by the wavefront and the elapsed time are related by the propagation velocity:

$$v_p = \frac{\Delta x}{\Delta t}$$

Rearranging (5.13) and substituting the propagation velocity gives the wavefront power in the desired form as the sum of an electric and magnetic field component.

$$\begin{aligned} P_{\text{wavefront}} &= \frac{\Delta d_H \Delta x}{\Delta t} + \frac{\Delta d_E \Delta x}{\Delta t} \\ &= \underbrace{v_p \Delta d_H}_{p_H} + \underbrace{v_p \Delta d_E}_{p_E} \end{aligned} \tag{5.14}$$

The power components of the wavefront for the magnetic and electric fields are defined in (5.15a) and (5.15b) respectively. The magnetic field power component is the change in magnetic field energy density multiplied by the propagation velocity. Similarly, the electric field power component is the change in electric field energy density multiplied by the propagation velocity. These are an important result which is used extensively in subsequent work.

$$\boxed{p_H \equiv v_p \Delta d_H} \tag{5.15a}$$

$$\boxed{p_E \equiv v_p \Delta d_E} \tag{5.15b}$$

One benefit of power components for describing the action of the wavefront is that they have common units so can be directly compared unlike voltage and current distributions. Applying dimensional analysis confirms that these power components have units consistent with a power:

$$\text{m/s} \times \text{J/m} = \text{J/s}$$

The power components in (5.15) are not powers in the regular sense like those obtained from circuit analysis by the multiplication of voltage and current. To emphasise their unusual origin, in this work power components are specified in units of Joules per second rather than Watts. Where we do use Watts for units of power, this will correspond to the regular power found on a circuit diagram.

This method of power components bears some resemblance to the work by Ferreira using Poynting vector [6], [11]. Ferreira acknowledges that an approach using Poynting vector is cumbersome and constrains his discussion only to the qualitative aspects of Poynting vector for power electronics. The power components provide a means to integrate the insights from underlying fields without directly dealing with

Poynting vector. The power components in (5.14) could be reformulated in terms of Poynting vector, but this would introduce additional complexity with limited benefit.

Due to the timing constraints imposed in this work, there is at most one wavefront in the transmission line at any time. The case where multiple wavefronts coexist in a transmission line is beyond the scope of this work. However, it should be noted that the transmission line can be segmented into regions around each wavefront according to the energy distributions and the power components computed for each wavefront.

5.5.1 Calculating power components

In conventional circuit analysis, power is computed by multiplying the current and voltage. However, that power quantity merges the behaviour of the magnetic and electric fields into a single value which makes a description of energy conversion difficult. Using (5.15) to decompose the transmission line power into its components facilitates insight into the nature of the underlying energy which is necessary to discuss the mechanism of energy conversion at the wavefront. Combining (5.11) and (5.15) gives the power components in terms of the current and voltage surrounding the wavefront.

$$\begin{aligned} p_H &= \frac{Z_{\text{line}}}{2}({I_1}^2 - {I_0}^2) \\ p_E &= \frac{1}{2Z_{\text{line}}}({V_1}^2 - {V_0}^2) \end{aligned} \tag{5.16}$$

The values of voltage V_1 and current I_1 are affected by the choice of load resistance, so the power components can also be expressed in terms of the load resistance as shown in (5.17). However, we prefer to use the form in (5.16) as this lends itself better to scaling this discussion to multiple reflections of the wavefront.

$$\begin{aligned} p_H &= -\frac{R_{\text{load}} Z_{\text{line}}(R_{\text{load}} + 2Z_{\text{line}})}{2(R_{\text{load}} + Z_{\text{line}})^2}(I_0)^2 \\ p_E &= \frac{(R_{\text{load}})^2 Z_{\text{line}}}{2(R_{\text{load}} + Z_{\text{line}})^2}(I_0)^2 \end{aligned} \tag{5.17}$$

Consider the wavefront power components for the transmission line inductor of the step-down converter that gave rise to the voltage and current distributions seen earlier in figure 5.2. Substituting the voltage and currents on either side of the wavefront from these distributions into (5.16) gives the wavefront power and components in figure 5.6.

The passive sign convention used when defining the current and voltage polarities aids in the interpretation of power components in figure 5.6. The magnetic field power component is negative and therefore the magnetic field supplies energy at the wavefront. On the other hand, the electric field component is positive, so the electric field is absorbing energy from the magnetic field.

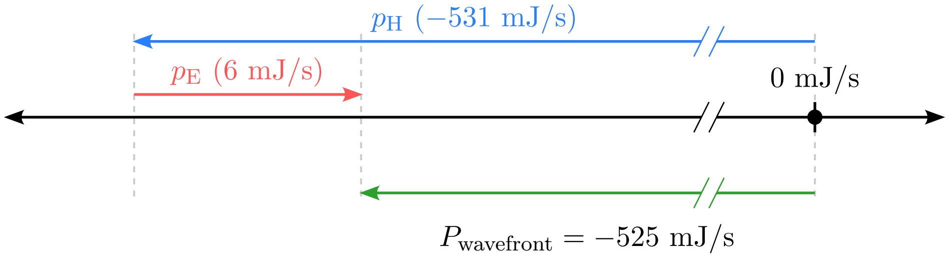

Figure 5.6: The wavefront power and its components where $0 < t < \tau$

The magnetic field power component is -531 mJ/s which is significantly greater in magnitude than the 6 mJ/s of the electric field component. Together the power components give the wavefront power of -525 mJ/s. Recall that the wavefront power is equal to the power at the terminals of the transmission line and thus the load resistor will dissipate energy at a rate of 525 mJ/s. Through straightforward circuit analysis it is verified that the load resistor indeed has a power of 525 mW. The conservation of power gives confidence that the approach of power components is valid.

From the perspective of wavefront power components, it appears that the wavefront extracts energy from the magnetic field for delivery at the terminals and, as a consequence, redistributes energy between the two fields. The magnetic field power component of -531 mJ/s is 6 mJ/s greater in magnitude than the wavefront power of -525 mJ/s because the magnetic field also supplies the 6 mJ/s of energy to the electric field.

5.5.2 Action of the wavefront

The voltage and current distributions show that the transmission line inductor produces the voltage and current at its terminals from energy stored purely in the magnetic field. The instantaneous power distribution shows that the wavefront is the site of energy conversion where energy initially at rest is put into motion. The magnetic field power component shows the wavefront causes the magnetic field of the inductor to supply energy at a greater rate than that which is conveyed down the line and delivered to the load resistor. The difference between these rates accounts for the energy which is deposited in the electric field at the wavefront as part of the conversion process. The energy in excess of the load requirement remains in the fields of the lossless transmission line between the site of the wavefront and the site of the terminals.

The wavefront appears to be the location and mechanism of energy conversion in the transmission line inductor. For lumped parameter models the wavefront is not visible and so the mechanism of energy conversion is hidden. The power at the terminals of the transmission line model is delivered from a fixed position, while the wavefront is mobile within the transmission line. Therefore, the site of energy conversion sweeps the entire length of the transmission line as the wavefront propagates.

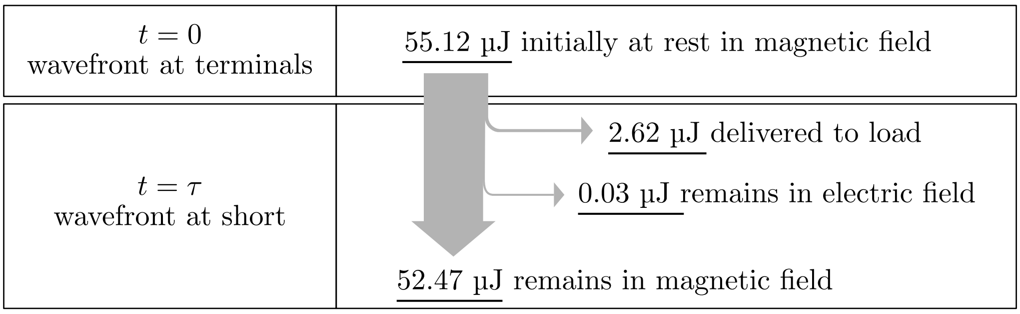

Figure 5.7: Division of energy in the transmission line inductor when the wavefront first reaches the end of the transmission line

Figure 5.7 shows how the initial energy at rest in the magnetic field of the inductor is divided at the time $t = \tau$ when the wavefront reaches the end of the transmission line. The widths of the arrows are proportional to the amount of energy, although the arrow for the electric field component is enlarged for visibility. Notably, the inductor now stores energy in its electric field, a result which is not predicted by the lumped inductor model.

Ferreira's [6], [11] work on transmission line modelling for circuit interconnects concludes that a deviation in the ratio of voltage to current in a transmission line from its characteristic impedance leads to deposition of energy along the transmission line thereby reducing the instantaneous power delivered to the load. Ferreira's approach can be applied to the results in this work by viewing the portion of the transmission line inductor between the terminals and the wavefront as an interconnect. The length of this interconnect grows or shrinks with the position the wavefront.

In the case of the transmission line inductor for the step-down converter, the voltage-to-current ratio is always significantly less that the $2\,\mathrm{k\Omega}$ characteristic impedance. According to Ferreira, the deviation between these quantities predicts that energy is deposited along the transmission line between the terminals and the wavefront. Accordingly, the instantaneous power delivered to the load will be less than the power extracted from the source. The source is the magnetic field immediately prior to the wavefront in the case of a transmission line inductor. Thus, the transmission line inductor provides the source of energy, the conditions for wavefront propagation, and the interconnect which conveys the outputs of the energy conversion process to the terminals.

5.6 Wavefront reflections

The transmission line is of finite length, so the wavefront must ultimately encounter the short circuit at the end of the transmission line and undergo a reflection. The reflection alters the action of the wavefront giving rise to different wavefront power components.

5.6.1 First reflection

Figure 5.8 shows the reflection diagram and corresponding voltage, current, and instantaneous power distributions following the first reflection of the wavefront in the transmission line. The outgoing wavefront has reflected at the short circuit and is returning towards the terminals. Again the total voltage and current distributions are obtained by summing up the initial conditions and the contribution of all prior waves in the reflection diagram.

The voltage reflection coefficient of the short circuit is -1, so the reflection sets up a returning voltage wave with the inverted voltage to the forward travelling wave. Therefore, the total voltage collapses to zero. The reflection also sets up a returning current wave with the same polarity as the forward travelling wave causing the total current in the line to again drop following the wavefront.

The load resistor will see the same power for the full duration of the round trip regardless of the reflection of the wavefront. The instantaneous power distribution shows the power to the right of the wavefront is again zero while the power to the left is the same as before the reflection occurred, so the wavefront power is unchanged. Again the wavefront power is decomposed into components according to the new voltage and current distributions:

$$\begin{aligned} p_H &= \frac{Z_{\text{line}}}{2}({I_2}^2 - {I_1}^2) \\ p_E &= \frac{1}{2Z_{\text{line}}}({V_2}^2 - {V_1}^2) \end{aligned}$$

More generally, (5.18) shows the power components indexed in terms of n, where n represents the number of reflections that the wavefront has undergone. Where $n = 0$, the wavefront exists in the line but has yet to undergo any reflections as discussed previously.

$$\begin{aligned} p_{Hn} &= \frac{Z_{\text{line}}}{2}({I_{n+1}}^2 - {I_n}^2) \quad \text{where} \quad n \in \mathbb{N}_0 \\ p_{En} &= \frac{1}{2Z_{\text{line}}}({V_{n+1}}^2 - {V_n}^2) \quad \text{where} \quad n \in \mathbb{N}_0 \end{aligned} \tag{5.18}$$

It is important to note that that energy density, which underpins the power components of the wavefront, is not a linear function of voltage or current, so the principle of superposition does not apply to power components. Therefore, the total voltage and current needed for the power components must be obtained as the sum of all prior waves in the reflection diagram.

Figure 5.9 shows the power components for the wavefront after the first reflection. The wavefront power is $-525\,\text{mJ/s}$ which is the same as before the reflection. The magnetic field power component is again negative so the magnetic field supplies energy. The magnetic field power component contributes $-519\,\text{mJ/s}$ to the wavefront power which is a smaller magnitude than its previous contribution of $-531\,\text{mJ/s}$. The electric field power component is now $-6\,\text{mJ/s}$ which is the same magnitude as before but with an inverted sign. Therefore, the electric field now supplies energy at the wavefront where before it absorbed energy.

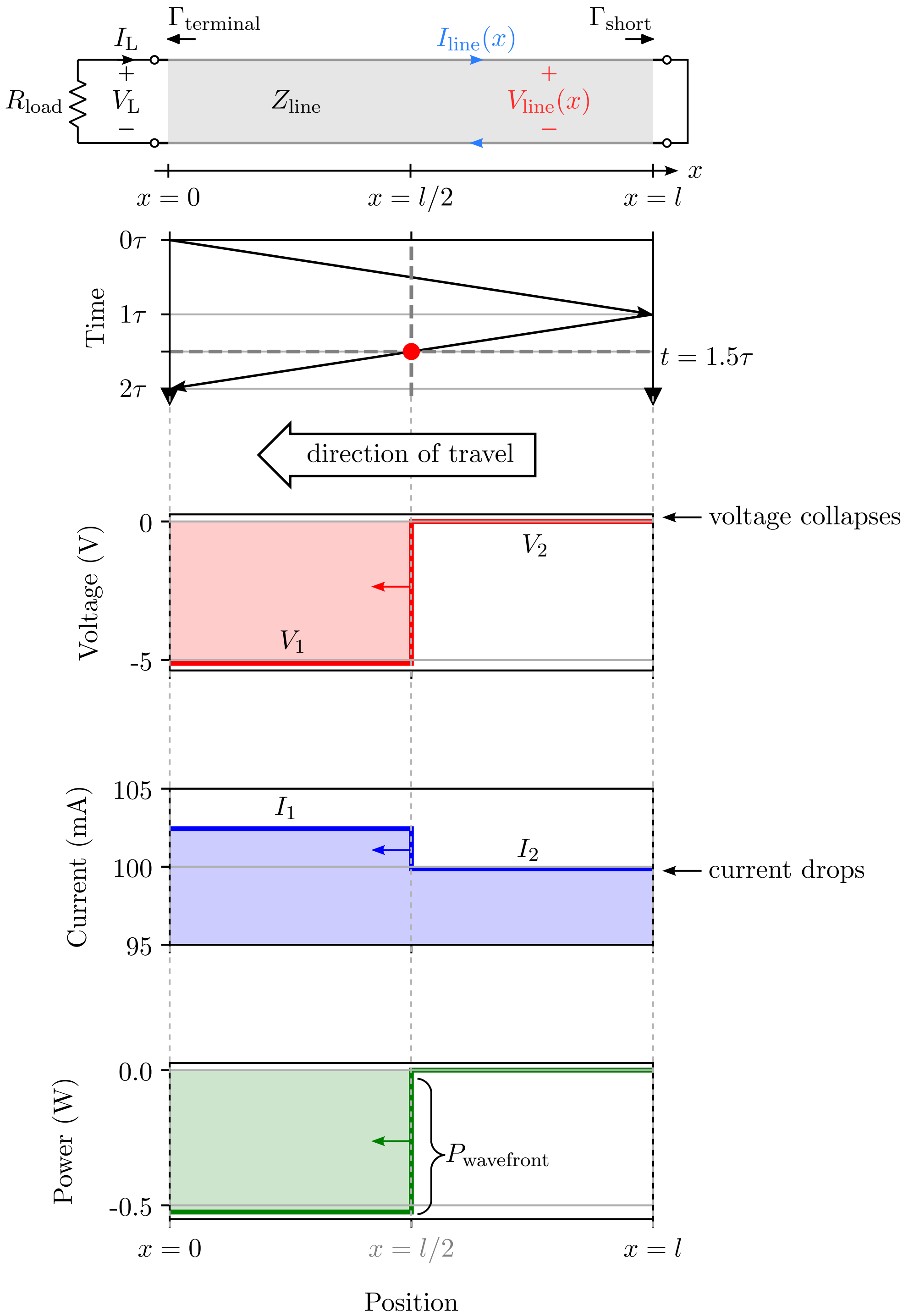

Figure 5.8: Voltage, current and instantaneous power distributions at $t = 1.5\tau$ for a wavefront reflected at the short circuit

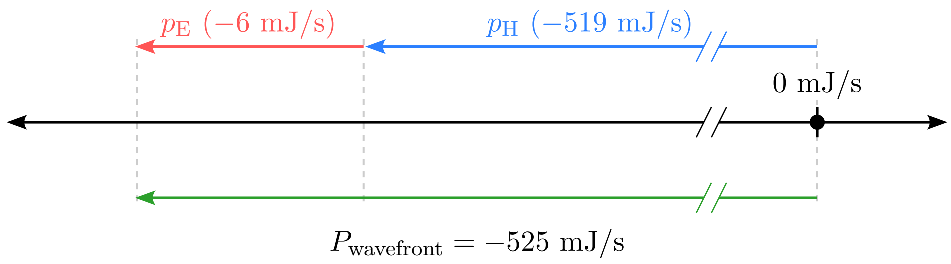

Figure 5.9: Wavefront power and its components after a single reflection at the short circuit where $\tau < t < 2\tau$

Ferreira [11] remarks that the energy deposited along a transmission line interconnect is recoverable under lossless conditions but may give rise to parasitic oscillations or voltage and current overshoots during switching. In the case of the transmission line inductor, the power components post-reflection in figure 5.9 indeed suggest that the energy deposited in the electric field prior to the reflection is fully recovered by the wavefront after the reflection. The reflection modifies the action of the wavefront, thereby reducing the contribution of the magnetic field by an amount equal to the energy recovered from the electric field.

5.6.2 Higher order reflections

The reflection diagram is employed for any number of reflections that take place in the transmission line. In figure 5.10 the spatial distributions are shown for the wavefront at $t = 2.5\tau$ after undergoing two reflections. The most recent reflection occurs at the terminal side of the transmission line inductor due to the mismatch between the transmission line impedance and load resistance. The voltage reflection coefficient is -0.95, so a large portion of the wavefront is reflected at the terminals. Therefore, many reflections of the wavefront will be necessary to get meaningful energy transfer between the inductor and load resistor.

There is a large degree of similarity between figures 5.8 and 5.10, only the magnitudes of the voltage, current and power distributions have diminished. It is expected that the distributions diminish in magnitude because the transmission line stores a finite amount of energy and, over time, the energy will be transferred out of the transmission line inductor and into the load resistor.

5.6.3 Time progression of power components

The energy conversion process repeats with each reflection of the wavefront and can be observed over time as shown in figure 5.11. The power of the lumped parameter inductor model is also shown. At the terminals of the inductor, the lumped parameter model and the transmission line model are in agreement. Steps in the terminal waveform occurs for even multiples of τ where the wavefront completes a round trip.

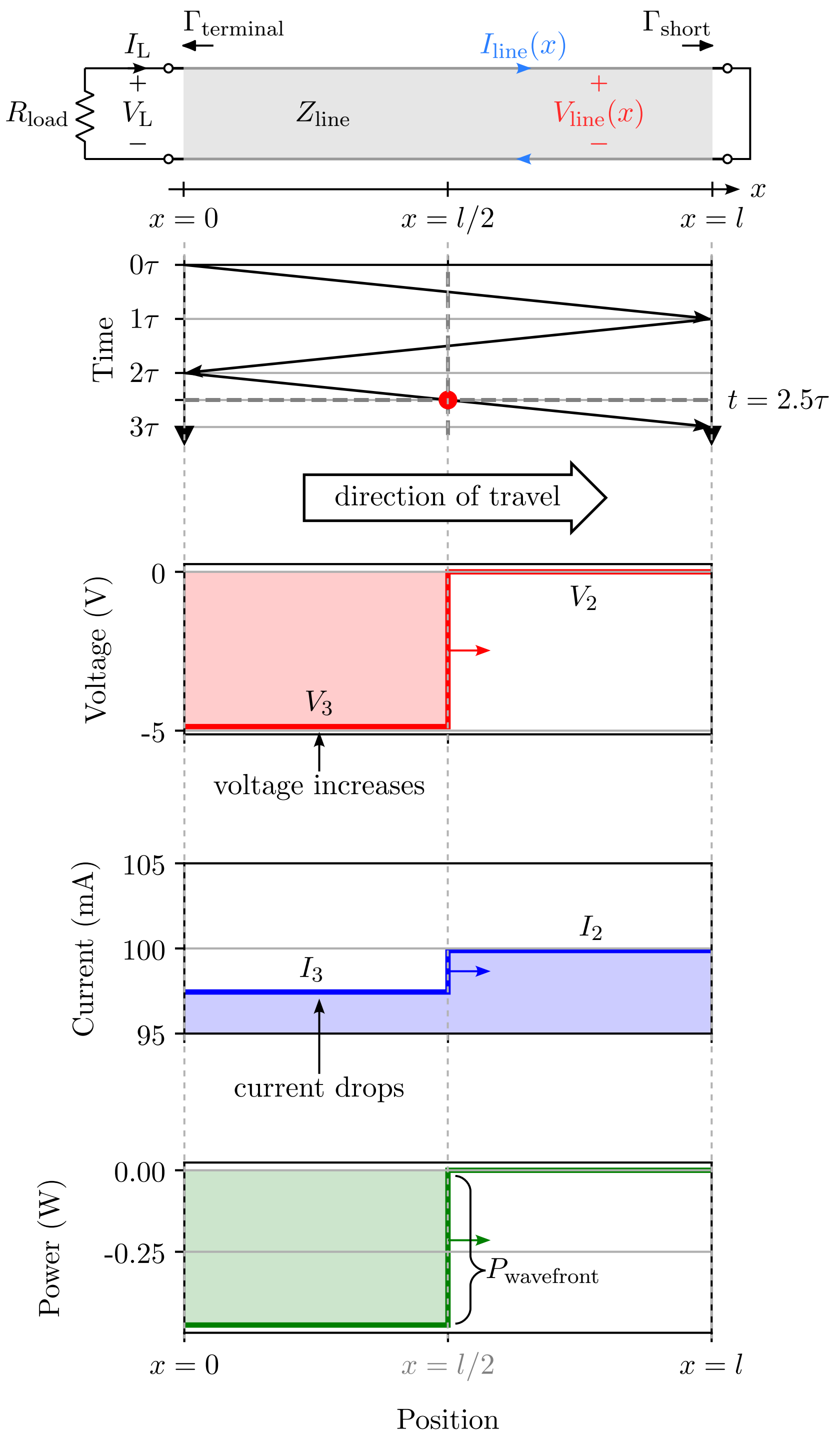

Figure 5.10: Voltage, current and instantaneous power distributions at $t = 2.5\tau$ for a wavefront reflected at the inductor terminals

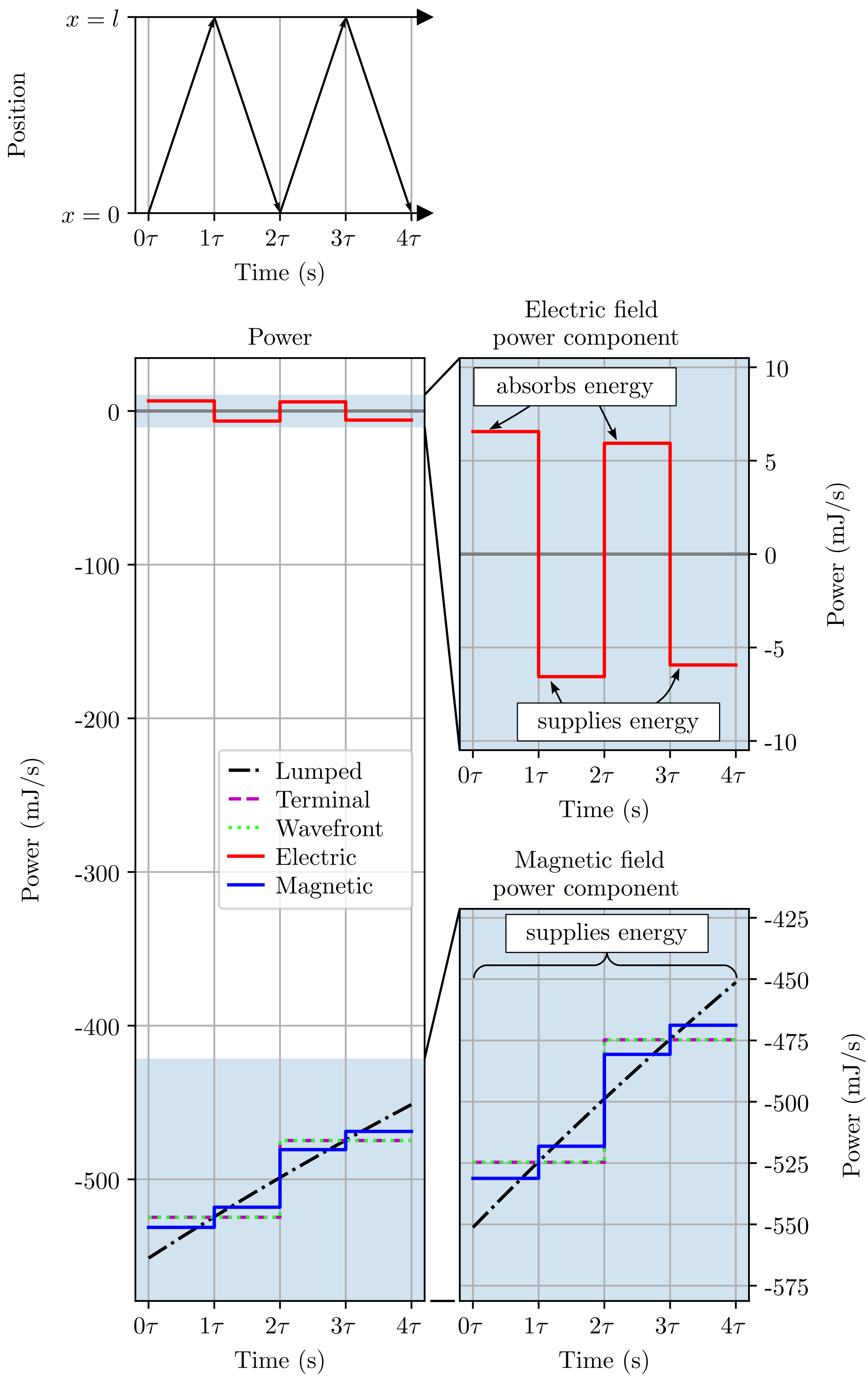

Figure 5.11: Wavefront power components in the transmission line inductor while discharging into the load resistor

Within the inductor, the wavefront power components change for each multiple of τ due to the reflection at the short circuit or terminals. The wavefront power remains constant for a round trip in spite of the reflection at the short circuit and thus overlays the curve for the terminal power. There is a sizable difference in magnitude between the electric field power component and the other curves so a zoomed-in view is provided.

At first, the electric field power component is approximately $-6\,\mathrm{mJ/s}$, so the electric field initially absorbs energy at the wavefront. Between 1τ and 2τ the electric field power component is approximately $6\,\mathrm{mJ/s}$ so the electric field supplies energy at the wavefront. This pattern repeats for each successive reflection with the electric power component alternating between absorbing and supplying energy in that order.

The electric field power component for the returning wavefront is always equal in magnitude but opposite in sign to the power component of the outgoing wavefront. Over time the power component decreases in magnitude. The presence of the electric field power component accounts for the vertical offset between the magnetic field component and the wavefront power. Over a round trip, the average power for the electric field component is $0\,\mathrm{J/s}$, so the electric field does not accumulate energy. The continued involvement of the electric field via an absorb-supply cycle suggests that it is an integral part of the energy conversion process of the inductor. The presence of electric field energy and the conversion process to and from it seem to be required for the operation of the inductor.

On the other hand, the magnetic field power component is always negative and large in magnitude in the region of $500\,\mathrm{mJ/s}$. Thus, the magnetic field continuously supplies energy which is conveyed to the terminals. This is what we come to expect from the lumped parameter model which is in good agreement with the magnetic field power component but neglects to describe the involvement of the electric field component seen in the transmission line. Overall the lumped parameter model is an appropriate approximation because the magnetic field component dominates the electric field component.

Figure 5.12 is an extension of figure 5.7 for reflections up to $t = 4\tau$ and shows how stored energy is apportioned between the magnetic field, electric field, and load at the time of each reflection. The energy in the magnetic field and electric field are denoted with the symbols U_H and U_E. The stored energy can be calculated in two ways: the wavefront power components can be integrated over time, or the energy density can be integrated over the length of the transmission line. Both methods produce the same results. The total energy view of the inductor in figure 5.12 is in agreement with the results offered by the wavefront power components.

The magnetic field acts as the primary store of energy with a small amount of energy directed to the electric field for odd multiples of the propagation delay. The energy imparted to the load is equal for the two halves of the round trip since the terminal power is constant. With each successive reflection the stored energy in the transmission line inductor decreases as the energy is delivered to the load resistor. This process will continue until there is no stored energy remaining. In the case of a step-down converter, the transmission line inductor must be charged up again to repeat the cycle. This is the topic of the next chapter.

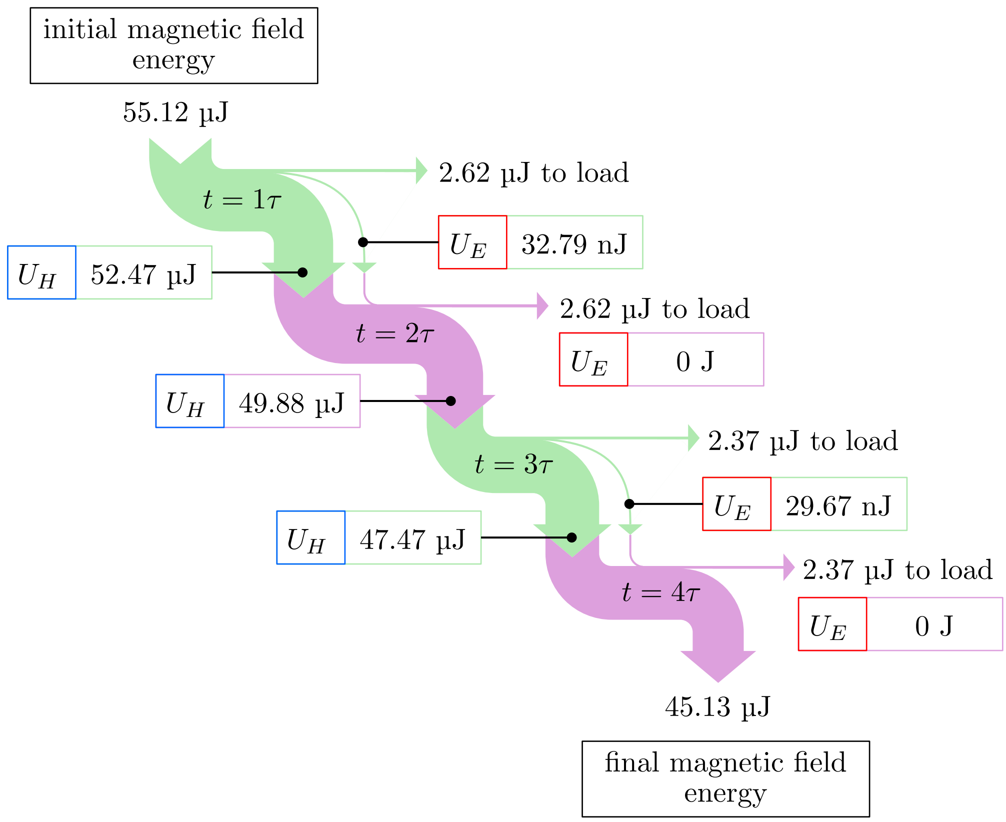

Figure 5.12: Sankey diagram showing how the stored energy within the transmission line is apportioned between the fields and load at each reflection of the wavefront

Chapter 6

Wavefront power components and the step-down converter

Over the course of every switching period of the step-down converter, the inductor accumulates and releases energy. The previous chapter considered the case where the transmission line inductor releases its stored energy into the load resistor. This chapter considers the remaining case where the transmission line inductor accumulates energy by charging from the voltage source as shown figure 6.1. To better understand the action of the wavefront in the energy conversion process, again the wavefront power is decomposed into components and observed over several reflections.

The insights from charging and discharging the transmission line inductor are then combined for a complete converter switching period. A discussion follows regarding lumped inductor models, the role of switching in power converters, and a suggestion for scaling this approach to numerous inductors and capacitors.

6.1 Charging circuit

The initial condition of the transmission line inductor is shown in figure 6.2a where the initial current I_0 is statically distributed in the transmission line and there is zero initial voltage. Section 6.2.1 explains in further detail why this is a valid

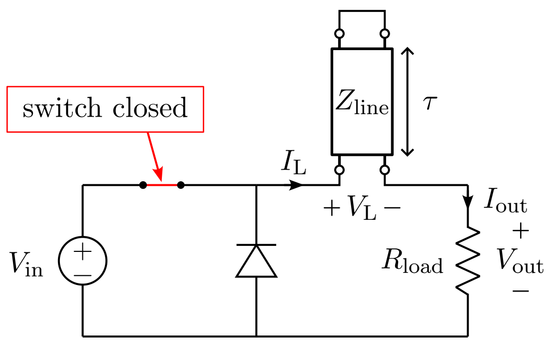

Figure 6.1: Step-down converter circuit with switch closed

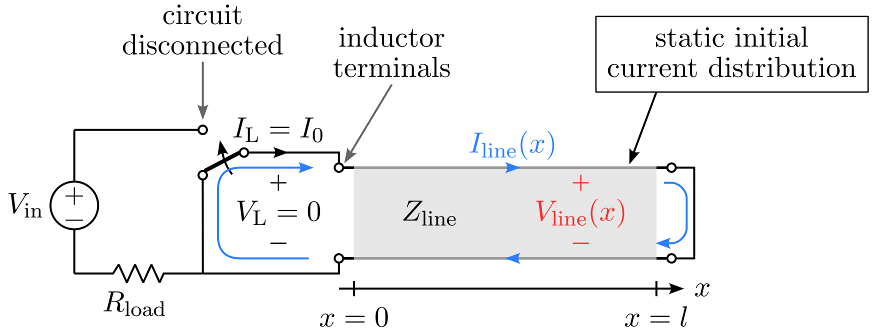

(a) Circuit for initial conditions (source bypassed)

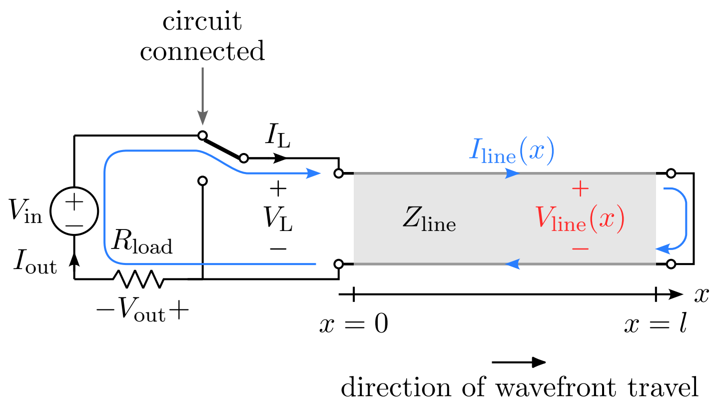

(b) Circuit for analysis (source connected)

Figure 6.2: The transmission line inductor with an initially static current distribution charges from the voltage source when connected via an ideal switch

representation of the initial state of the transmission line inductor for the step-down converter in the middle of the switching period.

Consider the wavefront that is initiated when the switch in figure 6.2b connects the voltage source and load resistor to the transmission line. The voltage and current of the wavefront are calculated in (6.1) using a system of equations obtained from the wave impedance and circuit analysis as done before in chapter 5.

$$\begin{aligned} I_{\text{wavefront}} &= \frac{1}{R_{\text{load}} + Z_{\text{line}}}(V_{\text{in}} - I_0 R_{\text{load}}) \\ V_{\text{wavefront}} &= \frac{Z_{\text{line}}}{R_{\text{load}} + Z_{\text{line}}}(V_{\text{in}} - I_0 R_{\text{load}}) \end{aligned} \tag{6.1}$$

The voltage and current at the terminals are given by (6.2).

$$\begin{aligned} I_{\text{L}} &= \frac{1}{R_{\text{load}} + Z_{\text{line}}}(V_{\text{in}} + Z_{\text{line}} I_0) \\ V_{\text{L}} &= \frac{Z_{\text{line}}}{R_{\text{load}} + Z_{\text{line}}}(V_{\text{in}} - R_{\text{load}} I_0) \end{aligned} \tag{6.2}$$

Equations (6.1) and (6.2) give the voltages and currents needed to construct spatial distributions prior to any reflections of the wavefront.

6.1.1 Spatial distributions

Recall that in steady state, the inductor had an initial current of 95 mA when the switch closes at the beginning of the charging cycle. Figure 6.3 shows spatial distributions of the voltage, current and instantaneous power in the transmission line inductor obtained from the initial conditions and reflection diagram.

A positive voltage of approximately 5 V follows the wavefront as it travels towards the short circuit where previously in chapter 5 the voltage was approximately −5 V. The total current at the terminals is now 97.5 mA which is greater than the initial current of 95 mA, so the wavefront current $I_{\text{wavefront}}$ is positive. The instantaneous power distribution shows a positive power of approximately 0.5 W follows the wavefront where previously it was negative. The transmission line absorbs energy from the voltage source. The wavefront power is positive, so energy flows into the transmission line from left to right.

The load resistor determines the impedance seen by the wavefront arriving at the inductor terminals. The voltage reflection coefficients remain unchanged despite the introduction of the voltage source. Figure 6.3 can be extended to several reflections although this not shown here since we shift focus to the power components of the wavefront.

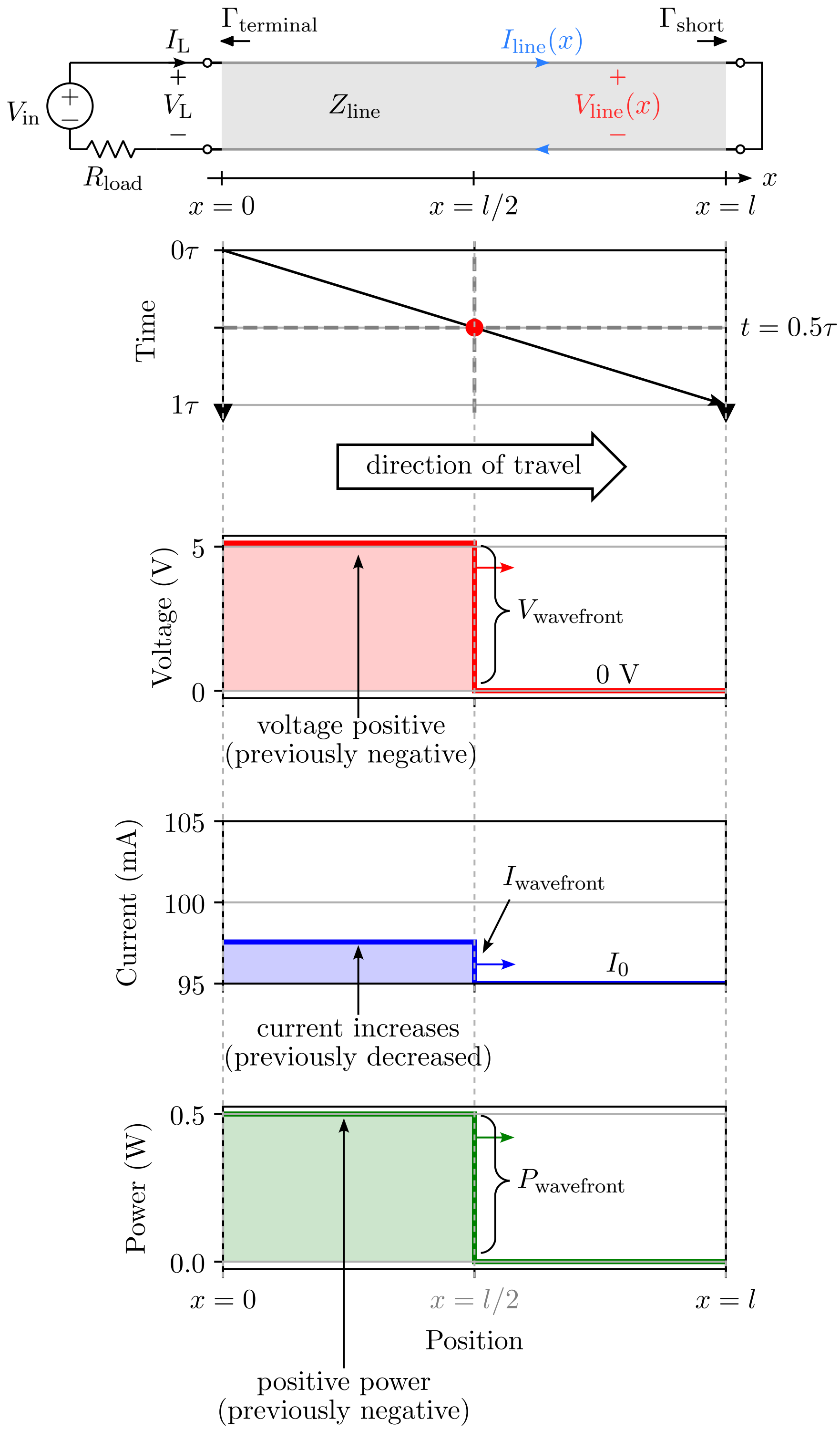

Figure 6.3: Reflection diagram and spatial distribution of voltage, current and instantaneous power for the initial passage of the wavefront at $t = 0.5\tau$ for a charging transmission line inductor

6.1.2 Power components

The procedure outlined in chapter 5 is repeated to obtain the power components for the initial wavefront in the transmission line in terms of circuit quantities as shown in (6.3). The similarity between the equivalent circuits means that (6.3) reduces to the same equations obtained in chapter 5 when V_{in} is set to 0 V.

$$\begin{aligned}
p_H &= \frac{Z_{\text{line}}}{2(R_{\text{load}} + Z_{\text{line}})^2}(V_{\text{in}} + Z_{\text{line}} I_0)^2 - \frac{Z_{\text{line}}}{2}(I_0)^2 \\
p_E &= \frac{Z_{\text{line}}}{2(R_{\text{load}} + Z_{\text{line}})^2}(V_{\text{in}} - R_{\text{load}} I_0)^2
\end{aligned} \tag{6.3}$$

Recall that the power components are indexed in terms of the number of reflections n where the cumulative voltages and currents are obtained from the reflection diagram.

$$\begin{aligned}
p_{Hn} &= \frac{Z_{\text{line}}}{2}({I_{n+1}}^2 - {I_n}^2) \quad \text{where} \quad n \in \mathbb{N}_0 \\
p_{En} &= \frac{1}{2Z_{\text{line}}}({V_{n+1}}^2 - {V_n}^2) \quad \text{where} \quad n \in \mathbb{N}_0
\end{aligned}$$

Figure 6.4 gives the power components for two round-trips of the wavefront in the transmission line inductor. The same fundamental relations seen in chapter 5 are visible. The power at the terminals and the wavefront power are equal with overlaid curves. The lumped inductor model and transmission line inductor model are in agreement regarding the power at the terminals.

The magnetic field power component closely follows the wavefront power and is strictly positive, so the magnetic field absorbs energy regardless of the wavefront reflections. Previously, the magnetic field power component was strictly negative, and the magnetic field always supplied power. The relative sizes of the electric and magnetic field power components indicate that the majority of energy absorbed from the voltage source is directed into the magnetic field as expected for an inductor.

Although the magnetic field is the dominant component of the wavefront power, again the electric field power component has a non-zero contribution. From 0τ to 1τ the electric field power component is positive, thus the electric field absorbs energy. From 1τ to 2τ the component is negative so the electric field supplies energy. This oscillation repeats for each round trip. The oscillations in the electric field power component have corresponding oscillations in the magnetic field power component. The electric field power component averages zero for each round trip with a slight decline in amplitude between each round trip.

The electric field component first absorbs then supplies energy which is the same sequence as when the inductor was discharged. For the odd multiples of τ, the wavefront reflects at the short circuit. Following the reflection, the magnetic field power component is larger than the terminal power. This means energy is deposited into the magnetic field faster than it is absorbed at the terminals. This apparent increase in power suggests that the energy initially deposited in the electric field is recovered in the magnetic field by the reflected wavefront. Thus the reflections

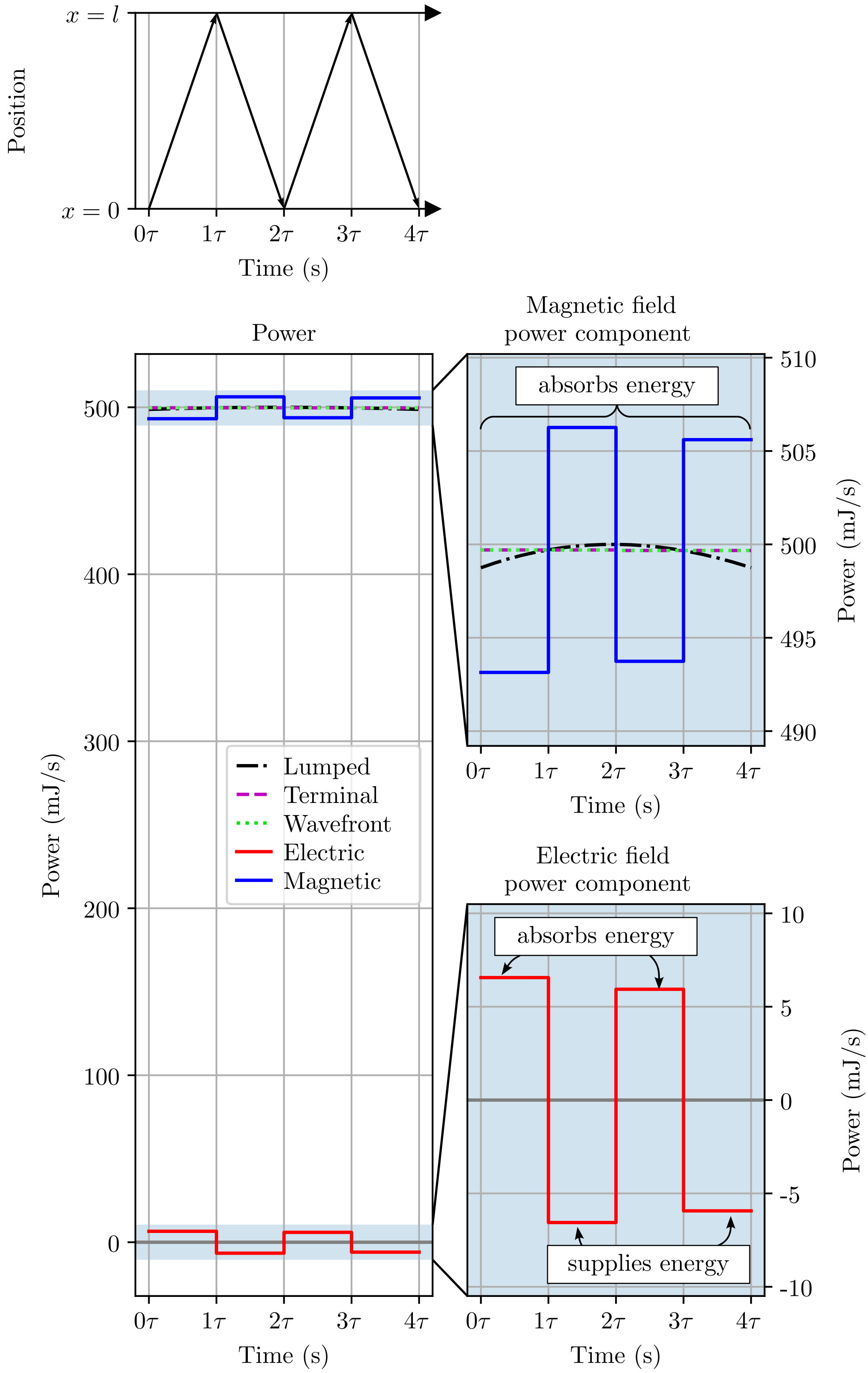

Figure 6.4: Wavefront power components in the transmission line inductor while charging from the voltage source

at the short circuit prevent a build up of energy in the electric field and bias the transmission line inductor towards storage of energy solely in the magnetic field. The reflections at the terminals opposite the short circuit restart the pattern by again causing the wavefront to deposit energy in the electric field for later recovery in the magnetic field. This mechanism moves energy into the transmission line and brings it to rest in the magnetic field.

6.2 Combined results

The step-down converter presented in chapter 4 has two distinct circuit configurations which have been considered independently. The portion of the switching period allocated to each of these circuits is determined by the duty cycle which is fixed at 50 %. The results of each circuit are combined for a complete view of the transmission line inductor over the course of a whole switching period.

6.2.1 Initial conditions at switching events

Steady state analysis of the step-down converter is achieved by applying a DC offset using an initial condition for the current in the inductor. Figure 6.5 depicts a uniform current and voltage in the transmission line in the region behind the wavefront as it travels towards the left. When the wavefront reaches the terminals at $x = 0$, the voltage and current are uniform along the full length of the line. The voltage in the transmission line inductor always collapses to zero due to the reflection at the short circuit.

Chapter 4 imposed the constraint that the round-trip delay of the transmission line cleanly divide between switching events. The switching event will introduce a new wavefront at the terminals of the transmission line inductor at the same instant that the existing wavefront arrives back at the terminals. The conditions within the line are uniform but not static due to the existing wavefront. It can be shown that the superposition of the existing wavefront and new wavefront is equivalent to using the new wavefront under uniform and static initial conditions. The uniform and

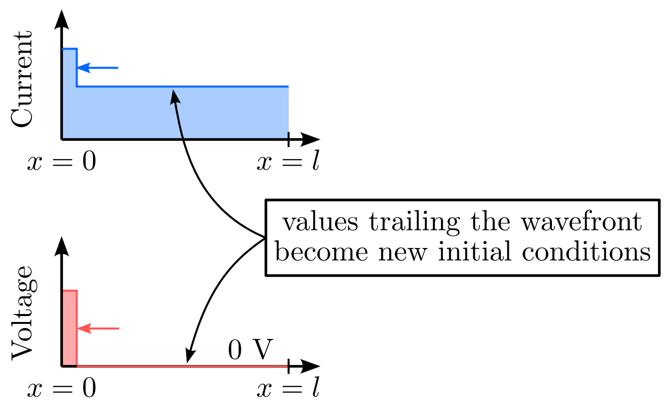

Figure 6.5: The voltage and current trailing the wavefront become the next set of initial conditions at a switching event

static initial conditions are given by the values which follow the existing wavefront in figure 6.5. Therefore, the results of the independent analysis of the converter circuits can simply be merged with prior observations transferrable to the complete converter switching period.

6.2.2 Power components over a switching period

Figure 6.6 shows the power components in the transmission line inductor for a full switching period of the step-down converter. The switching events are labelled on the time axis of the reflection diagram. The power components cover a wide range of values making it difficult to discern nuances in behaviour. Thus, the components are plotted again on separate axes at different scales. The magnetic field power component jumps from negative to positive when the switch closes, so a broken vertical axis is used to make the details visible at both extremes of magnitude.

The converter switch opens at $t = 0$ and the inductor supplies energy as it discharges into the load resistor. With each successive reflection, the magnitude of the power supplied at the terminals decreases. Since the primary store of energy is the magnetic field, it is appropriate that the magnetic field is the main contributor to the wavefront power. The electric field power component is small but non-zero. Together the electric and magnetic field conveys the energy converted at the wavefront to the terminals where it is available for the converter load.

At $t = 4\tau$ the switch closes, and the inductor starts to absorb energy from the input voltage source as shown by the positive power at the terminals. Energy is transported from the terminals to the wavefront where it is stored in the transmission line. The large magnetic field component indicates energy is primarily flowing into the magnetic field where its is stored until the next discharge cycle. Again, the electric field power component is small but non-zero. The wavefront power in figure 6.6 is the average of the magnetic field power. During charging, the magnetic field power oscillates about this average value with an amplitude equal to the electric field power component.

The electric field alternates between absorbing and supplying power regardless of whether the inductor is accumulating or releasing energy. This suggests that energy deposited in the electric field is required for the energy conversion process, allowing the storage and extraction of energy in the magnetic field of an inductor. If this is the case, then the electric field of the transmission line inductor can be minimised but can not be eliminated because it is fundamental to the functioning of the inductor.

It appears that the mechanism of energy conversion in an inductor is the exchange of energy between the electric and magnetic fields at the wavefront. Inductors and capacitors are structures which can support the wavefronts needed to perform energy conversion and thus are the fundamental building blocks of all power converters. Power converters exploit the internal energy conversion mechanism of reactive components using switches to introduce wavefronts which change the voltage and current levels of electrical energy.

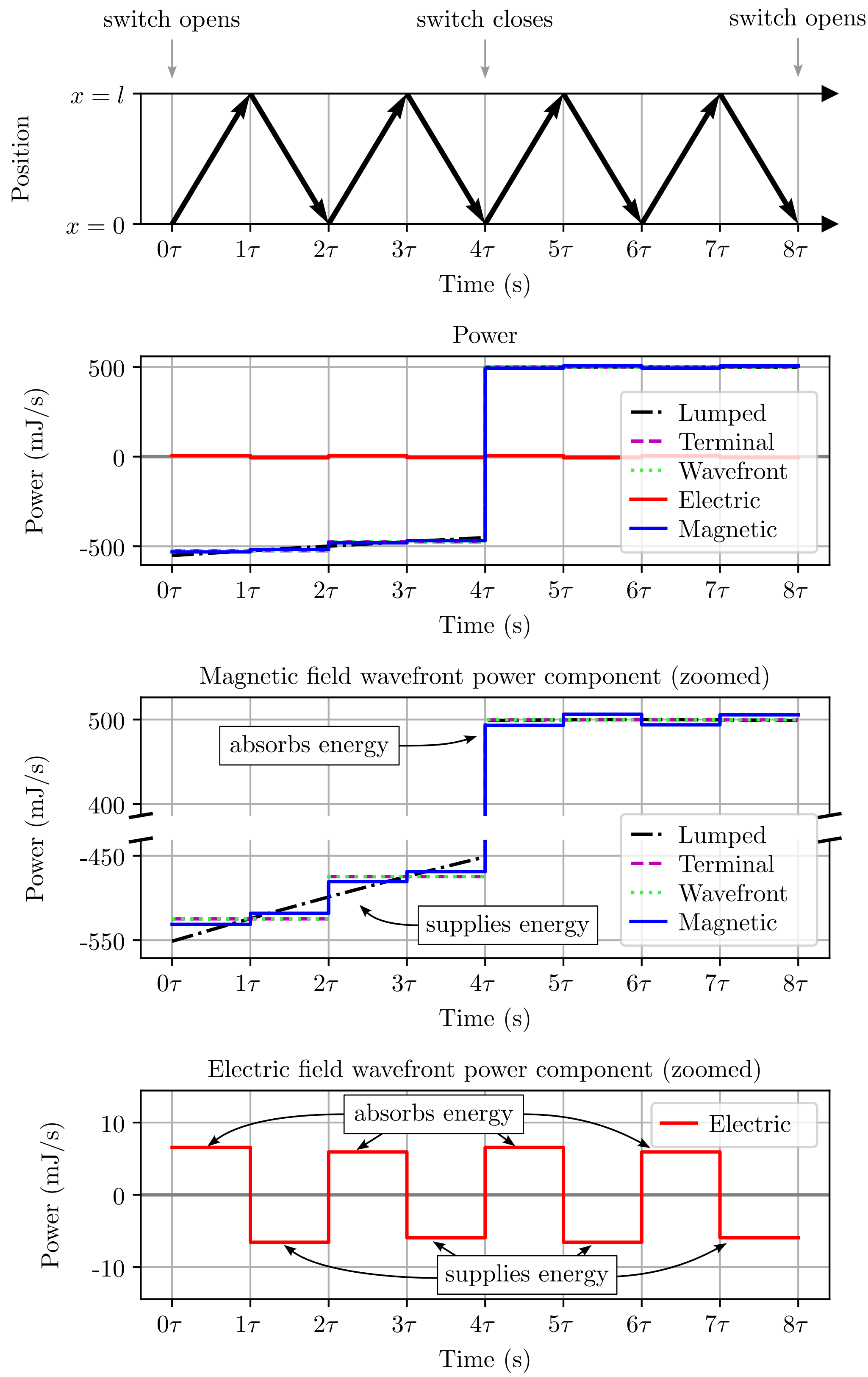

Figure 6.6: Wavefront power components for the transmission line inductor of the step-down converter over a switching period in steady state

6.3 Discussion

Observing the action of the wavefront over a full switching period gives rise to some general discussion points regarding lumped models, the role of switching in the converter, and the handling of topologies with numerous energy storage elements.

6.3.1 Lumped model as the limit of the transmission line model

In chapter 4 it is seen that the output waveform of the step-down converter using a transmission line inductor model approaches that of the lumped parameter model when the propagation delay is small. The shorter propagation delay results in smaller steps in the voltage and current waveforms. Smaller steps in voltage and current imply smaller changes in energy density and thus a reduction in the amplitude of oscillations in the magnetic and electric field power components. While the electric field component can be minimised, it cannot be entirely eliminated without fundamentally altering the transmission line model itself. The geometry of a physical inductor imposes a fundamental non-zero limit on the round-trip delay.

The wavefront power components in figure 6.6 suggest that the lumped inductor model is an appropriate approximation of the transmission line inductor. One can consider the lumped inductor model as the limit of the transmission line model as the propagation delay approaches zero. In this limit, the electric field power component approaches zero and thus could be neglected altogether. This explains the lumped view of an inductor which considers only the magnetic field.

6.3.2 Role of switching in the step-down converter

If energy conversion occurs at the wavefront, then the primary function of switching in the step-down converter is to create wavefronts in the inductor. The inductor can only absorb or supply a finite amount of energy under static circuit conditions. Thus, the magnitude of the wavefront diminishes over time as the voltage and current distributions approach a steady state. As the magnitude of the wavefront diminishes, less energy conversion takes place.

For the step-down converter to continuously accumulate and discharge energy in the inductor, new wavefronts must be continuously introduced to perform energy conversion. The repeated switching action provides a regular source of new wavefronts for the transmission line with each switching event. The circuit external to the transmission line inductor influences the properties of the wavefront and the reflections thereof. The nature of the wavefront alternates with each switching event as the transmission line inductor cycles between the accumulation and release of energy.

The conversion of energy at the wavefront explains the underlying effect which is exploited by the transmission line converter topologies proposed by Sander [5]. Sander proposes new topologies using transmission line models as the primary energy storage element. He recognises that careful switch timing switch can give rise to different modes of operation in the transmission line. Ultimately, controlling the timing of the switching action determines the spacing of wavefronts. The combination of these wavefronts enables different energy conversion outcomes at the converter terminals.

6.3.3 Circuits with numerous inductors and capacitors

The step-down converter was specifically chosen in this work because it had a single energy storage component. However, in practice, converter circuits have numerous inductors and capacitors. This raises the question: how can the insights gained from wavefront power components be applied to describe the energy conversion mechanisms in more complex topologies?

Generally, the approach of wavefront power components is more suited to foundational discussion than as a general analytical tool. While the scaling of power components to numerous transmission lines is beyond the scope of this work, one approach could be to construct a reflection diagram for each inductor or capacitor in the circuit, producing separate spatial distributions which can be analysed independently. However, transmission line modelling of circuits containing both inductors and capacitors is known to reveal complex interactions [9], [18]. Mofu [18] demonstrates that the complexity of this interaction is determined primarily by the propagation delays chosen for each transmission line with an irrational ratio of propagation delays giving rise to the most complex interactions. Where the propagation delays are integer multiples, the complex waveforms periodically merge together thereby simplifying the interaction.

Chapter 7

Impedance mismatch and energy conversion

The matching of impedances is an important consideration in many applications of transmission line modelling. Where the transmission line impedance matches the load, unwanted reflections are minimised and energy is delivered at maximum power from the source to the load. However, by definition a transmission line model of an inductor has a large characteristic impedance and is therefore unlikely to match the impedance of a connected load.

This chapter considers the effect of impedance mismatch on energy conversion at the wavefront in a transmission line inductor using wavefront power components. As shown in figure 7.1, the transmission line inductor is connected to a Thévenin equivalent circuit where the load resistance and supply voltage are varied. Simple values are chosen for parameters to produce numerical results that are easy to work with. Note that these values are separate to those used for the inductor of step-down converter in the previous chapters.

The case where the Thévenin voltage is 0 V is considered first. Impedance mismatch is most pronounced in the special cases of an open circuit and a short circuit. A trade-off is described between the degree of energy conversion in the inductor and the power at the terminals. The duality of inductors and capacitors modelled as transmission lines is briefly demonstrated. While this work does not discuss capacitors in detail, this treatment is included to provide a comparison of the wavefront power components for a capacitor and inductor at various levels of impedance mismatch.

Next, increasing Thévenin voltages are applied, and their effects on wavefront power components are observed across different degrees of impedance mismatch. Lastly, the Thévenin voltage is again set to 0 V, and the power components are described over several reflections of the wavefront using a sequence of curves.

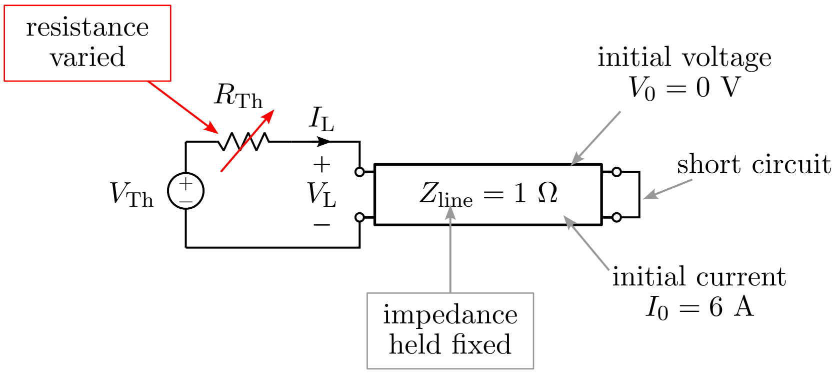

Figure 7.1: An impedance mismatch is created by varying the load resistance while the transmission line impedance is held fixed

7.1 Thévenin equivalent circuit

The setup in figure 7.1 is the basis for all further work in this chapter. Figure 7.1 shows a Thévenin equivalent circuit connected to a transmission line inductor with an initial current of 6 A and voltage of 0 V. The Thévenin circuit could represent any linear network like those seen in chapter 4 for the step-down converter.

The transmission line impedance is fixed at 1 Ω and the load resistance is varied to create different degrees of impedance mismatch. The load resistance is varied rather than the transmission line impedance so that the amount and nature of energy initially stored in the transmission line remains constant. Varying the polarities of the Thévenin voltage source and initial current is of little concern in this work, as they yield no unique additional insights. Additionally, the energy density which underpins the method of wavefront power components is independent of polarity because the voltage and current terms are squared.

7.2 Discharging inductor

In this section, only the properties of the initial wavefront are considered for a discharging inductor. The effect of reflections on the wavefront power components is left to section 7.4. In the case where the Thévenin voltage is 0 V, the inductor is the only source of energy in the circuit. As before, the energy in the inductor is initially at rest in the magnetic field. This creates a setup identical to the discharging inductor for the step-down converter in chapter 5, so the circuit analysis is not repeated here.

Figure 7.2 plots the initial conditions and the total voltage and current in the transmission line following the wavefront for values of R_{Th} in the range 1 mΩ to 1 kΩ. This range of load resistances is chosen to sufficiently reveal horizontal asymptotes in the curves. The resistance that matches the transmission line impedance is indicated with a vertical line at 1 Ω.

Figure 7.2 shows that the voltage in the transmission line following the wavefront approaches the initial voltage 0 V for small resistances and −6 V for large resistances. On the contrary, the current remains unchanged at its initial value of 6 A for small

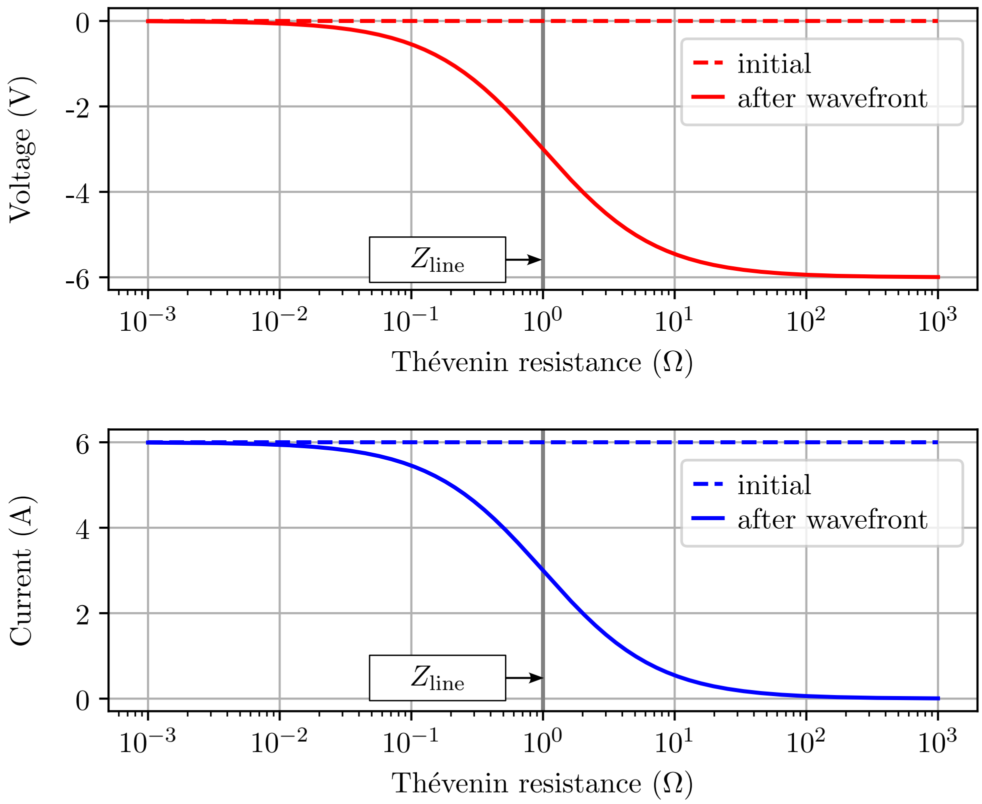

Figure 7.2: Voltage and current in the transmission line as a function of load resistance

resistances but approaches 0 A for large resistances. Therefore, the mismatch in impedance has a significant effect on the voltage and current which follow the wavefront. Significant changes in voltage and current will have corresponding changes in energy density.

7.2.1 Effect on energy density

Figure 7.3 plots the electric and magnetic field energy density in the transmission line before and after the initial wavefront. The initial density in the electric and magnetic fields is independent of resistance. After the wavefront, the magnetic field energy density drops to 0 J/m for large resistances or remains at 60 nJ/m for small resistances. The opposite is true for the electric field where the energy density increases from 0 J/m to 60 nJ/m with increasing resistance. Notably, where the resistance and transmission line impedance are matched, the energy density is equal in the electric field and magnetic fields. Recall that the change in energy density underpins the wavefront power components thus a similar dependence on resistance is expected for the wavefront power components.

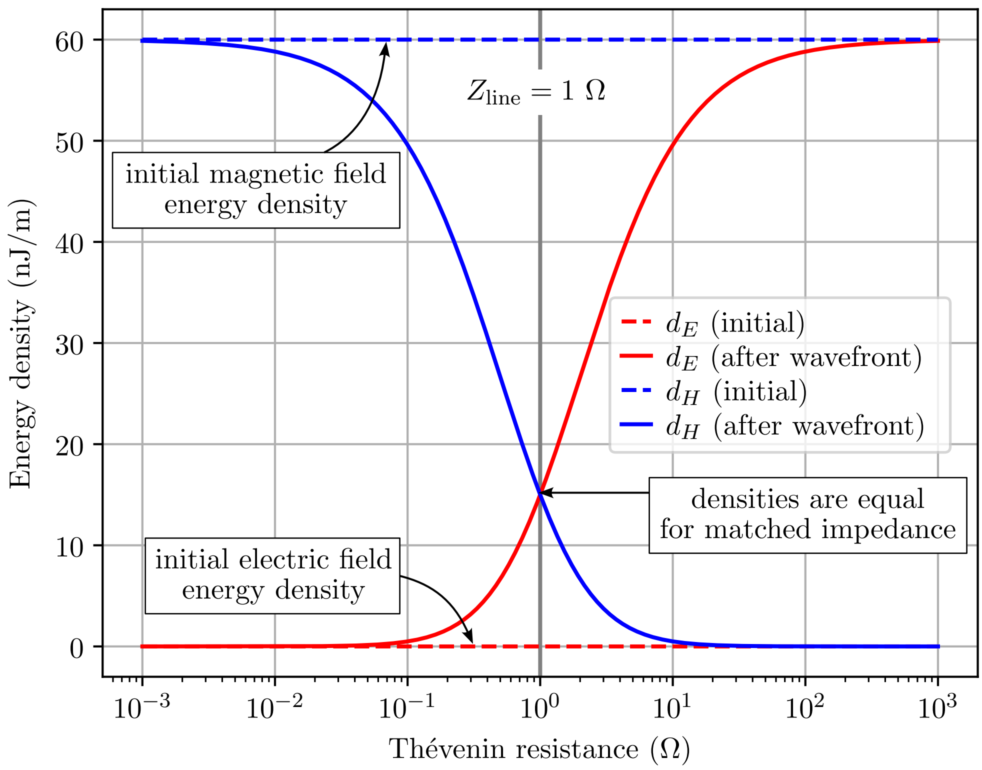

Figure 7.3: Electric and magnetic field energy density in the transmission line as a function of load resistance

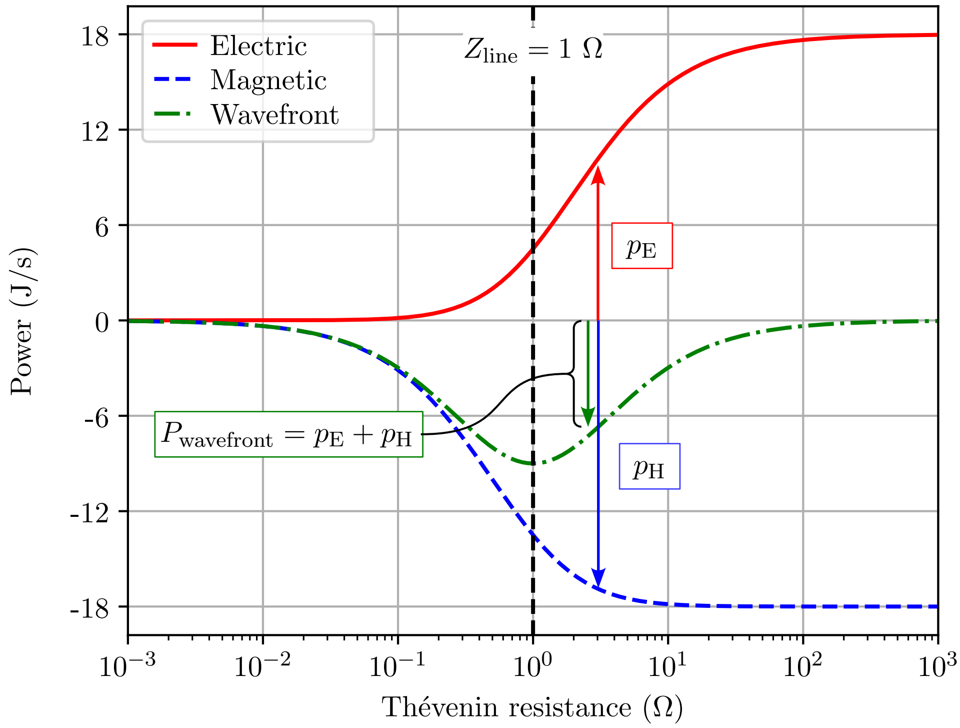

Figure 7.4: Wavefront power components as a function of load resistance for the initial passage of the wavefront

7.2.2 Effect on power components

Figure 7.4 shows the wavefront power and its components as functions of the load resistance. Previously in chapter 5, wavefront power components were represented using arrows on a number line. In figure 7.4 each point on the curve can be thought to represent the length of a power component arrow directed along the vertical axis. These curves are described by (7.1) which is reproduced from chapter 5.

$$\begin{aligned} p_H &= -\frac{R_{\text{Th}} Z_{\text{line}} (R_{\text{Th}} + 2Z_{\text{line}})}{2(R_{\text{Th}} + Z_{\text{line}})^2} (I_0)^2 \\ p_E &= \frac{(R_{\text{Th}})^2 Z_{\text{line}}}{2(R_{\text{Th}} + Z_{\text{line}})^2} (I_0)^2 \end{aligned} \tag{7.1}$$

In figure 7.4 the magnetic field power component is strictly negative thus the magnetic field supplies energy for all resistances. In contrast, the electric field power component is strictly positive so the electric field absorbs energy from the magnetic field for all resistances.

Chapter 5 establishes that the wavefront power is equal to the terminal power for the transmission line inductor. In figure 7.4 the wavefront power is strictly negative for all resistances. Likewise, the power at the terminals is also strictly negative. Therefore, a negative power at the terminals means the transmission line supplies the energy stored in its fields to the rest of the circuit at the rate equal to the wavefront power in figure 7.4.

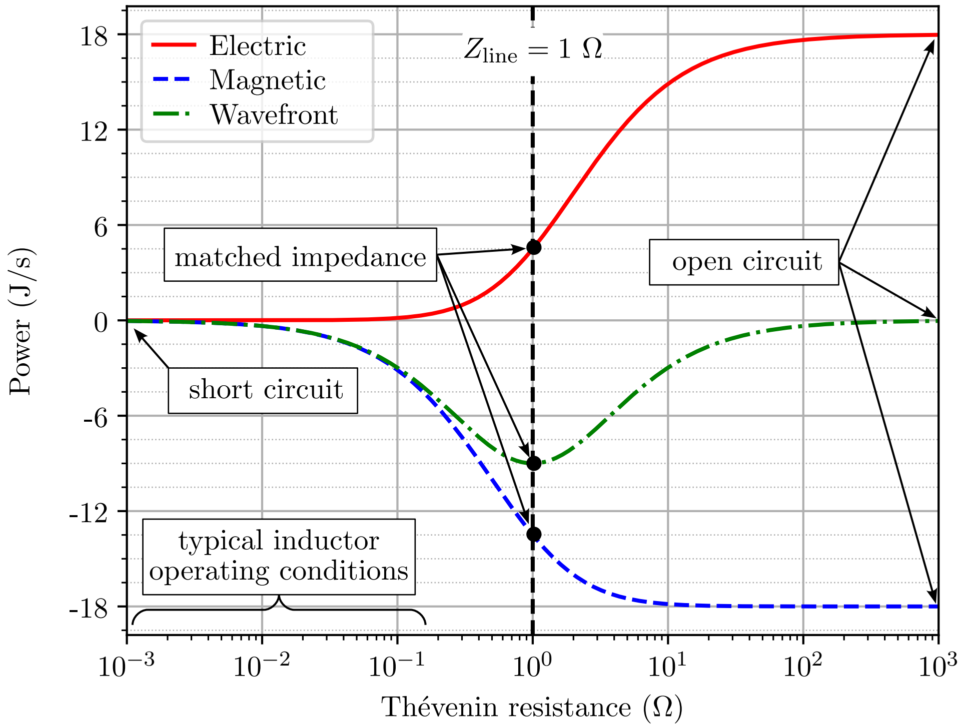

Figure 7.5: Wavefront power components annotated for salient values of resistance

When the load resistance is small, there is a substantial impedance mismatch, and the wavefront power and its components approach 0 J/s. When the load resistance is large, again there is a substantial impedance mismatch and the wavefront power approaches 0 J/s. However, there is interesting behaviour in the latter case since the power components approach horizontal asymptotes at 18 J/s and −18 J/s for the electric and magnetic field components, respectively. Although the wavefront power approaches zero for these high resistances, the wavefront power components indicate meaningful activity still takes place at the wavefront.

Figure 7.5 is an annotated version of figure 7.4 with the power components labelled at three salient resistances. When the resistance matches the transmission line impedance at 1 Ω the magnitude of the wavefront power is maximised. We also consider the outermost resistances at 1 mΩ and 1 kΩ which approximate the conditions of a short circuit and open circuit, respectively.

7.2.3 Small resistances

The region to the far left of figure 7.5 describes the scenario where the load resistance is small compared to the transmission line impedance. This is the region which best describes the impedance mismatch seen by the inductor under typical operating conditions in a power converter.

Where the resistance approaches 1 mΩ, the power components of the magnetic field and electric field both converge to 0 J/s. In the limit where the resistance is zero, the transmission line is effectively connected to a short circuit and the power components are zero. Thus, the energy is unchanged in the transmission line and remains at rest purely in the magnetic field.

For small resistances, the magnetic field power component is more sensitive to increases in the load resistance than the electric field component. The magnetic field component obtains a meaningful magnitude around $10\,\mathrm{m\Omega}$ while the electric field power component remains close to $0\,\mathrm{J/s}$. When the load resistance is an order of magnitude larger, around $100\,\mathrm{m\Omega}$, then the electric field component begins to show meaningful increase in magnitude.

The magnetic field power component follows the wavefront power, but the two curves begin to diverge as the resistance increases. Overall, the wavefront power components are small compared to those of larger resistances, suggesting that many reflections are needed to convert large amounts of energy. With a small wavefront power, many reflections are also needed to obtain meaningful energy transfer from the inductor to the load.

7.2.4 Matched impedance

In the case where the transmission line impedance is matched to the resistance at $1\,\Omega$, the wavefront power is maximised at $-9\,\mathrm{J/s}$. The rate of energy transfer can be measured by the power at the terminals. Since the wavefront power is equal to the power at the terminals of the transmission line inductor, the power delivered to the resistor is also maximised when the impedances are matched. This is a well-known result described by the maximum power transfer theorem.

For the matched impedance, the magnetic field power component is $-13.5\,\mathrm{J/s}$ while the electric field power component is $4.5\,\mathrm{J/s}$. Therefore, energy at rest in the magnetic field must be converted to energy in the electric field at a rate of $4.5\,\mathrm{J/s}$ by the wavefront. However, figure 7.5 shows that energy enters the electric field at even higher rates for larger resistances.

The wavefront power components suggest a conversion of energy occurs even when the impedance of the load is matched to the transmission line. This is explained by again considering Ferreira's [11] treatment of the voltage-to-current ratio. The initial current in the transmission line inductor leads to a voltage-to-current ratio which deviates from the characteristic impedance causing deposition of energy in the electric field. This deviation is commonplace for an inductor which stores energy purely in the magnetic field by design. Thus, the use of impedance matching alone will not stifle the energy conversion process in a transmission line inductor for the initial wavefront.

7.2.5 Large resistances

The case where the load resistance is much larger than the transmission line impedance is described by the region to the far right of figure 7.5. Where the load resistance approaches $1\,\mathrm{k\Omega}$, the magnetic field power component nears $-18\,\mathrm{J/s}$ while the electric field power component nears $18\,\mathrm{J/s}$. The sum of the components, given by the wavefront power, approaches $0\,\mathrm{J/s}$ hence little to no power is available for the load.

In the limit where the load resistor acts like an open circuit, the magnetic field supplies energy at the same rate that the electric field absorbs energy. The energy in the inductor remains in-place and is totally converted from magnetic field energy to electric field energy by the wavefront. This is an interesting result which could not be explained by a lumped inductor model with an initial current.

The trend in figure 7.5 is that electric and magnetic field power component curves diverge where a high degree of energy conversion occurs. A high degree of energy conversion means significant changes in the voltage and current levels in the transmission line result from the passage of the wavefront. However, the high degree of energy conversion comes at the expense of energy transfer to the load resistor because the wavefront power is small.

7.2.6 Conversion trade-offs

The energy conversion process at the wavefront can be manipulated through impedance mismatch. Figure 7.5 shows the value of load resistance has a significant impact on the wavefront power components prior to any reflections. As the magnitude of these power component vary, so does the degree of energy conversion and the rate at which energy is conveyed to the inductor terminals and transferred to the load.

Energy is neither transferred nor converted where the resistance is low. Where the impedances are matched, the rate of energy transfer between the transmission line and the load resistor is maximised, and some energy is converted. When the load resistance is high, almost no energy transfers to the load resistor, but much of the energy is converted. At these large resistances, a tradeoff between energy transfer and energy conversion is encountered: a high degree of energy conversion within the transmission line will result in less energy transfer out of the transmission line terminals.

This trade-off between energy conversion and energy transfer is further highlighted by figure 7.6. In figure 7.6 a lossless transmission line inductor is connected to an ideal switch. The inductor has an initial current. The switch is opened at $t = 0$. The voltage and current distributions are shown at $t = 0$ when the wavefront is at the left of the transmission line and at $t = \tau$ when the wavefront is at the right of the transmission line.

Initially there is only current and no voltage. After τ seconds have passed there is only voltage and no current. The wavefront introduced by the switch causes the magnetic field energy to totally convert into electric field energy so only a voltage exists. During this process all the energy remains confined to the transmission line. The total energy is constant, but the nature of that energy changes.

In order to perform both energy transfer and energy conversion, an impedance mismatch must be chosen to balance the two effects. The challenge is that each effect is optimised by different degrees of impedance mismatch. This is the trade-off between electrical energy conversion and transfer: prioritising large changes in voltage and current causes the energy to change form but remain trapped in-place. Prioritizing energy transfer instead causes the energy to exit from the transmission line faster but with smaller changes in voltage and current levels.

Typically, the motivation for performing energy conversion is to modify voltage and current levels while still retaining access to the energy. Therefore, the degree of

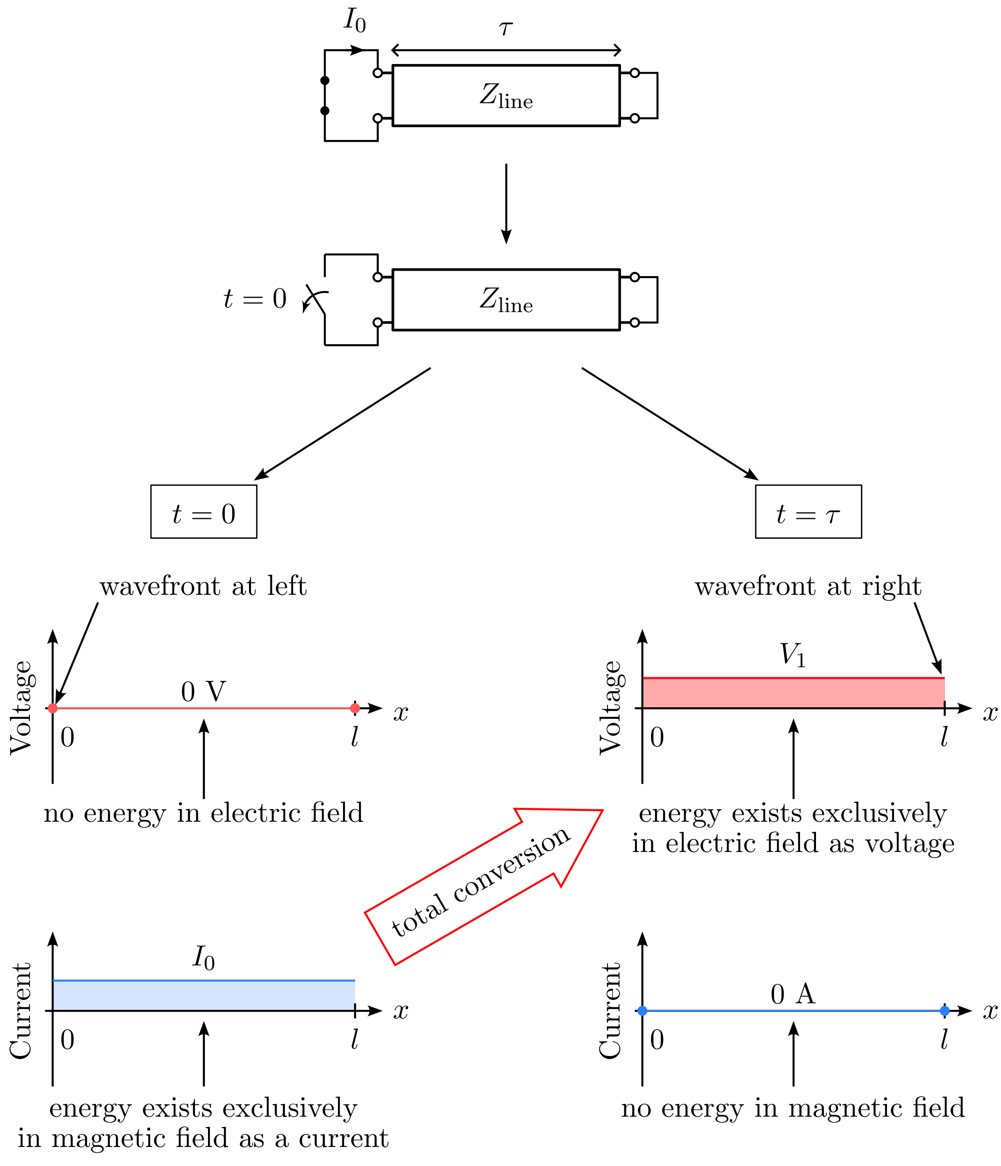

Figure 7.6: An open circuit causes all the magnetic field energy in the transmission line inductor to convert to electric field energy

energy conversion must necessarily be reduced so that the outputs of the conversion process can be transferred to do useful work. Additionally, it may be desirable to reduce the rate of energy transfer out of the inductor so the stored energy is delivered at a lower rate to the load.

7.2.7 Duality of inductors and capacitors

Chapter 3 discusses the duality of inductor and capacitors when modelled as transmission lines. So far we have seen how impedance mismatch affects the wavefront power components for a transmission line inductor. Figure 7.7 shows the wavefront power components can be equally applied to a transmission line capacitor model. The inductor has an initial current of 6 A, and the capacitor has an initial voltage of 6 V. The transmission line impedance is fixed at 1 Ω and the load resistance is varied. The capacitor power curves appear to be a transformation of the inductor curves: the electric and magnetic field power components are exchanged, and reflected about the vertical axis at the matched impedance.

For the transmission line capacitor the power components converge to 0 J/s for large resistances and diverge with smaller resistances. This is the opposite of what takes place for the transmission line inductor where the power components converge for small load resistances. The magnetic field component is positive for the capacitor but negative for the inductor. Similarly, the electric field component is negative for the capacitor but positive for the inductor. In both instances, where the impedances are matched the wavefront power is maximised.

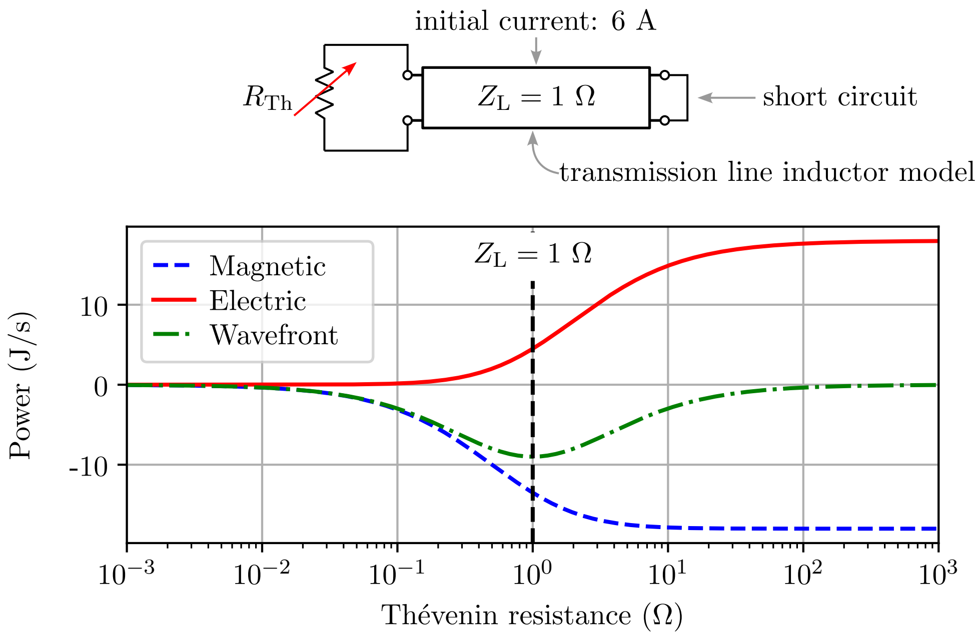

(a) Inductor wavefront power components

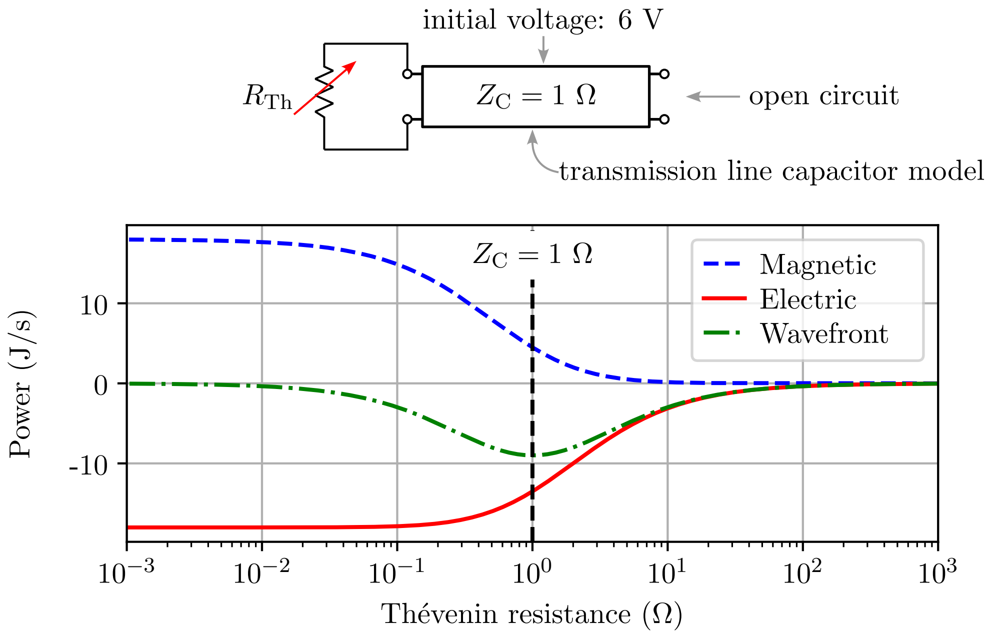

(b) Capacitor wavefront power components

Figure 7.7: Comparison of wavefront power and its components for transmission line models of (a) an inductor and (b) a capacitor

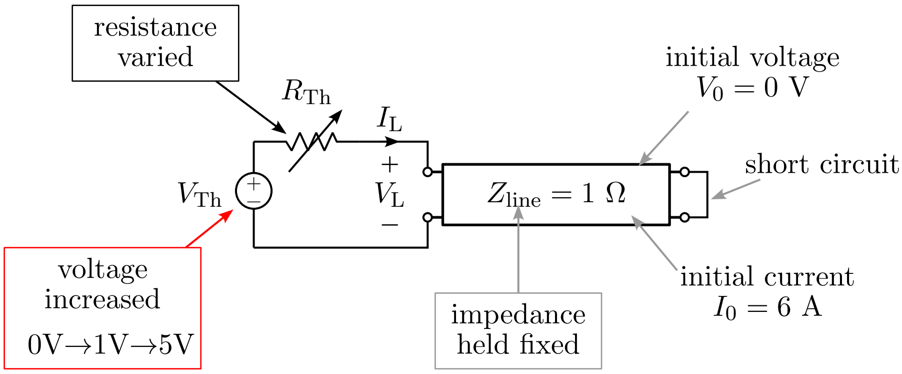

Figure 7.8: Circuit for charging the transmission line inductor with increasing voltages while varying the degree of impedance mismatch

7.3 Charging inductor

Charging a transmission line inductor requires the transfer of electrical energy from another source into the inductor. That energy is then brought to rest purely in the magnetic field of the inductor. We model the energy source with the Thévenin circuit in figure 7.8. The circuit in figure 7.8 is equivalent to the source and load resistor circuit of the step-down converter circuit seen earlier in chapter 6. Thus, the circuit analysis is not repeated here. Again, we look only at the case where the wavefront has not yet undergone any reflections.

Figure 7.9 plots the wavefront power components for a Thévenin voltage of 0 V, 1 V, and 5 V. The backgrounds of the plots in figure 7.9 are shaded to indicate the range of resistances for which the inductor absorbs or supplies energy. The case where the Thévenin voltage is 0 V in figure 7.9a has already been discussed in the previous section but is reproduced here for comparison. Where the transmission line is the only source of energy in the circuit, it supplies energy to the load resistor at its terminals regardless of the degree of impedance mismatch as seen in figure 7.9a.

The Thévenin voltage is set to 1 V in figure 7.9b. The transmission line inductor absorbs energy for the range of resistances to the left of the figure where the wavefront power is positive. This range of resistances is dependent on the applied voltage and initial current as expressed by (7.2). Therefore, the shaded region grows towards the right with increasing voltage as seen in figure 7.9c where 5 V is applied.

$$R_{Th} \leq \frac{V_{Th}}{I_0} \tag{7.2}$$

In figure 7.9a the wavefront power and its components approach zero for small resistances. As the source voltage is increased to 1 V in figure 7.9b and 5 V in figure 7.9c, the curves are shifted upwards on the vertical axis, becoming positive-valued for small resistances. Comparing figures 7.9b and 7.9c, it can be seen that the magnetic field power component is shifted upwards more than the electric field component for the same increase in voltage. Generally, the magnetic field component is large and the electric field component is small, so the majority of

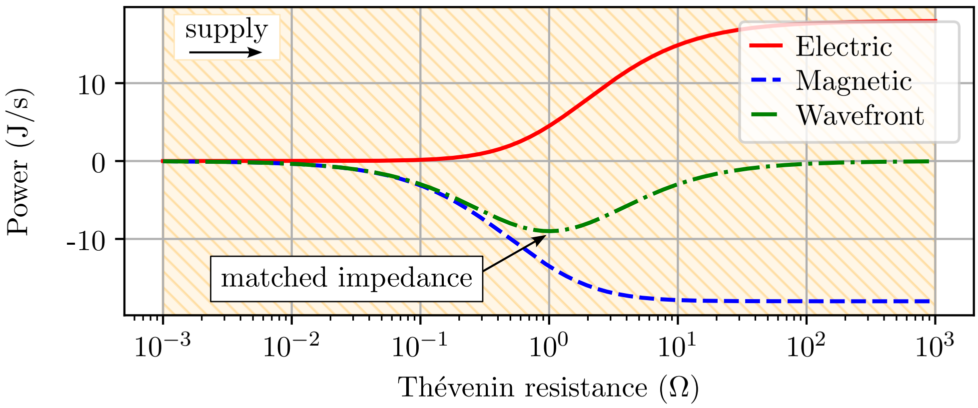

(a) 0 V source

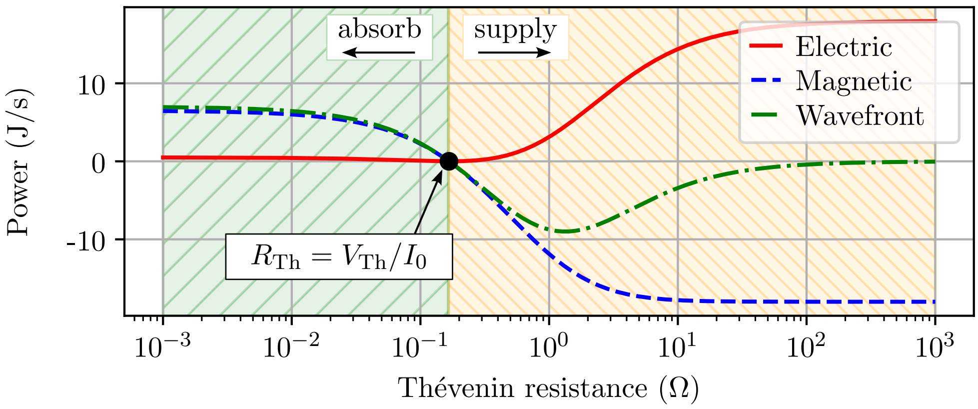

(b) 1 V source

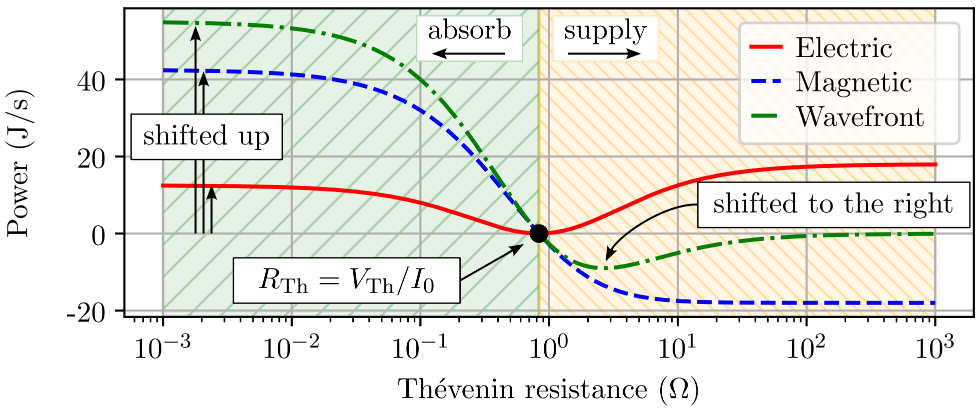

(c) 5 V source

Figure 7.9: Wavefront power components as a function of resistance with an applied voltage of (a) 0 V, (b) 1 V, and (c) 5 V

energy is directed into the magnetic field as expected for an inductor.

For the load resistance at the boundary between the shaded regions, the wavefront power and its components are all 0 J/s. At this load resistance, the voltage source of the Thévenin circuit maintains the initial current. The transmission line inductor remains in equilibrium regardless of switch position. There is no wavefront in the transmission line and energy conversion does not occur.

The state of equilibrium in the inductor coincides with the value of load resistance which minimise the electric field power component. This is an interesting result because it emphasises the participation of the electric field power component in the absorption and supply of energy by the transmission line inductor. This is in contrast to the lumped inductor model where the electric field is altogether neglected.

For charging the inductor, the maximum power transfer always occurs at the smallest load resistance. There the wavefront power has a maximum value. In figure 7.9c, the minimum value of the wavefront power is shifted towards the right as a result of the applied voltage. Thus, for discharging the inductor, the point of maximum power transfer out of the inductor is shifted to a load resistance greater than its characteristic impedance.

Moving to the right of figure 7.9 the load resistance is much greater than the transmission line impedance. In this case, the power components remain largely unchanged as the applied voltage increases. The large load resistance opposes the flow of current between the voltage source and the inductor. The impedance mismatch combined with the initial conditions leads to a wavefront which again extracts energy from the magnetic field. This is undesirable where the objective is to charge the inductor by storing energy in the magnetic field.

7.4 Discharging inductor over multiple reflections

Chapter 5 discusses how the electric and magnetic field components of the wavefront power are modified by the reflection of the wavefront at the ends of the transmission line inductor. The first reflection takes place at the short circuit and changes the contributions of the electric and magnetic field power components to the wavefront, but the wavefront power remains the same for the round trip. Over many reflections, the electric field power component oscillates between supplying and absorbing energy while the magnetic field component continuously supplied power. These observations were made for a single value of resistance connected to the transmission line inductor.

This section revisits the circuit from figure 7.1 where the transmission line inductor is discharged by setting the Thévenin voltage to 0 V. This section considers the effect of impedance mismatch on the wavefront power components over one and then multiple reflections. The same analysis could equally be applied where the Thévenin voltage is non-zero, but is not shown here.

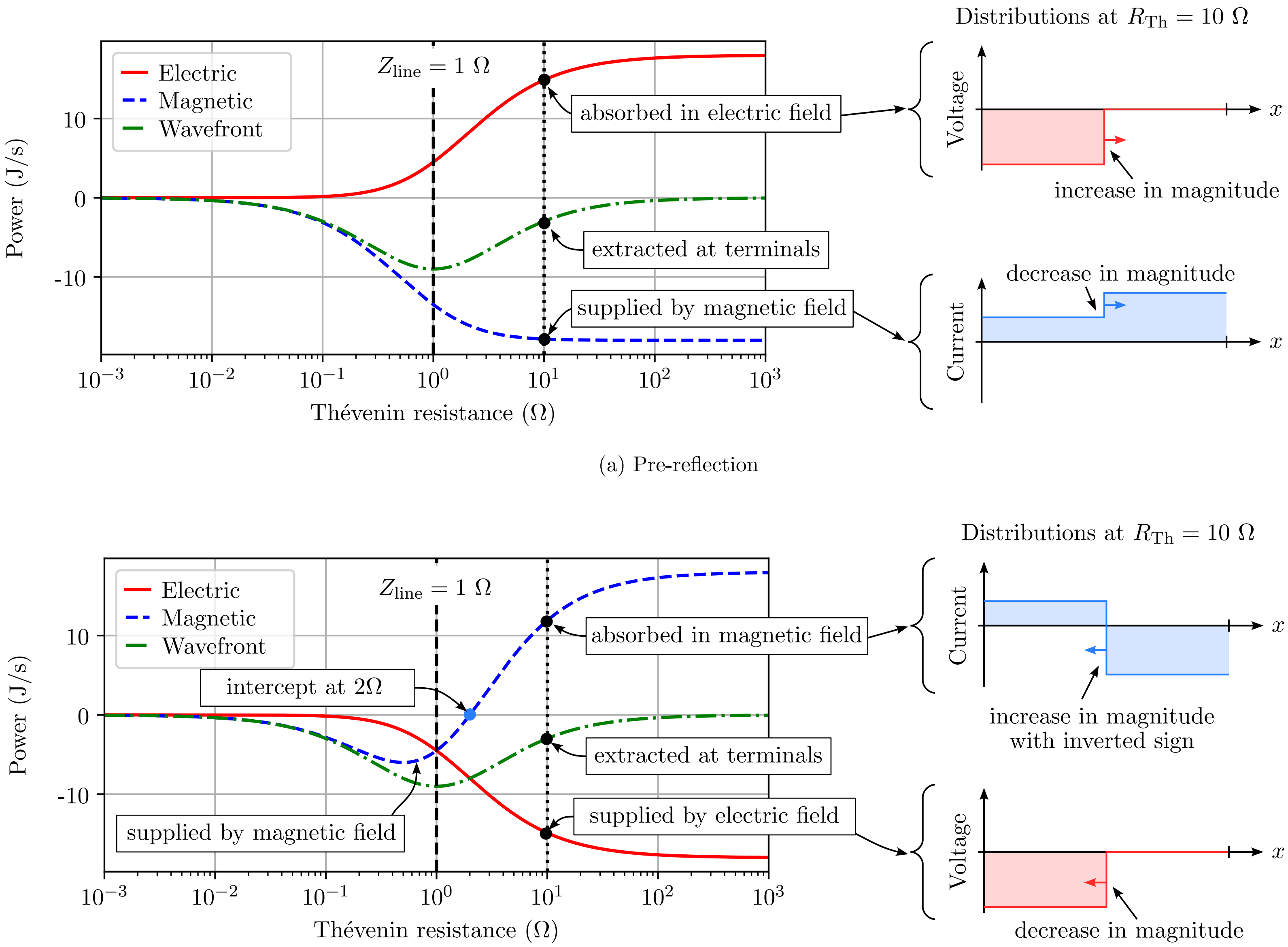

(a) Pre-reflection

(b) Post-reflection

Figure 7.10: Wavefront power and components (a) before and (b) after the first reflection in a discharging transmission line inductor

7.4.1 First reflection

Figure 7.10 plots the wavefront power components before and after the first reflection of the wavefront in the transmission line inductor. The pre-reflection curve in figure 7.10a is a reproduction of figure 7.4 and has already been discussed. It is shown again here to facilitate direct comparison with the post-reflection curve in figure 7.10b.

The wavefront power remains unchanged by the reflection for all resistances. In contrast, the wavefront power components are modified by the reflection, especially for large load resistances. Where the sign of a power component is inverted, the action of the wavefront on the energy in the underlying fields is reversed. For example, the electric field power component is positive for all resistances pre-reflection yet negative post-reflection. The magnetic field component shows interesting behaviour with the sign of the power components inverted post-reflection only for resistances greater than $2\,\Omega$.

Initially the wavefront travels in the transmission line towards the short circuit and after reflecting it travels back towards the terminals. The direction of travel is indicated on the voltage and current distributions to the right side of figure 7.10. These distributions are for a resistance of $10\,\Omega$ indicated by the dotted vertical line on the power curves. The pattern of behaviour at $10\,\Omega$ is representative of all resistances greater than $2\,\Omega$.

Prior to the reflection, in figure 7.10a where the resistance is $10\,\Omega$ the magnetic field power component is negative and the electric field power component is positive. Thus, the electric field absorbs energy from the magnetic field at the wavefront. The spatial distributions show a corresponding increase in voltage magnitude and decrease in current magnitude at the wavefront.

After the reflection, in figure 7.10b at $10\,\Omega$ the magnetic field power component becomes positive and the electric field power component becomes negative. Thus, the electric field supplies energy and the magnetic field absorbs energy. The voltage distribution shows the voltage collapses to zero behind the wavefront. At the same time, the current distribution shows an increase in magnitude behind the wavefront, albeit with the opposite polarity to before the reflection.

After the reflection, at $2\,\Omega$ the electric field exclusively contributes to the wavefront power while the magnetic field component is $0\,\mathrm{J/s}$. This intercept is interesting because it represents the resistance where wavefront reflection reverses the current direction but preserves the same magnitude. From a field perspective, the energy in the magnetic field is unchanged by the reversal of the current direction.

For resistances less than $2\,\Omega$, both the electric and magnetic field power components are negative. Thus, the reflection modifies the wavefront such that both the electric and magnetic field supply the wavefront power. The electric and magnetic fields contribute equally to the wavefront power where the curves intersect at $1\,\Omega$. This is the condition where the resistance and the transmission line impedance are matched.

Figure 7.10b shows the magnetic field component reaches a minimum of $-6\,\mathrm{J/s}$ at a resistance of $0.5\,\Omega$. This represents a peak in the magnitude of the power supplied by the magnetic field post-reflection. At $0.5\,\Omega$, the electric and magnetic fields initially contribute energy at a lower rate compared to when the impedance is matched. This means more energy remains in the fields. After the reflection, the change in energy density is greater at the wavefront and therefore the contribution of the magnetic field power component is greater than for a matched impedance.

Figures 7.10a and 7.10b exhibit a large degree of similarity for small resistances with all power components approaching 0 J/s. Therefore, the reflection has a diminishing effect for small resistances. This is the region which best describes the normal operating conditions for an inductor in the step-down converter. At 100 mΩ the wavefront power is the same as at 10 Ω. Thus, the inductor transfers same amount of energy to the load over the round trip but without the energy being first transferred into the electric field by the wavefront and then returned to the magnetic field after the reflection. Excess movement of energy incurs greater losses in physical circuits so it is appropriate that the normal operating conditions of an inductor minimise the movement of energy.

7.4.2 Multiple reflections

Figure 7.11 shows the wavefront power component curves over multiple reflections for the transmission line inductor discharging into the load resistor. The number of wavefront reflections is denoted by n. The cases where $n = 0$ and $n = 1$ were discussed in figures 7.10a and 7.10b for before and after the first reflection, respectively.

Each row of curves in figure 7.11 represents a round trip of the wavefront in the transmission line. The wavefront power is constant for a round trip, so the corresponding curve is identical across both plots in each row. Moving down the rows, the amplitude of the wavefront power diminishes for all resistances. This means that less power is delivered to the load resistor at the terminals for each successive round trip. For the first round trip, the wavefront power curve has a single minimum. For the second round trip and onwards, the wavefront power curve shows two local minima of equal value. As before, these two values of resistance produce the same wavefront power but with drastically different power components.

The even values of n form the column of plots on the left-hand side of figure 7.11. For the left column, the wavefront travels towards the short circuit from the terminals. For all resistances the electric field power component is positive and the magnetic field power component is negative, so the electric field always absorbs energy from the magnetic field.

The column of plots on the right-hand side of figure 7.11 is formed by the odd values of n. For the right column, the wavefront travels back towards the terminals and away from the short circuit. The electric field power component is negative for all values of resistance and thus supplies energy. The magnetic field power component is positive for large resistances and negative for small resistances.

The signs of the electric and magnetic field power components alternate for even and odd values of n at large resistances. This suggests that the initial wavefront mobilises energy from storage in excess of the load requirements. The excess energy continues to oscillate between storage in the electric and magnetic fields with each reflection. The oscillation leads to an excess amount of energy conversion to produce

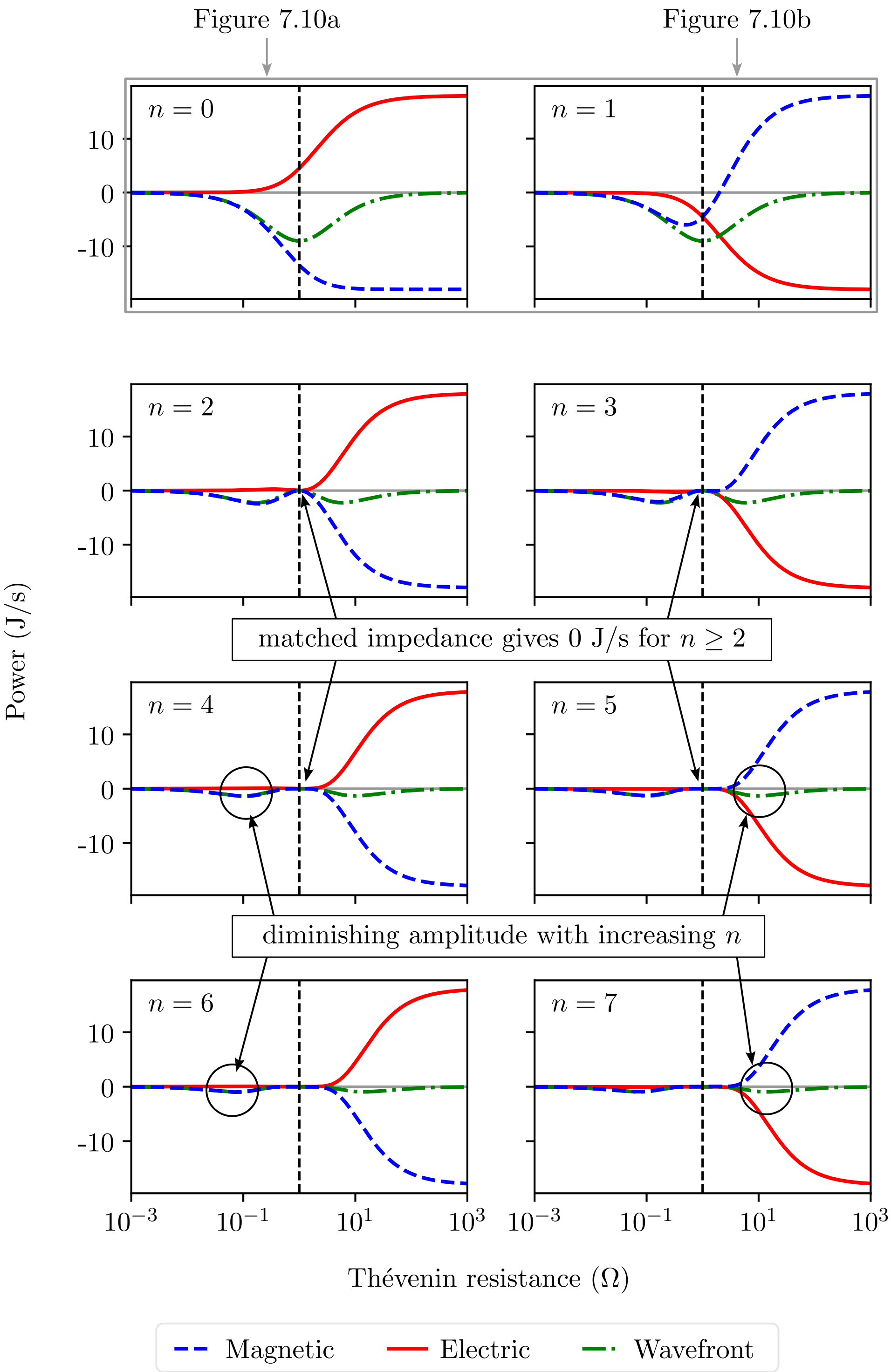

Figure 7.11: Wavefront power and its components for an increasing number of reflections

the same power output at the inductor terminals as for a smaller load resistance. Under lossy conditions, excess movement of energy between fields could lead to increased dissipation which is undesirable. Thus, it is appropriate that the load resistance be kept small in contrast to the impedance of the transmission line inductor.

For resistances of similar value to the transmission line impedance, the plots of wavefront power and its components see a marked drop in magnitude for $n \geq 2$. When the impedances are matched, energy transfers to the load at the highest rate, no reflection occurs when the wavefront returns to the load, and the transmission line is completely drained of its stored energy in one round trip. The wavefront power and its components are $0\,\mathrm{J/s}$ thereafter, since no further energy conversion is possible when the stored energy in the transmission line is depleted.

The general reduction in magnitude over time suggests that the rate of energy conversion that takes place in the transmission line decreases with each reflection. Thus, a wavefront introduced into a transmission line can only perform a finite amount of energy conversion despite undergoing many reflections. At the same time, the energy stored in the transmission line decreases. At some point the energy in the transmission line will be depleted, and the wavefront will cease to exist. The transmission line will need to be charged up again and a wavefront introduced to continue the energy conversion process.

Figure 7.11 suggests that an impedance mismatch generally extends the energy conversion process over many reflections. There are some applications, like a step-down converter, which set a desired voltage and current level for electrical energy at the inductor terminals. In these instances it is necessary to accept a reduced rate of energy transfer out of the inductor in exchange for an energy conversion process which takes many reflections to supply energy at the desired voltage and current levels. In that case, the impedance mismatch is a requirement for energy conversion as suggested by Sander [5] and Hofsajer [9].

Chapter 8

Conclusion

Although the outcomes of energy conversion are recognisable in DC-DC power converters, the functioning of inductors and capacitors with lumped parameter models cannot be explained from an electromagnetic field perspective. Distributed modelling has been used as an alternative to lumped parameter models for inductors and capacitors in literature, but an energy conversion mechanism is yet to be reported.

A step-down converter circuit is shown to function similarly with lumped and distributed models, providing a suitable context in which to study an inductor. An energy conversion process inside the inductor is identified and described using distributed modelling in the form of a high-impedance, lossless transmission line. A description is presented using reflection diagrams, spatial distributions, and a new method of wavefront power components.

The wavefront is identified as the primary centre of activity for the inductor. A reflection diagram for the wavefront yields spatial distributions of voltage and current. These distributions show the energy conversion process produces voltage and current inside the inductor from energy at rest purely in the magnetic field. The spatial distribution of instantaneous power suggests the wavefront is the site of energy conversion where energy initially at rest is put into motion. As the wavefront travels, energy conversion occurs at every position along the length of the transmission line inductor.

The wavefront power is decomposed into components for the electric and magnetic fields respectively using conservation of energy and changes in energy density. These components provide a means to describe the action of the wavefront on the underlying fields of the transmission line from an energy perspective. The power components are tracked over time in the absence and presence of an applied voltage as the wavefront undergoes reflections inside the transmission line.

When a transmission line inductor with an initial current discharges, electrical energy in the form of voltage and current is extracted by the travelling wavefront from the store of energy in the magnetic field. A reflection of the wavefront at the shorted end of the transmission line causes the electric field to offload its energy so only magnetic field energy remains. This is the process which ensures the magnetic field endures as the primary store of energy for the inductor. Similarly, for a charging inductor, with each round trip of the wavefront, the voltage and current at the terminals are converted into energy purely stored in the magnetic field along the length of the line. Notably, the presence of electric field energy in the inductor, and the associated conversion process to and from that electric field energy, appear to be essential for the operation of the inductor.

From the relative magnitudes of the wavefront power components in the transmission line inductor, it is evident that the lumped parameter model is an appropriate approximation of a physical inductor. The overwhelming majority of energy is indeed stored and processed in the magnetic field.

The wavefront power and its components are responsive to a mismatch transmission line impedance and load resistance. Extreme degrees of mismatch suppress or enhance the magnitude of the components for the same power output at the inductor terminals. A trade-off is observed between the degree of energy conversion and the ability of the inductor to absorb or supply energy at its terminals. Continuous conversion of energy under static circuit conditions is possible if the wavefront is maintained by confining energy inside the transmission line. However, if a power is present at the inductor terminals, the energy conversion process will eventually cease as the inductor is drained of energy or reaches maximum storage capacity. Applied to the inductor of the step-down converter, these insights highlight the necessity of switching for creating dynamic circuit conditions. Switching introduces new wavefronts which sustain the energy conversion process as energy accumulates and discharges.

This work prioritises conceptual understanding and therefore is limited in its treatment of complex concrete cases. Several modelling constraints were imposed to suppress sources of complexity and amplify the effects of interest. All forms of loss were eliminated using ideal switches and diodes, and a lossless transmission line model. The timing of switching events and propagation delays were specifically chosen to prevent substantial growth in the number of wavefronts which would overwhelm the analysis. While this work focussed on inductors, it is noted that this transmission line approach is equally applicable to capacitors. The duality that exists between transmission line inductors and capacitors can be utilized to extend the results of this work to capacitors.

The description put forward in this work on transmission line models offers a richer understanding of the mechanism of energy conversion in inductors which is not available using lumped parameter models. This work does not seek to change the established design techniques and foundational theory of power electronics. Rather, this description is intended to contribute to the body of conceptual knowledge for power electronics fundamentals. Additionally, given the richness of discussion from a simplified transmission line model, perhaps this work demonstrates that transmission lines are underutilized as a modelling tool in power electronics.

This work endeavours to describe a process in inductors that has long been overlooked because it was historically considered inconsequential. However, as technological advancements continually redefine the limits of power electronics, it is increasingly apparent that conceptual knowledge gaps need to be addressed. These conceptual knowledge gaps may yield insights which provide the theoretical foundation for further significant innovation in power electronics.

8.1 Future work

This work focusses on identifying and describing an energy conversion mechanism in a transmission line inductor model. This serves as a starting point for further discussion regarding the optimization of the energy conversion process and its sensitivity to various parameters. Suggestions for further avenues of research are primarily concerned with relaxing the constraints applied in this work.

One of those constraints is the requirement that the round-trip delay of the transmission line inductor coincide with the switching events in the step-down converter. This ensures there is at most one wavefront in the transmission line at any given time. Under normal operating conditions, the transmission line inductor may have numerous wavefronts travelling in one or both directions, especially as a result of a control strategy which modulates the converter duty cycle. Future work could consider the treatment of two or more wavefronts, each with an associated direction of travel. The work by Sander [5] may serve as a helpful starting point since it describes three modes of converter operation which depend on the relation between the round-trip delay of the transmission line and the switching times of a converter.

Another area of future work could consider different loads connected to the transmission line inductor. This work looked only at a resistive load, but interesting behaviour could arise from replacing the resistor with another transmission line. The interaction of the transmission lines would introduce an additional source of wavefronts in addition to the switching events. A key question to ask is: how does the introduction of wavefronts from adjacent transmission lines affect the overall energy conversion process? Again this would need careful treatment of the wavefronts at scale so the work by Mofu [18] describing the fracturing of wavefronts between adjacent transmission lines may be a helpful aid.

Parasitics refer to additional lumped circuit elements that are added into a circuit diagram to better account for effects observed in physical circuits. For example, a lumped capacitor may be connected to a lumped inductor to represent the total inter-winding capacitance. In modern power electronics with high frequency switches, parasitics cannot be assumed to be negligible, or added as an afterthought to explain away unexpected behaviour [6].

A particularly interesting avenue for future work is the role of parasitics in the energy conversion process for inductors and capacitors. In this work the electric field plays a fundamental part in the energy conversion process of a transmission line inductor. This raises questions around the nature of parasitics in an inductor. Are parasitics a necessary part of the energy conversion process? If it were possible to build an inductor without any parasitic capacitance would it still function? In the case of a transmission line inductor model, the inductive and capacitive elements are fundamentally integrated by the model and give rise to the characteristic impedance. If both inductance and capacitance are needed to support a wavefront, and the wavefront is needed to perform energy conversion, then perhaps parasitics are necessary for energy conversion. If that is indeed the case, then advances in techniques which minimise parasitics may ultimately impair the conversion of electrical energy.

References

[1] A. I. Petroianu, “Mathematical representations of electrical power: Vector or complex number? neither!” In *2014 IEEE Electrical Power and Energy Conference*, Nov. 2014, pp. 170–177.

[2] A. I. Petroianu, *Bridging Circuits and Fields: Foundational Questions in Power Theory.* Boca Raton: CRC Press, Nov. 30, 2021, 174 pp., ISBN: 978-1-315-20067-5.

[3] R. M. Strzelecki and G. Benysek, Eds., *Power Electronics in Smart Electrical Energy Networks* (Power Systems). London: Springer, 2008, ISBN: 978-1-84800-317-0 978-1-84800-318-7.

[4] N. Mohan, T. M. Undeland, and W. P. Robbins, *Power Electronics: Converters, Applications, and Design.* John Wiley & Sons, 2003, 802 pp., ISBN: 978-81-265-1090-0.

[5] S. Sander, “Buck and boost converters with transmission lines,” *IEEE Transactions on Power Electronics*, vol. 27, no. 9, pp. 4013–4020, Sep. 2012, Conference Name: IEEE Transactions on Power Electronics, ISSN: 1941-0107.

[6] J. Ferreira, “Application of the poynting vector for power conditioning and conversion,” *IEEE Transactions on Education*, vol. 31, no. 4, pp. 257–264, Nov. 1988, Conference Name: IEEE Transactions on Education, ISSN: 1557-9638.

[7] C. Sullivan and A. Kern, “Capacitors with fast current switching require distributed models,” in *2001 IEEE 32nd Annual Power Electronics Specialists Conference (IEEE Cat. No.01CH37230)*, ISSN: 0275-9306, vol. 3, Jun. 2001, 1497–1503 vol. 3.

[8] D. Smilovitz and S. Singer, “Using transmission lines properties for converter realization,” in *Proceedings of IEEE Power Electronics Specialist Conference - PESC ’93*, Jun. 1993, pp. 416–422.

[9] I. Hofsajer, “A new noise mechanism in power converters,” presented at the 2022 IEEE 31st International Symposium on Industrial Electronics (ISIE), 2022, pp. 604–607.

[10] D. Shmilovitz and S. Singer, “High-frequency-operated converters based on transmission lines,” *IEEE Transactions on Power Electronics*, vol. 11, no. 1, pp. 142–146, Jan. 1996, Conference Name: IEEE Transactions on Power Electronics, ISSN: 1941-0107.

[11] J. Ferreira, W. Cronje, and J. van Wyk, "Using poynting vector theory to model and optimise power electronic switching," *Transactions of the South African Institute of Electrical Engineers*, vol. 83, no. 3, Sep. 1992, Conference Name: Transactions of the South African Institute of Electrical Engineers, ISSN: 0038-2221.

[12] M. Ehsani, O. Stielau, J. van Wyk, and I. Pitel, "Integrated reactive components in power electronic circuits," *IEEE Transactions on Power Electronics*, vol. 8, no. 2, pp. 208–215, Apr. 1993, Conference Name: IEEE Transactions on Power Electronics, ISSN: 1941-0107.

[13] J. Ferreira and J. Van Wyk, "Electromagnetic energy propagation in power electronic converters: Toward future electromagnetic integration," *Proceedings of the IEEE*, vol. 89, no. 6, pp. 876–889, Jun. 2001, Conference Name: Proceedings of the IEEE, ISSN: 1558-2256.

[14] M. Smit, J. Ferreira, and J. Van Wyk, "Application of transmission line principles to high frequency power converters," in *PESC '92 Record. 23rd Annual IEEE Power Electronics Specialists Conference*, Jun. 1992, 1423–1430 vol.2.

[15] S. Sander and A. Karvonen, "Semiconductor component reduction in AC/DC converters with transmission lines," in *2013 15th European Conference on Power Electronics and Applications (EPE)*, Sep. 2013, pp. 1–10.

[16] C. Huang, F. Woittennek, and K. Röbenack, "Steady-state analysis of a distributed model of the buck converter," in *2013 European Conference on Circuit Theory and Design (ECCTD)*, Sep. 2013, pp. 1–4.

[17] J. Li, L. Yuan, B. Shi, and Z. Zhao, "Methodology of modeling and visualization of energy flow and energy topology for power converters," in *2016 19th International Conference on Electrical Machines and Systems (ICEMS)*, Nov. 2016, pp. 1–6.

[18] M. Mofu, "Investigation into energy manipulation in reactive components using transmission line modelling," M.S. thesis, University of the Witwatersrand, 2019.

[19] N. N. Rao, *Elements of Engineering Electromagnetics*. Pearson Prentice Hall, 2004, 876 pp., ISBN: 978-0-13-113961-9.

[20] M. Zahn, *Electromagnetic Field Theory: A Problem Solving Approach*. Wiley, May 31, 1979, 766 pp., ISBN: 978-0-471-02198-8.

[21] L. V. Bewley, "Traveling waves on transmission systems," *Transactions of the American Institute of Electrical Engineers*, vol. 50, no. 2, pp. 532–550, Jun. 1931, ISSN: 2330-9431.

[22] K. Röbenack and H. Bärnklau, "A spatially distributed boost converter - modeling and simulation," in *2023 27th International Conference on System Theory, Control and Computing (ICSTCC)*, ISSN: 2473-5698, Oct. 2023, pp. 480–486.

Appendix A

Circuit Simulation

The step-down converter in figure A.1 is simulated using the LTspice netlist given in listing A.1. The two circuits are represented within a single netlist to facilitate direct comparison of output waveforms in the time domain.

In the simulation, a pre-charge circuit sets the initial conditions of the transmission line inductor model since these cannot be directly set in LTspice. However, the pre-charge circuit introduces a time delay between the start of the simulation and the onset of the switching action in the converter. The lumped inductor model makes use of an identical pre-charge circuit to keep the waveforms aligned in the time domain.

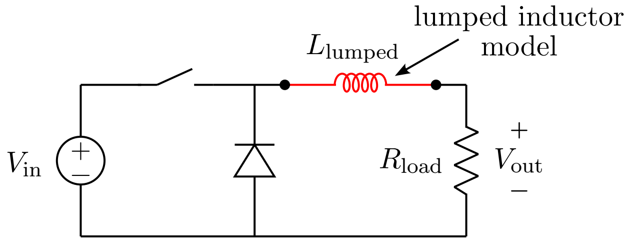

(a) Lumped inductor model

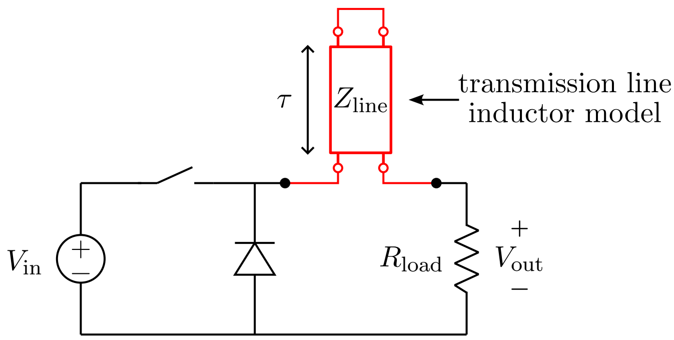

(b) Transmission line inductor model

Figure A.1: Step-down converter with lumped and distributed parameter inductor model for simulation with LTspice

Listing A.1: LTspice netlist for simulating the step-down converter

```
V4 pulse 0 PULSE({Vin} {0} {Tcharge} {Tswitch} {Tswitch}
    {Period*Duty} {Period})
R3 pulse Tout- R={Rload}
R1 pulse Lout- R={Rload}
L1 N004 0 {L} Rser=1u
T1 N002 0 0 0 Td={Delay} Z0={Z0}
I1 0 N001 {I0line}
R4 Tout- N002 R={if(time<Tcharge,10Meg, 10n)}
R5 Lout- N004 R={if(time<Tcharge,10Meg, 10n)}
I2 0 N003 {I0}
R6 N001 0 {Z0}
R7 N001 N002 R={if(time<Tcharge,100n,10Meg)}
R8 N003 N004 R={if(time<Tcharge,100n,10Meg)}
R9 N003 0 R={if(time<Tcharge,10Meg, 100n)}
.tran 0 {Tcharge+1*Period*1.1} {Tcharge} {Tstep}
.ic I(L1)={I0}
.param Rload=50 Vout=5 Vripple=0.5 Period={1/25e3}
.param Duty=0.5 Vin={Vout/Duty}
.param L={Rload*(1-Duty)*Period/(Vripple/Vout)}
.param Delay={Period*Duty/(2*trip)} Z0={L/Delay}
.param Tcharge={2*Delay}, Tswitch=0.1n
.param I0={(Vout+Vripple/2)/Rload}
.param I0line={I0}
.param Tstep=0.1n
.step param trip list 2 10
.backanno
.end
```